

BIOANALYTICAL MICROSYSTEMS FOR WATERBORNE PATHOGEN
DETECTION

A Dissertation

Presented to the Faculty of the Graduate School
of Cornell University

In Partial Fulfillment of the Requirements for the Degree of
Doctor of Philosophy

by

John Thomas Connelly

August 2011

© 2011 John Thomas Connelly

BIOANALYTICAL MICROSYSTEMS FOR WATERBORNE PATHOGEN DETECTION

John Thomas Connelly, Ph. D.

Cornell University 2011

Waterborne pathogens are a global health concern, with 1 billion people having no access to uncontaminated water sources and 2.2 million annual deaths resulting from infection. Biosensors offer the possibility of rapid, sensitive and specific detection of pathogens and, thus, the ability to provide warning systems prior to consumption and a means to monitor the efficacy of disinfection systems. However, in order for biosensors to be useful, one must be able to attain clinically relevant detection limits in real environmental samples and do so on a reasonable timescale. Thus, methods to increase the analytical sensitivity via pre-concentration and microfluidic device design are described herein. Firstly, employing a series of pre-concentration and purification steps followed by an enzymatic amplification of an mRNA sequence, it is shown that a limit of detection of one *Cryptosporidium parvum* oocyst can be attained and that this assay does work in real water samples. Secondly, integrating a liposome-based immunoassay and a nanoporous membrane for electrokinetic pre-concentration into a single microfluidic device for the detection of a human norovirus surrogate yielded an order-of-magnitude decrease in the limit of detection when compared to an optimized device foregoing pre-concentration. Finally, the optimization of microfluidic channel dimensions for assays using liposomal signal amplification is described; illustrating that a 60% reduction in channel height produces an order-of-magnitude reduction in the limit of detection. Taken together, the described work provides tools to advance the field of biosensors by demonstrating means to improve analytical sensitivity and overcome the obstacles presented by environmental water samples.

BIOGRAPHICAL SKETCH

Originally from Freeport, New York, John Thomas Connelly is the youngest son of John and Grace Connelly. He received his Master of Science from Cornell University in 2006, studying under Dr. Antje Baeumner, and his Bachelor of Science degree in Biological and Environmental Engineering from Cornell University in 2003. His research interests lie mainly in the field of biosensors, with his current work on those for waterborne pathogens and previous work on more clinical applications. Outside of science, John is a student of popular culture, photographer, music aficionado, advocate for social justice and equality, amateur genealogist, and dog lover.

This work is dedicated to my parents.

And Helo.

ACKNOWLEDGMENTS

I am deeply indebted to Dr. Antje Baeumner, my longtime academic and research mentor, for her support and encouragement not just throughout the course of this work, but throughout my academic career to date. Words cannot fully convey my heartfelt gratitude. I would also like to acknowledge my committee members, Dr. Richard Durst and Dr. Gregory Weiland, for their time, patience, guidance, and especially their patience, throughout my graduate work. I would like to thank the faculty and staff of the Department of Biological and Environmental Engineering for making Riley Robb Hall feel like home over the course of the last decade since I first matriculated at Cornell University as an undergraduate.

Several people have directly contributed to the work described in this dissertation as collaborators on specific projects and are listed as co-authors on the resultant publications. I would like to particularly acknowledge the contributions of Dr. Sam Nugen, with whom I worked directly on the biosensor for *Cryptosporidium parvum*, Dr. Brian Kirby and Dr. Sowmya Kondapalli, our key collaborators on the integrated concentration and detection device.

My colleagues in the Bioanalytical Microsystems and Biosensors Laboratory greatly contributed to this work through scientific discussion, training, assistance, moral support and comic relief. Dr. Katie Edwards, Barbara Leonard, Lauren Matlock-Colangelo, and Sarah Reinholt, thank you for the conversations, intellectual and otherwise.

TABLE OF CONTENTS

BIOGRAPHICAL SKETCH.....	iii
DEDICATION	iv
ACKNOWLEDGEMENTS	v
TABLE OF CONTENTS	vi
LIST OF FIGURES	x
LIST OF TABLES	xi
LIST OF ABBREVIATIONS	xii
CHAPTER 1	1
BIOSENSORS FOR THE DETECTION OF WATERBORNE PATHOGENS	1
ABSTRACT.....	1
IMPORTANCE AND CHALLENGE OF WATERBORNE PATHOGENS	1
INDICATOR ORGANISMS	4
STANDARD TECHNIQUES FOR WATERBORNE PATHOGEN DETECTION .	5
BIOSENSORS AS NOVEL DETECTION METHODS.....	7
CRITERIA FOR BIOSENSORS DEVELOPMENT	7
OBSTACLES TO DETECTION	9
FUTURE IMPROVEMENTS FOR WATERBORNE PATHOGEN	
IMMUNOSENSORS.....	14
IMPROVEMENTS FOR DNA-BASED BIOSENSORS.....	17
CONCLUSIONS.....	19
REFERENCES	21
CHAPTER 2.....	32
HUMAN PATHOGENIC <i>CRYPTOSPORIDIUM</i> SPECIES BIOANALYTICAL	
DETECTION SYSTEM WITH SINGLE OOCYST LIMIT OF DETECTION	
.....	32
ABSTRACT.....	32
INTRODUCTION	33
MATERIALS & METHODS	35

IMMUNOMAGNETIC SEPARATION (IMS).....	37
HEAT SHOCK, LYSIS AND mRNA ISOLATION.....	37
NASBA PROCEDURE	38
LATERAL FLOW ASSAY	39
VERIFICATION OF VIABILITY DETECTION WITH DAPI/PI STAINING..	40
PREPARATION OF ENVIRONMENTAL WATER SAMPLES	42
RESULTS & DISCUSSION.....	43
DETECTION OF HUMAN PATHOGENIC <i>CRYPTOSPORIDIUM SPP.</i>	43
SPECIFICITY FOR HUMAN PATHOGENIC <i>CRYPTOSPORIDIUM</i>	44
DETECTION IN THE PRESENCE OF CONTAMINATING ORGANISMS....	44
ANALYTICAL SENSITIVITY.	45
DISCRIMINATION BETWEEN VIABLE AND NON-VIABLE OOCYSTS ...	46
COMPARISON TO EPA METHOD 1622	48
SPIKED ENVIRONMENTAL WATER SAMPLES.....	49
CONCLUSIONS.....	51
ACKNOWLEDGEMENT	51
REFERENCES	53
CHAPTER 3.....	55
INTEGRATED MICROFLUIDIC PRE-CONCENTRATION AND IMMUNOBIOSENSOR.....	55
ABSTRACT.....	55
INTRODUCTION	55
EXPERIMENTAL METHODS.....	59
FABRICATION OF MICROFLUIDIC CHANNELS	59
WAFER BONDING	60
MEMBRANE FABRICATION AND SURFACE TREATMENT.....	60
LIPOSOME AND MAGNETIC BEAD PREPARATION	62
SAMPLE LOADING, CONCENTRATION AND DETECTION.....	63
RESULTS	65
ELECTROPHORETIC CONCENTRATION OF FLUORESCENT LIPOSOMES	65

INTEGRATED CONCENTRATION AND DETECTION EXPERIMENTS.....	67
COMPARISON OF DEVICE PERFORMANCE WITH AND WITHOUT CONCENTRATION.....	68
DISCUSSION.....	70
CONCLUSION.....	71
ACKNOWLEDGEMENTS.....	72
REFERENCES.....	73
CHAPTER 4.....	79
MICRO-TOTAL ANALYSIS SYSTEM FOR VIRUS DETECTION: MICROFLUIDIC PRE-CONCENTRATION COUPLED TO LIPOSOME- BASED DETECTION.....	79
ABSTRACT.....	79
INTRODUCTION.....	80
MATERIALS & METHODS.....	85
FCV PURIFICATION AND TITRATION.....	85
BIOTINYLATION OF ANTIBODIES.....	85
PREPARATION OF CAPTURE BEADS.....	86
PREPARATION OF STREPTAVIDIN-CONJUGATED LIPOSOMES.....	86
MICROTITER PLATE LIPOSOME IMMUNOASSAY (LIA) FOR ANTIBODY SELECTION.....	87
CONCENTRATION AND DETECTION OF FCV.....	88
DETECTION OF FCV WITHOUT ELECTROKINETIC CONCENTRATION	90
RESULTS & DISCUSSION.....	91
SELECTION OF ANTIBODIES AND ASSAY OPTIMIZATION.....	92
COMPARISON OF FCV DETECTION WITH AND WITHOUT ELECTROKINETIC CONCENTRATION.....	94
CONCLUSION.....	97
ACKNOWLEDGEMENTS.....	98
REFERENCES.....	99
CHAPTER 5.....	104

OPTIMIZATION OF MICROFLUIDIC ELECTROCHEMICAL DETECTION CHANNELS FOR LIPOSOME NANOVESICLE-BASED SIGNAL AMPLIFICATION	104
ABSTRACT	104
INTRODUCTION	105
MATERIALS & METHODS	106
FABRICATION OF MICROFLUIDIC CHANNELS	107
FABRICATION OF IDUAS	109
IDUA CHARACTERIZATION	109
IDUA FLOW RESPONSE	109
LIPOSOME AND MAGNETIC BEAD PREPARATION	110
DNA HYBRIDIZATION ASSAY	111
RESULTS & DISCUSSION.....	111
IDUA FABRICATION.....	112
BUFFER OPTIMIZATION.....	113
IDUA ELECTROCHEMICAL RESPONSE WITH VARYING CHANNEL DIMENSIONS	115
EFFECT OF DIMENSION CHANGES ON DNA HYBRIDIZATION ASSAY	117
CONCLUSION.....	118
ACKNOWLEDGEMENTS	119
REFERENCES	120
CHAPTER 6.....	122
CONCLUSION	122

LIST OF FIGURES

Figure 1.1: Typical Process Flow for Detection of Pathogens in Environmental Water Samples	13
Figure 2.1: <i>Cryptosporidium</i> Detection in the Presence of Contaminating Organisms	45
Figure 2.2: Lateral Flow Test Strips from 1 Oocyst <i>C. parvum</i> Samples	46
Figure 2.3: DAPI/PI Viability Staining Results	47
Figure 2.4: Lateral Flow Test Strips for Environmental Water Samples	50
Figure 3.1: Image of the Integrated Glass Microfluidic Device.....	58
Figure 3.2: Image Sequence Showing Liposome Concentration and Elution.....	66
Figure 3.3: Concentration Factors During Liposome Concentration	66
Figure 3.4: Fluorescent Liposomes Captured at the Bead Bed	67
Figure 3.5: Snapshots of the Fluorescence Measurement Window During Lysis	68
Figure 3.6: Fluorescence Intensity Profiles from the Bead Bed During OG Injection for Experiments With and Without Preconcentration	69
Figure 4.1: Schematic of Assays with and without Pre-concentration.....	84
Figure 4.2: Combined Concentration and Detection Device.....	89
Figure 4.3: Device without Pre-concentration Module	91
Figure 4.4: Dose-Response Curves for Polyclonal Capture Antibody with Monoclonal Reporter Antibodies.....	93
Figure 4.5: Optimized Assay for FCV Detection in Cell Culture Lysate	93
Figure 4.6: FCV Detection after Electrokinetic Concentration.....	94
Figure 4.7: FCV Detection without Pre-concentration.....	95
Figure 5.1: Fully Assembled Microfluidic Device.....	108
Figure 5.2: Effect of Encapsulant and Diluent Buffers on Liposome Performance...	114
Figure 5.3: Calibration Curve for 50 μ m Deep Channels of Specified Widths	116
Figure 5.4: Calibration Curve for 500 μ m Wide Channels of Specified Depths	116
Figure 5.5: Dose-Response Curves for Channels of two Different Depths Using a DNA Sandwich-Hybridization Assay	118

LIST OF TABLES

Table 1.1: World Health Organization (WHO) List of Relevant Waterborne Pathogens	2
Table 2.1: NASBA Primers	38
Table 2.2: Probes for Detection.....	39
Table 2.3: Correlation of Viability to Staining and DIC Visualization.....	41
Table 2.4: Characteristics of Environmental Water Samples.....	42
Table 2.5: Percentage of Samples Testing Positive at Varying Oocyst Numbers for the Three Human Pathogenic <i>Cryptosporidium</i> species	43
Table 2.6: Comparison of Results Obtained from Experimental Methods and EPA Method 1622 for Samples Containing 10 or 25 Oocysts	49
Table 5.1: Flow Rates Required for Equal Linear Velocities in Channels of Varying Cross-Sections	117

LIST OF ABBREVIATION

AFM	Atomic Force Microscopy
BSS	Borate Saline Sucrose
CFU	Colony Forming Unit
CPE	Cytopathogenic Effects
CRFK	Crandell-Reese Feline Kidney
DAPI	4',6-diamidino-2-phenylindole
DIC	Differential Interference Contrast
DMEM	Dulbecco's Modified Eagle's Media
DPPC	1,2-Dipalmitoyl- <i>sn</i> -Glycero-3-Phosphocholine
DPPE	1,2-Dipalmitoyl- <i>sn</i> -Glycero-3-Phosphatidylethanolamine
DPPG	1,2-Dipalmitoyl- <i>sn</i> -Glycero-3-[Phospho- <i>rac</i> -(1-Glycerol)], sodium salt
EDTA	Ethylenediaminetetraacetic acid
ELISA	Enzyme-Linked Immunosorbent Assay
FCV	Feline Calicivirus
FDA	US Food & Drug Administration
FITC	Fluorocein isothiocyanate
HBSS	Hank's Balanced Salt Solution
HEPES	4-(2-hydroxyethyl)-1-piperazineethanesulfonic acid
HSS	HEPES Saline Sucrose
IDUA	Interdigitated Ultramicroelectrode Array

IMS	Immunomagnetic Separation
LFA	Lateral Flow Assay
LIA	Liposome Immunoassay
mAb	Monoclonal antibody
μ TAS	Micro Total Analysis System
NASBA	Nucleic Acid Sequence-Based Amplification
OG	octyl- β -D-glucopyranoside
pAb	Polyclonal antibody
PBS	Phosphate Buffered Saline
PCR	Polymerase Chain Reaction
PDMS	Polydimethylsiloxane
PMMA	Polymethylmethacrylate
PFU	Plaque Forming Unit
PI	Propidium iodide
PMT	Photomultiplier Tube
PSS	Phosphate Saline Sucrose
RIE	Reactive Ion Etching
RT-PCR	Reverse Transcriptase PCR
SERS	Surface Enhanced Raman Spectroscopy
SNT	Serum Neutralization Test
SPR	Surface Plasmon Resonance

SRB	Sulforhodamine B
UPT	Up-converting Phosphor Technology
US EPA	United States Environmental Protection Agency
WHO	World Health Organization

CHAPTER 1

BIOSENSORS FOR THE DETECTION OF WATERBORNE PATHOGENS

Abstract

Waterborne bacterial, viral and parasitic pathogens are a global health concern and their rapid and specific detection in contaminated potable water is of utmost importance. Biosensors have been reported employing various biorecognition molecules and transduction methodologies as they have promise to provide highly sensitive detection of the analyte of interest in a short time frame and a high degree of specificity. However, there are several obstacles to the detection of waterborne pathogens; namely they tend to be present at very low concentrations in the environment and environmental samples contain numerous inhibitors of enzymatic reactions and interfering organisms and particulates. Here we present a review of the current state of biosensor technology with respect to the needed improvements over standard detection methods and the challenges presented by real environmental samples. Further, we identify future areas of focus necessary to realize novel detection devices capable of supplanting the gold standards of today.

Importance and challenge of waterborne pathogens

Lack of access to safe, potable water is a global health concern that, in combination with poor hygiene and sanitation facilities, impacts more than half the population of the developing world. Almost 1 billion people rely on contaminated water sources, contributing to the 2.2 million annual deaths caused by diarrheal diseases (1), which the World Health Organization (WHO) estimates as at least 4% of the global disease

burden (2). This lack of access to safe water and proper sanitation facilities disproportionately effects children; those under 5-years-old account for over 90% of the annual deaths from diarrheal diseases with about 5,000 children dying per day (3).

Table 1.1: World Health Organization (WHO) List of Relevant Waterborne Pathogens[†]

Pathogen	Associated Disease	Relative Infectivity	Persistence in water	Resistance to Disinfection
Bacteria				
<i>Burkholderia pseudomallei</i>	melioidosis	Low	May multiply	Low
<i>Campylobacter jejuni</i> , <i>C. coli</i>	gastroenteritis	Moderate	Moderate	Low
<i>Escherichia coli</i> - pathogenic	gastroenteritis	Low	Moderate	Low
<i>E. coli</i> O157:H7 (enterohaemorrhagic)	gastroenteritis, hemolytic-uremia	High	Moderate	Low
<i>Legionella</i> spp.	Legionnaires' disease	Moderate	May multiply	Low
Non-tuberculous mycobacteria	Pulmonary disease, skin infection	Low	May multiply	High
<i>Pseudomonas aeruginosa</i>	Pulmonary disease, skin infection [‡]	Low	May multiply	Moderate
<i>Salmonella</i> Typhi	Typhoid Fever	Low	Moderate	Low
<i>Salmonella enterica</i>	Salmonellosis	Low	May multiply	Low
<i>Shigella</i> spp.	Shigellosis	High	Short	Low
<i>Vibrio cholerae</i>	Cholera	Low	Bioaccumulates	Low
<i>Yersinia enterocolitica</i>	gastroenteritis	Low	Long	Low
Viruses				
Adenoviruses	gastroenteritis, respiratory infection	High	Long	Moderate
Enteroviruses	gastroenteritis	High	Long	Moderate
poliovirus	poliomyelitis	High	Long	Moderate
coxsackievirus	meningitis	High	Long	Moderate
Astroviruses	gastroenteritis	High	Long	Moderate
Hepatitis viruses A,E	Hepatitis	High	Long	Moderate
Noroviruses	gastroenteritis	High	Long	Moderate
Sapoviruses	gastroenteritis	High	Long	Moderate
Rotavirus	gastroenteritis	High	Long	Moderate
Protozoa				
<i>Acanthamoeba</i> spp.	keratitis, encephalitis	High	May multiply	Low
<i>Cryptosporidium</i> spp.	Cryptosporidiosis	High	Long	High
<i>Cyclospora cayetanensis</i>	gastroenteritis	High	Long	High
<i>Entamoeba histolytica</i>	amoebic dysentery	High	Moderate	High
<i>Giardia lamblia</i>	Giardiasis (Beaver fever)	High	Moderate	High
<i>Naegleria fowleri</i>	Primary amoebic meningoencephalitis	Moderate	May multiply	Low
<i>Toxoplasma gondii</i>	Toxoplasmosis	High	Long	High
Helminths				
<i>Dracunculus medinensis</i>	Dracunculiasis (Guinea worm disease)	High	Moderate	Moderate
<i>Schistosoma</i> spp.	Schistosomiasis	High	Short	Moderate
† Adapted from WHO Guidelines for Drinking Water Quality (10)				
‡ immunocomprised individuals				

Waterborne pathogens are also a problem in developed nations. The annual number of cases of acute gastrointestinal illness in the United States caused by the consumption of contaminated water has been estimated to be from 4.26 million (4) to as high as

32.9 million (5). Some of the largest outbreaks resulting from protozoan parasites, like *Cryptosporidium* and *Giardia*, have been in developed nations. The 1993 outbreak in Milwaukee, Wisconsin, is still the largest caused by *Cryptosporidium*; over 400,000 people were infected and 100 deaths were attributed to the contamination of the municipal water supply (6, 7). A crisis hit Sydney, Australia, in 1998 when severe weather systems flooded the water treatment facilities with *Cryptosporidium* oocysts and *Giardia* cysts that were ultimately detected in filtered water triggering 70 days of boil water alerts (8). In Western Europe, higher hygiene standards have led to decreased immunity to enteric viruses, like hepatitis A, causing a spike in cases (9).

The causative agents of most waterborne diseases can be divided into three categories: bacteria, viruses, and parasites, the latter consisting of protozoan and helminths. Those of greatest concern, shown in Table 1.1 adapted from the WHO (10), are those that are capable of causing severe disease and persist in the environment for a long time and can withstand common disinfection methods, either due to a resistant state such as a spore or vegetative phase for bacteria, the cysts, oocysts and ova of parasites and most viruses. In all cases, infected people and animals shed large numbers of microbes in feces, which can then directly contaminate water supplies through untreated or undertreated sewage or through accidental release. Additionally, the practice of using livestock waste for fertilization can result in contamination of reservoirs and wells via runoff or permeation into the groundwater as well (11). As a result, some countries are considering restrictions on this practice based on pathogenic content modeled after current US EPA rules (12). The use of untreated wastewater for irrigation of crops,

particularly those consumed raw, can also result in exposure to pathogens and infection (13). Contamination of marine environments can result in the bioaccumulation of bacteria, like *Vibrio cholerae* (6), and viruses in shellfish (11, 14). Many of these microbes remain infective for long periods in aqueous environments, allowing them to travel long distances from the initial source (15). In this regard, viruses are of utmost concern. Their longevity permit them to contaminate deep aquifers - water sources long thought to be untouched by microbes and thus, safe and pure (16). As waterborne pathogens travel through the environment they are typically diluted to low, but clinically concerning, concentrations creating a detection challenge.

Indicator organisms

In 1989, the United States Environmental Protection Agency (US EPA) established rules for water quality monitoring, setting benchmarks, limiting the potential risk of infection to no more than 1 in 10,000 per year (17), that have served as a guideline for regulation in other countries (18). The cornerstone of these regulations is the monitoring of total coliform bacteria in source and finished water to assess disinfection efficiency and trigger further testing for specific pathogens (19). Coliform bacteria include bacteria that are typically found in feces, collectively called fecal coliform, such as *Escherichia coli*, *Enterococcus* spp. and *Clostridium perfringens*, and is, therefore, an indicator for fecal contamination, which in turn is an indicator of the potential for pathogenic microbes (20). This method is flawed as significant pathogens persist in water far longer than coliform bacteria, namely enteric viruses, which can be found in low concentrations in samples showing no other sign of fecal

contamination. Due to this, some non-pathogenic viruses have been evaluated as indicators of contamination or to aid in the assessment of disinfection techniques (20, 21). The use of these indicator organisms remains the gold-standard of monitoring and regulation due to the prohibitive cost of testing for multiple, individual pathogens spanning a diverse array of microbe types.

Standard techniques for waterborne pathogen detection

Detection for bacteria, both fecal indicators and pathogens, and viruses are dominated by culture techniques and molecular biology methods. For bacterial detection, standard bacterial cell culture methods are employed and the presence of bacterial growth can be measured via the development of colonies that may be counted, for plated cultures (22, 23). Similarly, the presence of viral pathogens can often be determined via cell culture plaque assays. Here, a sample is added to a monolayer of mammalian cells that is then fixed in agar. The plates are then observed for plaques, regions of dead cells exhibiting cytopathogenic effects (CPE) (24). Culture methods are time consuming, bacteria can take days to grow (25) while some viruses can take several weeks to develop plaques. Some viruses will never form plaques as they are very slow growing, do not produce CPE, or no cell lines have been determined on which they grow (26). More rapid methods for coliform bacteria have been developed, marketed as Colilert® and Colisure®, that rely on chromogenic substrates added to culture media that yield a visible color change as it is cleaved by bacterial enzymes (27).

Immunological methods, such as serum neutralization tests (SNT), immunofluorescence, and Enzyme-Linked Immunosorbent Assays (ELISA) have been used for detection of waterborne pathogens. SNT is used for the serotyping of viruses and calls for mixing a sample, extracted from a plaque assay, with antiserum and then assessing the decrease of infectivity by plaque assay (28). These tests are extremely time consuming as they require two rounds of cell culture. Immunofluorescence assays for viruses allow for a shortening of assay time compared to SNT as it eliminates the second round of cell culture and employs fluorophore-labeled antibodies for detection via microscopy (29) or flow cytometry (30). Assays based on immunofluorescence and immunomagnetic separation (IMS) are the gold standard for the detection of protozoan parasites. The US EPA have established methods 1623 for the combined detection of *Cryptosporidium* spp. and *Giardia* spp. (31), or 1622 for *Cryptosporidium* spp. alone (32), both of which employ IMS followed by immunostaining and fluorescent microscopy. ELISA has been used for the detection of waterborne pathogens (33, 34), but has not been as popular for environmental samples as in clinical analyses (35). Immunological methods suffer from the inability to determine infectivity, as living and dead organisms appear the same, and in addition are very time-consuming.

Since it was first published in 1988, the Polymerase Chain-Reaction (PCR) (36), and modifications like reverse transcriptase PCR (RT-PCR), real-time, quantitative, nested, and multiplex PCR (37-42), have become indispensable tools for the detection and identification of pathogens. Other techniques, such as Nucleic Acid Sequence-

Based Amplification (NASBA), have also been used for assays to detect waterborne pathogens (43-46). When compared to cell culture, molecular techniques are far more appealing due to the shorter time to result, typically no more than a few hours as opposed to days or weeks, as well as increased sensitivity (37). Also, by allowing for the detection of sequences specific to only the pathogen of interest, molecular biological techniques create a level of discrimination unavailable in cell culture. However, particularly with respect to viruses, these methods do not provide information on the infectivity of the pathogen being detected.

Biosensors as novel detection methods

Biosensors are devices or assays that employ a biorecognition element coupled to a signal transducer to detect an analyte of interest (47). Common biorecognition elements include oligonucleotide probes, antibodies, aptamers, cell surface molecules (48), and phages (49). Transduction methodologies can be roughly divided into three primary types: optical, electrochemical and mechanical. Biosensors offer the promise of substantial improvements over the standard methods and have been reported employing the full spectrum of biorecognition molecules and transduction methods for the detection of waterborne pathogens, with oligonucleotide probes and antibodies being the most common.

Criteria for biosensors development

New detection methods for waterborne pathogens must be superior to the current standards in one or more of three key characteristics: sensitivity, specificity, and

speed. Also important, though secondary to these three areas, are reductions in the susceptibility of the method to user error and the portability of the biosensor.

Sensitivity, in most cases, is defined as the ability to detect very few organisms in a sample (rather than the degree of discrimination between various concentration levels). How sensitive an assay must be is dependent on the specific pathogen's ability to cause disease as well as governmental regulations and regulatory goals. For instance, as few as 10 viable *C. parvum* oocysts can cause infection in healthy adults (50) and the US EPA regulatory goal is the complete absence of these oocysts from finished drinking water (17). Therefore, an effective new analytical method must meet this goal and be capable of detecting a single viable oocyst.

New methods can also seek to improve the specificity of detection with respect to discerning one closely related species from another or even viable organisms from dead. Some standard methods are very effective with respect to these two criteria. For example, cell culture methods can be used to detect a single CFU or PFU and inherently provide discrimination with respect to viability status. US EPA method 1622 can easily detect 10 *Cryptosporidium* spp. oocyst (51), but cannot discriminate between pathogenic and non-pathogenic species or viable and dead oocysts without additional analytical steps such as staining. Further, all of these methods fail with respect to the third criterion, providing rapid results.

Novel methods can, do, and will make trade-offs with respect to these key areas as do the standard methods. In developing a new assay these trade-offs are inherent in the selection of the detection methodology, especially between molecular biological and immunological. Molecular biological methods are often sensitive enough to detect a single organism but can sacrifice speed as they require time for the enzymatic amplification of the nucleic acid target and the processing of the sample in order to access the genetic material of the organism. For example, Taniuchi *et al.* reported a multiplex PCR reaction for protozoan parasites using Luminex® beads with limits of detection of 10^2 *Cryptosporidium* spp. oocysts, 10^3 *Giardia lamblia* cysts and 10^1 *Entamoeba histolytica* trophozoites (52). However, the assay includes an extensive DNA purification procedure requiring well over an hour to complete. Immunological assays tend to be faster, as less sample pre-processing is required, but can sacrifice sensitivity. The lower limits of detection of immunoassays range from 10^3 to 10^6 cells, cysts, oocysts or CFU per mL, but can yield results in as little as 10 minutes(53-59). Both methodologies can have high levels of specificity. However, the specificity of antibody-based detection is highly dependent on the availability of quality antibodies whereas nucleic acid amplification requires the ability to identify a unique sequence in the genome of the organism of interest and designing suitable primers and probes.

Obstacles to detection

Environmental samples pose a number of challenges to assay development due to the numerous potential microbial, particulate, and other organic and inorganic contaminants. Also, as previously stated, waterborne pathogens, especially those that

persist for long times, are typically present at low concentrations in environmental samples, itself an obstacle to detection. Taken together, these present a formidable hurdle to overcome; thus, sample pre-treatment that is compatible with the selected method of detection must be considered when comparing the relative merits of two assays and included in the development of a novel method.

The current standard for sample filtration and concentration is commercially-available charged membrane filters through which large volumes of water can be processed and various buffer changes are required for the adsorption and elution of the analyte of interest (33, 42, 60). Microfluidic devices for pre-processing have been developed exploiting similar principles. Balasubramanian *et al.* took advantage of the net surface charge of waterborne microbes in the development of a microfluidic electrostatic trapping device, consisting of a microchannel with electrodes as two of the walls, capable of concentrating *E. coli*, *Salmonella* and *Pseudomonas* with over 99% capture efficiencies (61).

Size-based microfluidic filtration techniques have also been implemented for pre-concentration. Taguchi *et al.* fabricated a stainless steel filter with conical pores integrated into a microfluidic device. Under negative pressure, a sample is pulled through the pores and larger particles are captured and the analyte of interest, here *C. parvum* oocysts, can be visualized and quantified using fluorophore-conjugated antibodies (62). Microfluidic devices using electrokinesis and *in situ* photopolymerized nanoporous membranes have been demonstrated for concentration

of analytes (63) while allowing for removal of smaller competing molecules (64). Similar membranes have been combined into a single microfluidic device with downstream liposome-based detection in an immunoassay for a human norovirus surrogate, yielding an order of magnitude improvement in the analytical sensitivity (65). Implementing a device replicating a macro-scale weir, Zhu *et al.* captured *C. parvum* oocysts or *G. lamblia* cysts where the channel depth dramatically reduces, again allowing for detection via immunofluorescence (66).

Filtration methods are particularly useful when processing large sample volumes – on the scale of liters – and provide the much needed initial purification necessary when handling environmental samples. However, filtration cannot provide the specificity of IMS, which has become an invaluable tool for both concentrating the analyte of interest and purifying the sample solution. The latter is of particular interest as environmental samples often contain organic and inorganic compounds that can act as inhibitors of the enzymes required for molecular amplification techniques (67). As magnetic particles are available in a range of sizes, IMS is also appealing for implementation in micro-total analysis systems. Microfluidic devices employing IMS prior to PCR-based detection have been reported for *E. coli* O157:H7, with a detection limit of 0.2 CFU/ μ L (68) and 10^2 PFU/mL enterovirus 71 (38, 39). Foregoing magnetic beads and directly immobilizing the capture antibodies inside of a microchannel, which can minimize user error, Dharmasiri *et al.* reported a device capable of detecting only 6 CFU *E. coli* O157:H7 (69). The use of IMS and other antibody-capture techniques as a pre-processing step in molecular biology-based

assays very clearly elucidates why immunoassays can be dramatically faster. Figure 1.1 compares the typical process flow for immunoassays and DNA biosensors employing common signal transduction techniques. Detection of nucleic acid sequences requires 2 to 3 additional pre-processing steps after immunoseparation, whereas the introduction of a second, labeled antibody creates the sandwich immunoassay commonly used with various detection platforms (59, 70-73).

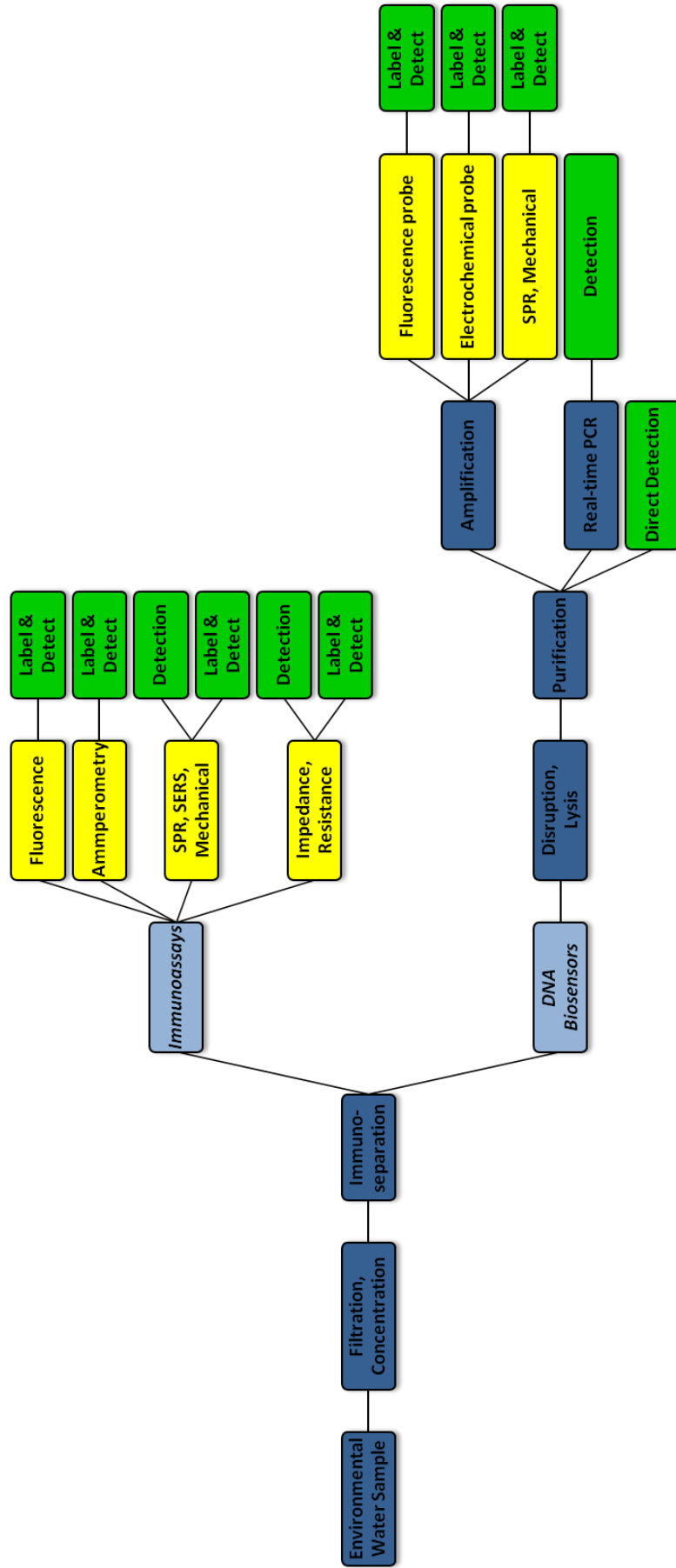


Figure 1.1: Typical Process Flow for Detection of Pathogens in Environmental Water Samples
 Regardless of detection method, water samples must be passed through filtration and concentration steps in order to retain all potential pathogens for analysis and reduce the volume of the sample proceeding through the process. Many assays will then employ and immunoseparation step, such as IMS. Processes diverge at this point, with immunoassays requiring only labeling and/or detection and DNA biosensors calling for more pre-processing and, most often, enzymatic amplification. Processing steps are shown in dark blue, final signal output steps in green with techniques in yellow.

Future improvements for waterborne pathogen immunosensors

Key to the future potential of immunoassays for waterborne pathogens is the increase of the analytical sensitivity to levels more in line with the detection limits required to meet public health and water safety goals. Lower limits paired with the already short time to results would make these biosensors indispensable. To achieve these increases in analytical sensitivity, methods for the amplification of specific signals and reduction of the background noise must be investigated.

Signal amplification employing enzyme-labels, as in traditional ELISAs, is well established in biosensors (53). However, as this amplification is reliant on the enzyme's action on a provided substrate over time, this method is less desirable.

Liposome nanovesicles encapsulating a fluorescent dye, employed as a marker, have been demonstrated to provide substantial, instantaneous signal amplification and high sensitivity compared to single fluorophore labels (74). Biosensor immunoassays using liposomes for the detection of whole *E. coli* O157:H7 have shown the benefit of liposome lysis for increasing the analytical sensitivity; intact liposomes produced a limit of detection of 10^3 CFU/mL (75), while lysed liposomes produced readable signals for 1 CFU/mL (76). As liposomes can encapsulate a range of water soluble molecules, they can be used for signal amplification with other transduction techniques, such as electrochemical detection (77, 78).

Exploring other transduction techniques for a wide range of signal amplification strategies can be chosen. For example, using a portable surface plasmon resonance

(SPR) system, Soelberg *et al.* employed antibody-labeled magnetic beads to produce an 80-fold amplification of the signal in an assay for a microbial enterotoxin (70). Here, as the change in the measured refractive index in SPR biosensors is relative to the size of particles binding to the surface, signal amplification can be produced simply with a large particle. Similarly, the increase in mass provided by gold nanoparticle labels has been used to produce signal amplification leading to four orders-of-magnitude improvement in sensitivity for surface acoustic wave biosensors (79, 80).

An interesting methodology for enhanced sensitivity is the integrating waveguide biosensor. Here, antibodies immobilized on the interior surface of a glass capillary tube and those conjugated to a fluorophore bind the pathogen of interest. Light is incident normal to the capillary for excitation while emitted light couples into the capillary waveguide and is collected by a photomultiplier tube (PMT). In this format, the sensitivity is enhanced as the specific signal increases with the length of the capillary while the background noise remains the same, yielding a two orders-of-magnitude decrease in detection limit compared to fiber optic biosensors (81). Zhu *et al.* showed the integrating waveguide biosensor could detect as few as 10 cells of *E. coli* O157 per capillary (82), corresponding to a concentration of about 10^2 CFU/mL.

The integrating waveguide biosensor elucidates that importance of not only signal amplification but the reduction of background noise. Though in that system the noise simply does not increase, the development of systems that reduce the contribution

noise can reduce detection limits by increasing the signal-to-noise ratio. Biosensors that take advantage of the evanescent wave generated by total internal reflectance of light confined within an optical fiber or waveguide, allows for the specific excitation of fluorophores immobilized on the surface of the fiber and not those in the bulk sample, reducing potential noise. Extensive research on evanescent wave fluoroimmunoassays has been conducted at the US Naval Research Laboratory resulting in the commercialization of the portable RAPTOR system available from Research International. The RAPTOR allows four samples to be analyzed in parallel, with a 10min assay time, and has been used to detect waterborne pathogens at concentrations such as 5×10^4 *G. lamblia* cysts/mL (54), 10^5 *C. parvum* oocyst/mL (55), 10^4 CFU/mL of *E. coli* O157:H7 (57) and 10^3 CFU/mL of *S. enterica* Enteritidis (58) and fecal indicators, like enterococci, in environmental samples at 10^5 CFU/mL (56).

Biosensors employing the signal amplification and noise reducing techniques described can benefit, or have benefited, from the increases in sensitivity commonly achieved with microfluidics or microfabricated sensor elements. As a result of working on a dimensional scale closer to the size of the microbial and viral pathogens found in water, limits of detection nearing single cell may be possible. For example, with devices employing antibody-coated, 200nm diameter polypyrrole nanowires individually suspended between two electrodes to create a field-effect transistor, Shirale *et al.* detected down to 1 PFU/L of an enterovirus surrogate in urban runoff water (83). The binding of virions to the surface of the nanowire produces a

measurable change in increase in resistance as the close proximity of negative moieties of the analyte depletes available charge carriers in the bulk of the wire. This effect is measurable for such a low virus concentration due to the nanoscale dimensions of the sensor (84).

Improvements for DNA-based biosensors

Nucleic acid biosensors already provide the desired sensitivity for detecting waterborne pathogens present at low concentrations, with some reporting single organism limits (52, 85). The primary area to focus improvement efforts necessary for these biosensors is the overall assay time required to realize detection in real samples. Starting with environmental water samples requires, first, the purification and concentration of the pathogen of interest, followed by steps to disrupt the cell membrane, oocyst wall, spore coat, or viral capsid and purify the genetic material prior to amplification and detection. Clearly defined protocols and commercially available kits exist for these tasks, such as Dynal's IMS kits and beads and Qiagen's nucleic acid purification line of products. These pre-processing steps, while necessary, add time. Thus, investigations to shorten, eliminate, or provide alternatives to these methods.

Many pre-processing methods can benefit from miniaturization. Confining a reaction within a micro or nanoscale fluidic channel has great potential to decrease assay time as the smaller volume reduces diffusion limitations (86) as well as simplify assay procedures by stringing multiple operations together into micro Total Analysis

Systems (μ TAS) (87). Microfluidic devices for some sample preparation steps have already been reported, including immunoseparation and pre-concentration as discussed previously, as well as for mRNA isolation (88), PCR (39, 89-94) and isothermal amplification reactions (95).

As is the case with immunosensors, methods that improve the analytical sensitivity are also of interest. However, as PCR-based methods already allow for low limits of detection with respect to numbers of pathogenic organisms, methods that can provide similar limits without amplification should be the primary focus. This promises to reduce both assay time and complexity. Bio-barcode assays, for example, have been used to produce signal amplification as Zhang *et al.* demonstrated in an assay for *S. enterica* Enteritidis. Here, gold nanoparticles coated in a target-specific probe and fluorescein-labeled barcode DNA in a 1:100 ratio were used along with magnetic beads in a sandwich hybridization assay capable of detecting 0.25 fmol of target DNA(96). This is similar to the limits achieved when using the aforementioned liposomal signal amplification in DNA-based sensors(78, 97). However, this is not sensitive enough by itself for detection of unamplified target. Using multiple liposome-tagged probes in a lateral flow assay, Nugen *et al.* selected bacterial 16S rRNA as a potential target as 80% of the total RNA in a cell is rRNA (98). This assay was capable of detecting 135ng of total bacterial RNA without enzymatic amplification in only 20 minutes (99), demonstrating the future promise of liposome-based signal amplification.

Another method that has proven capable of yielding specific signals in assays without enzymatic amplification is up-converting phosphor technology (UPT). Using inorganic microcrystals which emit visible light when excited by an infrared laser, UPT can produce specific signals with very low background due to a lack of autofluorescence (100). With PCR amplification, assays using these reporter molecules were capable of detecting 3 amol of specific target DNA (101). Zuiderwijk *et al.* employed 4 probes, 2 labeled with biotin for capture of the desired target and 2 labeled with digoxigenin, and UPT-reporter molecules labeled with an anti-digoxigen antibody (102). With the assistance of the multiple probes, this assay was capable of detecting 1ng of genomic DNA, or approximately 10^6 bacterial cells.

Conclusion

Waterborne pathogens represent a critical, global health problem and methods that can rapidly, sensitively, and specifically detect their presence in accordance with water safety regulations and clinically significant levels are imperative for the improvement of the health and quality of life for millions of people. While DNA biosensors have proven effective at detecting low concentrations, they typically require time consuming purification processes upstream. Immunosensors require relatively fewer sample processing steps, thus less time. Through various signal amplification and background noise reduction techniques, coupled with the improvements in sensitivity promised by miniaturization, antibody-based detection methods have great potential for rapid, sensitive analysis of all forms of waterborne pathogens.

Current and future research efforts need to be focused on the detection of pathogens from their actual environmental matrix and on the needed pre-processing steps. This includes miniaturization strategies, materials research, and an emphasis on multiplexing so that ideally all relevant pathogens for a specific scenario can be detected at once. Taken together, this will produce novel methods capable of providing the necessary sensitivity, specificity and speed to replace the current standards and, hopefully, improve access to safe drinking water and decrease the global health burden of waterborne disease.

REFERENCES

1. Miagostovich MP, Ferreira FFM, Guimaraes FR, Fumian TM, Diniz-Mendes L, Luz SLB, et al. Molecular detection and characterization of gastroenteritis viruses occurring naturally in the stream waters of Manaus, central Amazonia, Brazil. *Applied and Environmental Microbiology* 2008;74:375.
2. World Health Organization. Facts and Figures on Water Quality and Health. http://www.who.int/water_sanitation_health/facts_figures/en/index.html (Accessed March 25 2011).
3. UNICEF. Water, Sanitation and Hygiene. http://www.unicef.org/wash/index_3951.html (Accessed March 25 2011).
4. Colford JM, Roy SL, Beach MJ, Hightower A, Shaw SE, Wade TJ. A review of household drinking water intervention trials and an approach to the estimation of endemic waterborne gastroenteritis in the United States. *Journal of Water and Health* 2006;4:71-88.
5. Messner M, Shaw S, Regli S, Rotert K, Blank V, Soller J. An approach for developing a national estimate of waterborne disease due to drinking water and a national estimate model application. *Journal of Water and Health* 2006;4:201-40.
6. Philip RB. *Ecosystems and Human Health: Toxicology and Environmental Hazards*. 2nd ed. Boca Raton, FL: Lewis Publishers, 2001:328pp.
7. Wilkinson SL. Eating Healthy in a Dirty World. *Chemical & Engineering News* 1997;75:24-33.
8. Cox P, Hawkins P, Warnecke M, Ferguson C, Deere D, Bustamante H, et al. The Risk of *Cryptosporidium* to Sydney's Drinking Water Supply. In: Thompson RCA, Armson A, Ryan UM, eds. *Cryptosporidium: From Molecules to Disease*, Vol. First ed. ed. Amsterdam, the Netherlands: Elsevier B.V., 2003:325-40.
9. Koopmans M, Duizer E. Foodborne viruses: an emerging problem. *International Journal of Food Microbiology* 2004;90:23-41.

10. World Health Organization. Guidelines for drinking-water quality. Vol. 1. 3rd ed. Geneva: World Health Organization, 2008.
11. Bosch A. Human enteric viruses in the water environment: a minireview. *International Microbiology* 1998;1:191-6.
12. US Environmental Protection Agency. Standards for the use and disposal of sewage sludge; final rule. *Federal Register* 1993;58:9248-415.
13. Hamilton AJ, Stagnitti F, Premier R, Boland A-M, Hale G. Quantitative Microbial Risk Assessment Models for Consumption of Raw Vegetables Irrigated with Reclaimed Water. *Appl Environ Microbiol* 2006;72:3284-90.
14. Le Guyader FS, Atmar RL. Viruses in Shellfish. In: Bosch A, ed. *Human Viruses in Water*, Vol. 17. Amsterdam, The Netherland: Elsevier, 2007:205-26.
15. Fong T-T, Lipp EK. Enteric Viruses of Humans and Animals in Aquatic Environments: Health Risks, Detection, and Potential Water Quality Assessment Tools. *Microbiol Mol Biol Rev* 2005;69:357-71.
16. Borchardt MA, Bradbury KR, Gotkowitz MB, Cherry JA, Parker BL. Human Enteric Viruses in Groundwater from a Confined Bedrock Aquifer. *Environ Sci Technol* 2007;41:6606-12.
17. US Environmental Protection Agency. National primary drinking water regulations; maximum contaminant level goals for microbial contaminants. *Federal Register* 1989;54:27527.
18. Grabow WOK. Overview of Health-Related Water Virology. In: Bosch A, ed. *Human Viruses in Water*, Vol. 17. Amsterdam, the Netherlands: Elsevier B.V., 2007:1-25.
19. US Environmental Protection Agency. National primary drinking water regulations; total coliforms (including fecal coliforms and *E. coli*); final rule. *Federal Register* 1989;54:27544-68.

20. Jofre J. Indicators of Waterborne Enteric Viruses. In: Bosch A, ed. Human Viruses in Water, Vol. 17. Amsterdam, The Netherlands: Elsevier, 2007:227-49.
21. Tree JA, Adams MR, Lees DN. Disinfection of feline calicivirus (a surrogate for Norovirus) in wastewaters. *Journal of Applied Microbiology* 2005;98:155-62.
22. Office of Water. Method 1604: Total Coliforms and *Escherichia coli* in Water by Membrane Filtration Using a Simultaneous Detection Technique (MI Medium). US Environmental Protection Agency, 2002.
23. American Public Health Association, American Water Works Association, Water Environment Federation. Standard methods for the examination of water and wastewater. 21 ed. Washington, DC: American Public Health Association, 2005.
24. Block JC, Schwartzbrod L. Viruses in water systems : detection and identification. New York, N.Y.; Weinheim, Federal Republic of Germany: VCH Publishers ; VCH Verlagsgesellschaft, 1989.
25. de Boer E, Beumer RR. Methodology for detection and typing of foodborne microorganisms. *International Journal of Food Microbiology* 1999;50:119-30.
26. Wyn-Jones P. The Detection of Waterborne Viruses. In: Bosch A, ed. Human Viruses in Water, Vol. 17. Amsterdam, The Netherlands: Elsevier, 2007:177-204.
27. Straub TM, Chandler DP. Towards a unified system for detecting waterborne pathogens. *Journal of Microbiological Methods* 2003;53:185-97.
28. Hsiung GD, Fong CKY, Landry ML. Hsiung's diagnostic virology. 4 ed. New Haven: Yale University Press, 1994.
29. Rigonan AS, Mann L, Chonmaitree T. Use of Monoclonal Antibodies To Identify Serotypes of Enterovirus Isolates. *J Clin Microbiol* 1998;36:1877-81.

30. Barardi CRM, Emslie KR, Vesey G, Williams KL. Development of a rapid and sensitive quantitative assay for rotavirus based on flow cytometry. *Journal of Virological Methods* 1998;74:31-8.
31. Office of Water. Method 1623: *Cryptosporidium* and *Giardia* in Water by Filtration/IMS/FA. US Environmental Protection Agency, 2001.
32. Office of Water. Method 1622: *Cryptosporidium* in Water by Filtration/IMS/FA. US Environmental Protection Agency, 2001.
33. Kittigul L, Khamoun P, Sujirarat D, Utrarachkij F, Chitpirom K, Chaichantanakit N, Vathanophas K. An improved method for concentrating rotavirus from water samples. *Memórias do Instituto Oswaldo Cruz* 2001;96:815-21.
34. Tajima T, Takeda Y, Tohya Y, Sugii S. Reactivities of Feline Calicivirus Field Isolates with Monoclonal Antibodies Detected by Enzyme-Linked Immunosorbent Assay. *The Journal of Veterinary Medical Science* 1998;60:753-5.
35. Wyn-Jones AP, Sellwood J. Enteric viruses in the aquatic environment. *Journal of Applied Microbiology* 2001;91:945-62.
36. Saiki RK, Gelfand DH, Stoffel S, Scharf SJ, Higuchi R, Horn GT, et al. Primer-directed enzymatic amplification of DNA with a thermostable DNA polymerase. *Science* 1988;239:487-91.
37. Kopecka H, Dubrou S, Prevot J, Marechal J, Lopez-Pila JM. Detection of naturally occurring enteroviruses in waters by reverse transcription, polymerase chain reaction, and hybridization. *Appl Environ Microbiol* 1993;59:1213-9.
38. Lien K-Y, Lee W-C, Lei H-Y, Lee G-B. Integrated reverse transcription polymerase chain reaction systems for virus detection. *Biosensors and Bioelectronics* 2007;22:1739-48.
39. Lee W-C, Lien K-Y, Lee G-B, Lei H-Y. An integrated microfluidic system using magnetic beads for virus detection. *Diagnostic Microbiology and Infectious Disease* 2008;60:51-8.

40. Li Y, Zhang C, Xing D. Fast identification of foodborne pathogenic viruses using continuous-flow reverse transcription-PCR with fluorescence detection. *Microfluidics and Nanofluidics* 2011;10:367-80.
41. Kovac K, Gutiérrez-Aguirre I, Banjac M, Peterka M, Poljsak-Prijatelj M, Ravnikar M, et al. A novel method for concentrating hepatitis A virus and caliciviruses from bottled water. *Journal of Virological Methods* 2009;162:272-5.
42. Kittigul L, Ekchaloemkiet S, Utrarachkij F, Siripanichgon K, Sujirarat D, Pungchitton S, Boonthum A. An efficient virus concentration method and RT-nested PCR for detection of rotaviruses in environmental water samples. *Journal of Virological Methods* 2005;124:117-22.
43. Rutjes SA, van den Berg HHJL, Lodder WJ, de Roda Husman AM. Real-Time Detection of Noroviruses in Surface Water by Use of a Broadly Reactive Nucleic Acid Sequence-Based Amplification Assay. *Appl Environ Microbiol* 2006;72:5349-58.
44. Lamhoujeb S, Fliss I, Ngazoa SE, Jean J. Evaluation of the Persistence of Infectious Human Noroviruses on Food Surfaces by Using Real-Time Nucleic Acid Sequence-Based Amplification. *Appl Environ Microbiol* 2008;74:3349-55.
45. Baeumner AJ, Cohen RN, Miksic V, Min JH. RNA Biosensor for the Rapid Detection of Viable *Escherichia coli* in Drinking Water. *Biosensors & Bioelectronics* 2003;18:405 – 13.
46. Baeumner AJ, Humiston M, Montagna RA, Durst RA. Detection of Viable Oocysts of *Cryptosporidium parvum* Following Nucleic Acid Sequence Based Amplification. *Analytical Chemistry* 2001;73:1176-80.
47. Turner APF, Karube I, Wilson GS. *Biosensors: fundamentals and applications*: Oxford University Press, USA, 1987.
48. Rider TH, Petrovick MS, Nargi FE, Harper JD, Schwoebel ED, Mathews RH, et al. A B cell-based sensor for rapid identification of pathogens. *Science* 2003;301:213.

49. Arya SK, Singh A, Naidoo R, Wu P, McDermott MT, Evoy S. Chemically immobilized T4-bacteriophage for specific *Escherichia coli* detection using surface plasmon resonance. *Analyst* 2011;136:486-92.
50. Chappell CL, Okhuysen PC, Sterling CR, DuPont HL. *Cryptosporidium parvum*: Intensity of infection and oocyst excretion patterns in healthy volunteers. *Journal of Infectious Diseases* 1996;173:232-6.
51. McCuin RM, Clancy JL. Modifications to United States Environmental Protection Agency Methods 1622 and 1623 for Detection of *Cryptosporidium* Oocysts and *Giardia* Cysts in Water. *Appl Environ Microbiol* 2003;69:267-74.
52. Taniuchi M, Verweij JJ, Noor Z, Sobuz SU, Lieshout Lv, Petri WA, Jr., et al. High Throughput Multiplex PCR and Probe-based Detection with Luminex Beads for Seven Intestinal Parasites. *Am J Trop Med Hyg* 2011;84:332-7.
53. Wolter A, Niessner R, Seidel M. Detection of *Escherichia coli* O157: H7, *Salmonella typhimurium*, and *Legionella pneumophila* in water using a flow-through chemiluminescence microarray readout system. *Analytical Chemistry* 2008;80:5854-63.
54. Anderson GP, Rowe-Taitt CA. Water quality monitoring using an automated portable fiber optic biosensor: RAPTOR. *Photonic Detection and Intervention Technologies for Safe Food*, Vol. 4206. 1 ed. Boston, MA, USA: SPIE, 2001:58-63.
55. Kramer MF, Vesey G, Look NL, Herbert BR, Simpson-Stroot JM, Lim DV. Development of a *Cryptosporidium* oocyst assay using an automated fiber optic-based biosensor. *Journal of biological engineering* 2007;1:3.
56. Leskinen SD, Lim DV. Rapid Ultrafiltration Concentration and Biosensor Detection of Enterococci from Large Volumes of Florida Recreational Water. *Appl Environ Microbiol* 2008;74:4792-8.
57. Lim DV. Detection of microorganisms and toxins with evanescent wave fiber-optic biosensors. *Proceedings of the IEEE* 2003;91:902-7.

58. Valadez AM, Lana CA, Tu SI, Morgan MT, Bhunia AK. Evanescent wave fiber optic biosensor for *Salmonella* detection in food. *Sensors* 2009;9:5810-24.
59. Kang CD, Lee SW, Park TH, Sim SJ. Performance enhancement of real-time detection of protozoan parasite, *Cryptosporidium* oocyst by a modified surface plasmon resonance (SPR) biosensor. *Enzyme and Microbial Technology* 2006;39:387-90.
60. Katayama H, Shimasaki A, Ohgaki S. Development of a Virus Concentration Method and Its Application to Detection of Enterovirus and Norwalk Virus from Coastal Seawater. *Appl Environ Microbiol* 2002;68:1033-9.
61. Balasubramanian AK, Soni KA, Beskok A, Pillai SD. A microfluidic device for continuous capture and concentration of microorganisms from potable water. *Lab on a Chip* 2007;7:1315-21.
62. Taguchi T, Arakaki A, Takeyama H, Haraguchi S, Yoshino M, Kaneko M, et al. Detection of *Cryptosporidium parvum* oocysts using a microfluidic device equipped with the SUS micromesh and FITC-labeled antibody. *Biotechnology and Bioengineering* 2007;96:272-80.
63. Song S, Singh AK, Kirby BJ. Electrophoretic Concentration of Proteins at Laser-Patterned Nanoporous Membranes in Microchips. *Anal Chem* 2004;76:4589-92.
64. Song S, Singh AK, Shepodd TJ, Kirby BJ. Microchip Dialysis of Proteins Using in Situ Photopatterned Nanoporous Polymer Membranes. *Anal Chem* 2004;76:2367-73.
65. Connelly JT, Kondapalli S, Parker JSL, Kirby BJ, Baeumner AJ. Micro-total analysis system for virus detection: Microfluidic pre-concentration coupled to liposome-based detection. *Anal Bioanal Chem* 2011;(submitted).
66. Zhu L, Zhang Q, Feng H, Ang S, Chau FS, Liu W-T. Filter-based microfluidic device as a platform for immunofluorescent assay of microbial cells. *Lab on a Chip* 2004;4:337-41.

67. Fout GS, Martinson BC, Moyer MWN, Dahling DR. A Multiplex Reverse Transcription-PCR Method for Detection of Human Enteric Viruses in Groundwater. *Appl Environ Microbiol* 2003;69:3158-64.
68. Beyor N, Yi L, Seo TS, Mathies RA. Integrated Capture, Concentration, Polymerase Chain Reaction, and Capillary Electrophoretic Analysis of Pathogens on a Chip. *Analytical Chemistry* 2009;81:3523-8.
69. Dharmasiri U, Witek MgA, Adams AA, Osiri JK, Hupert ML, Bianchi TS, et al. Enrichment and Detection of *Escherichia coli* O157:H7 from Water Samples Using an Antibody Modified Microfluidic Chip. *Analytical Chemistry* 2010;82:2844-9.
70. Soelberg SD, Stevens RC, Limaye AP, Furlong CE. Surface Plasmon Resonance Detection Using Antibody-Linked Magnetic Nanoparticles for Analyte Capture, Purification, Concentration, and Signal Amplification. *Analytical Chemistry* 2009;81:2357-63.
71. Porter MD, Driskell JD, Kwarta KM, Lipert RJ, Neill JD, Ridpath JF. Detection of Viruses: Atomic Force Microscopy and Surface Enhanced Raman Spectroscopy. *Developments in Biologicals* 2006;126:31-9.
72. Porter MD, Lipert RJ, Siperko LM, Wang G, Narayanan R. SERS as a bioassay platform: fundamentals, design, and applications. *Chem Soc Rev* 2008;37:1001-11.
73. Settingington EB, Alocilja EC. Rapid electrochemical detection of polyaniline-labeled *Escherichia coli* O157:H7. *Biosensors and Bioelectronics* 2011;26:2208-14.
74. Edwards KA, Baeumner AJ. Liposomes in Analyses. *Talanta* 2006;68:1421-31.
75. Kim M, Oh S, Durst RA. Detection of *Escherichia coli* O157:H7 Using Combined Procedure of Immunomagnetic Separation and Test Strip Liposome Immunoassay. *Journal of Microbiology and Biotechnology* 2003;13:509-16.
76. DeCory T, Durst RA, Zimmerman S, Garringer L, Paluca G, DeCory H, Montagna RA. Development of an Immunomagnetic Bead-Immunoliposome

Fluorescence Assay for Rapid Detection of *Escherichia coli* O157:H7 in Aqueous Samples and Comparison of the Assay with Standard Microbiology Method. *Applied and Environmental Microbiology* 2005;71:1856-64.

77. Bunyakul N, Edwards K, Promptmas C, Baeumner A. Cholera toxin subunit B detection in microfluidic devices. *Analytical and Bioanalytical Chemistry* 2008.
78. Goral VN, Zaytseva NV, Baeumner AJ. Electrochemical microfluidic biosensor for the detection of nucleic acid sequences. *Lab on a Chip* 2006;6:414-21.
79. Cai J, Yao C, Xia J, Wang J, Chen M, Huang J, et al. Rapid parallelized and quantitative analysis of five pathogenic bacteria by ITS hybridization using QCM biosensor. *Sensors and Actuators B: Chemical* 2011;In Press, Corrected Proof.
80. Deisingh AK, Thompson M. Sequences of *E. coli* O157:H7 detected by a PCR-acoustic wave sensor combination. *Analyst* 2001;126:2153-8.
81. Ligler FS, Breimer M, Golden JP, Nivens DA, Dodson JP, Green TM, et al. Integrating Waveguide Biosensor. *Analytical Chemistry* 2001;74:713-9.
82. Zhu P, Shelton DR, Karns JS, Sundaram A, Li S, Amstutz P, Tang C-M. Detection of water-borne *E. coli* O157 using the integrating waveguide biosensor. *Biosensors and Bioelectronics* 2005;21:678-83.
83. Shirale DJ, Bangar MA, Park M, Yates MV, Chen W, Myung NV, Mulchandani A. Label-Free Chemiresistive Immunosensors for Viruses. *Environmental Science & Technology* 2010;44:9030-5.
84. Cui Y, Wei Q, Park H, Lieber CM. Nanowire Nanosensors for Highly Sensitive and Selective Detection of Biological and Chemical Species. *Science* 2001;293:1289-92.
85. Connelly J, Nugen S, Borejsza-Wysocki W, Durst R, Montagna R, Baeumner A. Human pathogenic *Cryptosporidium* species bioanalytical detection method with single oocyst detection capability. *Analytical and Bioanalytical Chemistry* 2008;391:487-95.

86. Heyries KA, Loughran MG, Hoffmann D, Homsy A, Blum LJ, Marquette CA. Microfluidic biochip for chemiluminescent detection of allergen-specific antibodies. *Biosensors and Bioelectronics* 2008;23:1812-8.
87. Reyes DR, Iossifidis D, Auroux PA, Manz A. Micro total analysis systems. 1. Introduction, theory, and technology. *Analytical Chemistry* 2002;74:2623-36.
88. Nugen SR, Asiello PJ, Baeumner AJ. Design and fabrication of a microfluidic device for near-single cell mRNA isolation using a copper hot embossing master. *Microsystem Technologies* 2009;15:477-83.
89. Kopp MU, Mello AJ, Manz A. Chemical amplification: continuous-flow PCR on a chip. *Science* 1998;280:1046.
90. Hashimoto M, Chen P-C, Mitchell MW, Nikitopoulos DE, Soper SA, Murphy MC. Rapid PCR in a continuous flow device. *Lab on a Chip* 2004;4:638-45.
91. Zhang C, Xing D. Miniaturized PCR chips for nucleic acid amplification and analysis: latest advances and future trends. *Nucleic Acids Research* 2007;35:4223-37.
92. Zhang C, Xu J, Ma W, Zheng W. PCR microfluidic devices for DNA amplification. *Biotechnology Advances* 2006;24:243-84.
93. Sun K, Yamaguchi A, Ishida Y, Matsuo S, Misawa H. A heater-integrated transparent microchannel chip for continuous-flow PCR. *Sensors and Actuators B: Chemical* 2002;84:283-9.
94. Obeid PJ, Christopoulos TK, Crabtree HJ, Backhouse CJ. Microfabricated Device for DNA and RNA Amplification by Continuous-Flow Polymerase Chain Reaction and Reverse Transcription-Polymerase Chain Reaction with Cycle Number Selection. *Analytical Chemistry* 2002;75:288-95.
95. Asiello PJ, Baeumner AJ. Miniaturized isothermal nucleic acid amplification, a review. *Lab on a Chip* 2011.

96. Zhang D, Carr DJ, Alocilja EC. Fluorescent bio-barcode DNA assay for the detection of *Salmonella enterica* serovar Enteritidis. *Biosensors and Bioelectronics* 2009;24:1377-81.
97. Zaytseva NV, Montagna RA, Baeumner AJ. Microfluidic biosensor for the serotype-specific detection of Dengue virus. *Anal Chem* 2005;77:7520-7.
98. Brown TA. *Genomes 3*. New York: Garland Science Pub., 2007.
99. Nugen SR, Leonard B, Baeumner AJ. Application of a unique server-based oligonucleotide probe selection tool toward a novel biosensor for the detection of *Streptococcus pyogenes*. *Biosensors and Bioelectronics* 2007;22:2442-8.
100. Zijlmans HJMAA, Bonnet J, Burton J, Kardos K, Vail T, Niedbala RS, Tanke HJ. Detection of cell and tissue surface antigens using up-converting phosphors: a new reporter technology. *Anal Biochem* 1999;267:30-6.
101. Corstjens P, Zuiderwijk M, Brink A, Li S, Feindt H, Niedbala RS, Tanke HJ. Use of up-converting phosphor reporters in lateral-flow assays to detect specific nucleic acid sequences: a rapid, sensitive DNA test to identify human papilloma-virus type 16 infection. *Clin Chem* 2001;47.
102. Zuiderwijk M, Tanke HJ, Niedbala RS, Corstjens PLAM. An amplification-free hybridization-based DNA assay to detect *Streptococcus pneumoniae* utilizing the up-converting phosphor technology. *Clinical Biochemistry* 2003;36:401-3.

CHAPTER 2

HUMAN PATHOGENIC *CRYPTOSPORIDIUM* SPECIES BIOANALYTICAL DETECTION SYSTEM WITH SINGLE OOCYST LIMIT OF DETECTION

Abstract

A bioanalytical detection method for specific detection of viable human pathogenic *Cryptosporidium* species, *C. parvum*, *C. hominis*, and *C. meleagridis* is described. Oocysts were isolated from water samples via immunomagnetic separation, and mRNA was extracted with oligo-dT magnetic beads, amplified using nucleic acid sequence-based amplification (NASBA), and then detected in a nucleic acid hybridization lateral flow assay. The amplified target sequence employed was a portion of the *hsp70* mRNA specific to the pathogenic species, production of which is stimulated via a brief heat shock. The described method was capable of detecting one oocyst in 10 μ L using flow-cytometer-counted samples. Only viable oocysts were detected, as confirmed using 4',6-diamidino-2-phenylindole and propidium iodide (DAPI/PI) staining. The detection system was challenged by detecting oocysts in the presence of large numbers of common waterborne microorganisms and packed pellet material filtered from environmental water samples. When the method was compared with EPA Method 1622 for *C. parvum* detection, highly comparable results were obtained. Since the described detection system yields unambiguous results within 4.5 h, it is an ideal method for monitoring the safety of drinking water.

Introduction

Cryptosporidium is a waterborne protozoan parasite, several species of which can cause cryptosporidiosis, an intestinal disease in humans and domestic mammals. In immunocompromised or immunosuppressed patients cryptosporidiosis can be fatal. Three species are known to cause infection in humans; *C. parvum*, *C. hominis* and *C. meleagridis* have all been implicated as the causative agents in the infection of humans, regardless of immunological status (1, 2). Outbreaks of cryptosporidiosis have occurred on a worldwide basis from various contaminated sources, with the largest outbreak occurring in 1993 in Milwaukee, Wisconsin with over 400,000 people infected and over 100 deaths after contamination of the municipal water supply (3). More recently, in August 2005, about 4,000 people were infected with *Cryptosporidium* at the Seneca Lake State Park in Geneva, New York, after chlorinated recreational water became contaminated. An estimated 300,000 cases of cryptosporidiosis occur each year in the United States resulting in approximately 66 deaths (4). Most commonly used water treatment methods, i.e. chlorination, are ineffective in the prevention of transmission of *Cryptosporidium* as part of the parasite's life cycle is a resilient oocyst phase. Although the number of oocysts often found in contaminated water is generally very low, a volunteer study showed that 10 oocysts could cause illness in healthy people (5) and the FDA suggests that as few as one oocyst could cause infection. Therefore, a sensitive diagnostic method is necessary for effective detection.

Detection of *Cryptosporidium* in public water treatment systems relies on the EPA-approved Method 1622 (6). This method requires filtration and immunomagnetic separation of oocysts from the resuspended captured material. Captured oocysts are then stained using fluorescein-isothiocyanate conjugated anti-*Cryptosporidium* species monoclonal antibody as well as a nucleic acid stain to determine oocyst concentrations via fluorescence microscopy. This method, however, is unable to discriminate between species pathogenic or nonpathogenic to humans. Furthermore, Method 1622 can not distinguish between viable and, therefore, pathogenic oocysts and non-viable, non-pathogenic oocysts. These shortcomings can lead to false positive results. Additional staining methods need to be applied in order to obtain additional information on the viability of the oocysts. Alternatively, excystation of the oocysts or infectivity assays can be performed, but they require additional expertise, are extremely time consuming and labor intensive. Thus they are not suitable for routine water analysis (7, 8).

As only viable oocysts can cause infection, detection of only these oocysts is desirable. Messenger RNA (mRNA) is a short-lived and often inducible molecule and is optimal for distinguishing viable from non-viable organisms. In this study, a mRNA for a heat shock protein, *hsp70*, common to *C. parvum*, *C. hominis*, and *C. meleagridis* was chosen as the target sequence (9). As an mRNA for a heat shock protein, this molecule will be produced in large amounts when the oocysts are subjected to elevated temperatures; we will show this mRNA is only produced in viable organisms.

Lateral flow sandwich assays using dye-encapsulating liposomes as a signal amplification system have been well established. Previously, nucleic acid hybridization-based sandwich assays using liposome technology have been reported for the detection of pathogenic organisms including *B. anthracis* (10), Dengue virus (11), and *E. coli* (12). These assays are inexpensive, rapid, specific, and simple to run.

Previously, we have reported the detection of *C. parvum* via its *hsp70* mRNA using an electrochemiluminescence assay that demonstrated the specificity and potential for the development of a much simpler *C. parvum* assay system. Since then, we have also reported the use of a competitive liposome-lateral flow assay that was not as sensitive as other LFAs for other nucleic acid sequences using sandwich hybridization (13). Fritsch and colleagues have reported the detection of *C. parvum* via the same RNA using an electrochemical micro-vessel sensor (14). In the present work, we have integrated immunomagnetic separation directly into the assay and optimized the *C. parvum* detection using oligo-dT mRNA isolation. We have proven the extreme sensitivity of the assay using flow-cytometer counted samples of *C. parvum* and have proven that the assay can detect all human-pathogenic *Cryptosporidium* species. Finally, we compared the detection system with EPA Method 1622.

Materials & Methods

Several kits were used in this study, including the Dynabeads® mRNA DIRECT Micro Kit and the Dynabeads® anti-*Cryptosporidium* Kit from Dynal Biotech, a division of Invitrogen Corporation (Frederick, MD). Also used was the NucliSens®

Basic Kit amplification reagents to perform the NASBA from bioMérieux, Inc (Durham, NC). All phospholipids and cholesterol were obtained from Avanti Polar Lipids, Inc. (Alabaster, AL), streptavidin, sulforhodamine B (SRB) were purchased from Invitrogen Corporation. Polyethersulfone test strip material was purchased from Pall Corporation (Port Washington, NY) and nitrocellulose test strip material was obtained from Hanomy, LLC (Cheshire, CT). All oligonucleotides were ordered from Operon Biotechnologies (Huntsville, AL). Crypt-a-Glo™ FITC-labeled antibody was purchased from Waterborne, Inc. (New Orleans, LA).

Stock solutions of *C. parvum* oocysts used in this study were provided by Clancy Environmental Consultants, Inc. (St. Albans, VT) and were from the Iowa isolate maintained at Waterborne, Inc. All samples of oocysts counted by flow cytometry were provided by the Wisconsin State Laboratory of Hygiene (Madison, WI). *C. hominis* oocysts were provided by Dr. Giovanni Widmer and *C. meleagridis* oocysts were provided by Dr. Sal Tzipori, both of the Tufts University School of Veterinary Medicine (North Grafton, MA). *C. muris* oocysts were also obtained from Waterborne, Inc., via Clancy Environmental Consultants, Inc. Both samples of *Giardia intestinalis* and *Oocystis minuta* were provided by Clancy Environmental Consultants, Inc. as well as all packed pellet material from environmental water samples. *Escherichia coli* O157:H7 was purchased from ATCC, number 43888.

Immunomagnetic Separation (IMS)

Some alterations were made to the use of the Dynabeads® anti-*Cryptosporidium* Kit, in that recommended volumes were halved. Thus, 5 mL sample volumes were used and 500 µL each of SL™-A and SL™-B buffers were added. Fifty microliters of anti-*Cryptosporidium* IMS beads were added to each tube and incubated for 90 minutes at room temperature under constant rotation. Each tube was then placed in a magnetic particle concentrator (MPC) for two minutes and the supernatant aspirated. The bead-oocyst complex was resuspended in 500 µL 1X SL™-A buffer and transferred to a sterile nuclease-free 1.5 mL Eppendorf tube. The tubes were allowed to stand in the MPC with the magnet in place for two minutes. The supernatant was aspirated from each tube and the magnet removed. Samples being processed through the Dynabeads mRNA DIRECT Micro Kit were then resuspended in 100 µL nuclease-free water.

Heat Shock, Lysis, and mRNA Isolation

One-hundred microliter oocyst samples were heat shocked at 42°C for 20 minutes. The oocysts were then lysed by a freeze thaw process (15) consisting of five cycles of freezing in an ethanol/dry ice bath and thawing in a 65°C water bath, with each treatment lasting for one minute.

The samples were processed using the Dynabeads® mRNA DIRECT Micro Kit for isolation of mRNA using oligo-d(T)₂₅ superparamagnetic beads as per the manufacturer's directions. Briefly, the samples were mixed with 100 µL of a Lysis/Binding Buffer, containing 100 mM Tris-HCl pH 7.5, 500 mM LiCl, 10 mM

EDTA pH 8.0, 1% lithium dodecyl sulfate (LiDS) and 5 mM dithiothreitol prior to lysis and mixed with 20 μ L of an oligo-d(T)₂₅ bead solution by pipetting. The solution was gently shaken, to prevent settling, at 23°C for five minutes before being placed on a magnetic stand and supernatant aspirated. The beads were then washed by twice adding and aspirating 100 μ L of Wash Buffer A, containing 10 mM Tris-HCl pH 7.5, 0.15 M LiCl, 1 mM EDTA, 0.1% LiDS, and twice adding and aspirating 100 μ L Wash Buffer B, containing 10 mM Tris-HCl pH 7.5, 0.15 M LiCl, 1 mM EDTA. Finally the beads were resuspended in 5 μ L of nuclease-free water.

NASBA Procedure

NASBA was conducted using the NucliSens® Basic Kit amplification reagents as per the manufacturer's instructions in a final volume of 20 μ L. Briefly, 10 μ L of the Reagent Mix, including 2 pmol per reaction of each of the primers shown in *Table 2.1*, were added to the 5 μ L samples containing the resuspended oligo-d(T)₂₅ beads and incubated at 65°C for five minutes and then at 41°C for five minutes. Five microliters of the Enzyme Mix was then added and the samples were returned to the 41°C heat block for five minutes. Samples were then transferred to a 41°C water bath for a 90 minute incubation. The primers used in these experiments have previously shown to be extremely sensitive and specific for the detection of *C. parvum* (9).

Table 2.1: NASBA Primers

Component	5'→ 3'	Concentration
Primer 1	aat tct aat acg act cac tat agg gag aag gta gaa cca cca acc aat aca	2.0 pmol/assay
Primer 2	aga ttc gaa gaa ctc tgc gct ga	2.0 pmol/assay

Lateral Flow Assay

One microliter of NASBA product was aspirated from the sample, still containing the oligo-d(T)₂₅ beads, and mixed with 2 μ L of liposomes tagged with the reporter probe shown in *Table 2.2*, prepared as previously reported (16), and 5 μ L of hybridization buffer, containing 20% formamide, 4X SSC, 0.2% Ficoll type 400 and 0.125 M sucrose, and allowed to incubate at 41°C for 20 minutes. A lateral flow test strip with the capture probe (*Table 2.2*) immobilized was inserted into the tube and after the mixture migrated into the test strip an additional 35 μ L of the running buffer was added to complete the assay. Signals were then read at the capture zone and a background reading was taken just below this zone using an ESECO handheld Biosmart Reflectometer BR-10, $\lambda = 560$ nm (Cushing, OK). Capture and background readings were subtracted to yield the final signals. The probes used in this assay have previously shown to provide sensitive and specific detection of *C. parvum* (9). Test strips were prepared as previously described using a Camag Linomat IV for consistent application of the streptavidin-capture probe solution (11, 17), with 60 pmol of biotinylated capture probe and 20 pmol of streptavidin immobilized on each test strip. A positive signal is defined as a reflectometer reading at the capture zone that is more than 5 above the background reading, with any sample yielding a difference less than this considered to be negative.

Table 2.2: Probes for Detection

Probe	5' → 3'
Reporter	gtg caa ctt tag ctc cag tt –cholesterol
Capture	biotin-aga ttc gaa gaa ctc tgc gc

Verification of Viability Detection with DAPI/PI Staining

A stock sample containing 5.9×10^4 oocysts of *C. parvum* per 100 μL was split to provide 4 aliquots of 1 mL each in screw-top, gasket-sealed microcentrifuge tubes. Of these aliquots, 2 were placed in boiling water for a total of 15 minutes, removed every 5 minutes to vortex. All 4 samples were then allowed to rest at room temperature for 72 hours to allow any *hsp70* mRNA produced at the early stages of boiling to degrade.

One boiled sample and one control sample were centrifuged at 12,000 rpm for 1 minute in a microcentrifuge and the supernatant was aspirated, leaving the pellet and less than 50 μL of the supernatant. One milliliter of acidified Hanks' Balanced Salt Solution (HBSS), pH 2.75, was added to the samples and they were allowed to incubate at 37°C for 1 hour. The samples were centrifuged as before, the supernatant removed and 1 mL of normal HBSS added to resuspend the pellet. This wash step was then repeated and the sample was centrifuged and the supernatant aspirated once again, and the pellet was resuspended in 100 μL of normal HBSS.

To each sample, 10 μL of 2 mg/mL DAPI in methanol and 10 μL of 1 mg/mL PI in 1XPBS, pH 7.2 were added. The samples were then incubated in the dark for 90 minutes at 37°C. Seven microliters of a 1X working solution of Crypt-a-Glo™ FITC-labeled antibody was added to each sample and it was allowed to incubate for another 30 minutes at 37°C. Upon removal from incubation 1mL of normal HBSS was added to each sample and mixed by vortexing.

Slides were prepared by placing 5 μL of a sample on each slide and covering with a 18 mm^2 coverslip, which was then sealed with clear nail-polish. Samples were then examined at 600X using the appropriate filters and DIC optics in order to classify oocysts based on inclusion or exclusion of DAPI and PI, and visualization of the contents of the oocysts as shown in *Table 2.3*.

Table 2.3: Correlation of Viability to Staining and DIC Visualization

<i>Type of Oocyst</i>	<i>Viability Status</i>
PI+	Dead
DAPI+/PI-	Viable at Assay
DAPI-/PI-	Viable with further trigger
Cytoplasmic DAPI+/PI-	Dead
Ghost	Dead

Boiled samples were to be examined until a minimum of 200 oocysts were counted and non-boiled control samples were examined to confirm the presence of viable oocysts.

These samples were then compared to the corresponding boiled and non-boiled samples which were heat shocked and lysed as described. The samples were then diluted from the original oocyst concentration to 10 oocysts per 100 μL and divided into 100 μL aliquots prior to mRNA isolation, amplification and detection as described.

Preparation of Environmental Water Samples

Environmental water samples were filtered as per method 1622 and all material captured on the filter was eluted and collected by Clancy Environmental Consultants, Inc. Each sample was characterized based on biological and inorganic contaminants, as shown in *Table 2.4*. Some of the samples were shipped containing formalin. In order to wash out any formalin, each of the environmental water samples were centrifuged for 20 minutes at 1,200xg, the supernatants were removed, and the packed pellet volume estimated. Each sample was then diluted to 5% packed pellet volume prior to being split into replicates. Environmental water samples were spiked into tubes containing 100 oocysts of *C. parvum* in 500 µL nuclease-free water sorted by flow cytometry and the total volume was brought to 5 mL with nuclease-free water providing packed pellet volumes of 1 to 4.5% per replicate.

Table 2.4: Characteristics of Environmental Water Samples

Sample ID	Source Type	Water Type	Equivalent Volume (L)	Percentage Pellet Volume per Replicate	Characteristics
256-6	River	Source	~ 6	4.5%	Algae, diatoms and vegetative debris – typical river water
201-1	River	Source	34	1%	High concentration of algae, diatoms, rotifers, free-living protozoa and vegetative debris
094-3	River/Reservoir	Raw	10	4.5%	Very high levels of biological particles and inorganic debris
243-2	Lake	Source	102	2.5%	High in algae and Diatoms
270-3	Well	Source	4690	3.5%	High inorganic debris. Low in biologicals

Results & Discussion

Detection of Human Pathogenic Cryptosporidium spp.

Samples containing 0, 5, 25, 50, 100, 250, and 500 oocysts of *C. parvum*, *C. hominis*, or *C. meleagridis*, respectively in 100 µL of nuclease-free water were prepared and heat shocked, lysed and the mRNA isolated as described above. The samples were then amplified via NASBA and the samples quantified using the lateral flow assay. All three species were successfully identified at concentration levels as low as 5 oocysts (Table 2.5). Since samples were generated via serial dilution from a stock solution containing 5×10^3 oocysts/mL, the oocyst concentrations shown here are not as accurate as those performed later. However, the data demonstrate that all three human-pathogenic species of *Cryptosporidium* can be detected with the biosensor assay using the same primers and detection probes.

Table 2.5: Percentage of samples testing positive at varying oocyst numbers for the three human pathogenic *Cryptosporidium* species †

Number of Oocysts	<i>C. parvum</i>	<i>C. hominis</i>	<i>C. meleagridis</i>
0	0%	0%	0%
5	67%	100%	33%
25	100%	100%	67%
50	100%	100%	100%
100	100%	100%	100%
250	100%	100%	100%
500	100%	100%	100%

† Six replicates were tested for each number of oocysts for each species.

Initial experiments employed total RNA isolation using the Qiagen RNeasy Mini Kit. However, as the target molecule is mRNA and *Cryptosporidium* is eukaryotic, mRNA isolation using oligo-d(T)₂₅ magnetic beads was also investigated and found to be better due to the more specific isolation of mRNA molecules via their poly-A tail and

elimination of potentially contaminating rRNAs and tRNAs. Thus, this procedure yielded more consistent results, especially at low oocyst concentrations and was employed in all experiments described here.

Specificity for Human Pathogenic Cryptosporidium

Eight samples containing 500 oocysts of *C. muris* in 100 µL of nuclease-free water were treated as described above and amplified with a negative control and a positive control, a sample containing mRNA isolated from 500 oocysts of *C. meleagridis*. The negative control as well as all eight samples containing oocysts of *C. muris* produced negative signals on the lateral flow test strips while the positive control generated a strong positive signal at the capture zone. This indicated that no false positive signals will be generated by non-human pathogenic *C. muris*.

Detection in the Presence of Contaminating Organisms

Samples containing 10 oocysts of *C. parvum* and approximately 5×10^4 cells of *E. coli* O157:H7, *Giardia intestinalis*, or *Oocystis minuta*, respectively in 5 mL were processed using the IMS procedure described above. The samples were then heat shocked, lysed, isolated, and amplified as described above. Each combination of contaminating organism and *C. parvum* were analyzed in quadruplicate and compared to samples containing 10 oocysts of *C. parvum* aliquoted from the same stock run in parallel.

The samples containing *C. parvum* oocysts and contaminating organisms tested positive in all cases, as shown in *Figure 2.1*. One sample out of 4 containing only 10 oocysts of *C. parvum* yielded a negative result. It is assumed that either this sample was not handled correctly, or that less than 5 viable oocysts were present since samples were generated via dilution only.

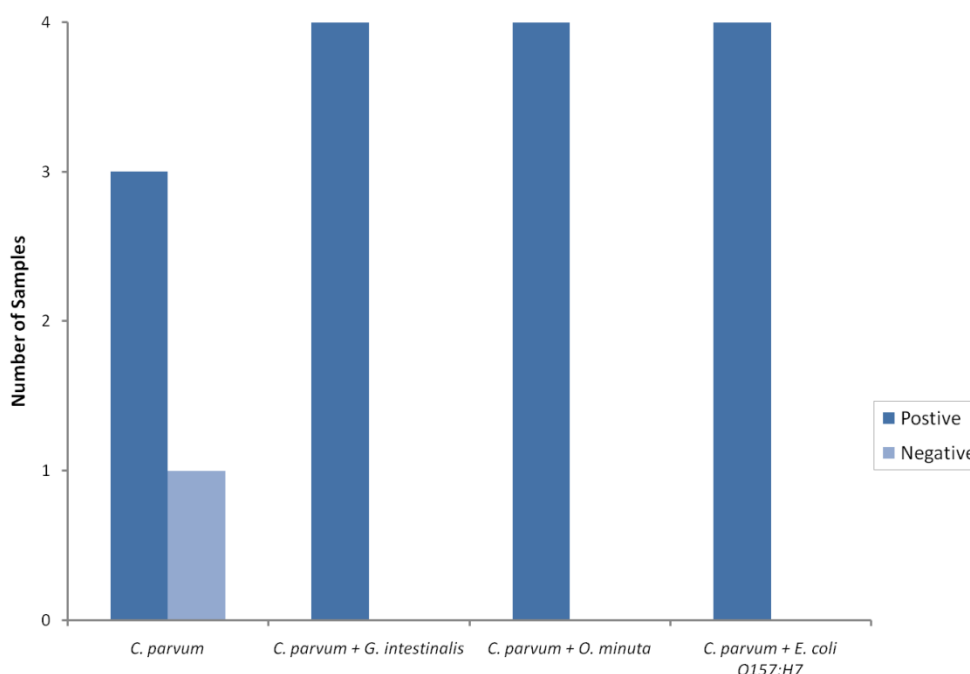


Figure 2.1: *Cryptosporidium* Detection in the Presence of Contaminating Organisms. Each sample was analyzed in quadruplicate and contained 10 oocysts of *C. parvum*. Those containing *G. intestinalis* or *O. minuta* had 54,000 cells and samples with *E. coli* O157:H7 had 8.6×10^4 CFU.

Analytical Sensitivity

Samples containing 1, 2, 3, 4, 5 or 10 oocysts of *C. parvum* in 10 μ L counted into tubes by flow cytometry were obtained from the Wisconsin State Laboratory of Hygiene. Prior to shipping, these samples were heat shocked as described and 100 μ L of the Lysis/Binding Buffer from the Dynabeads mRNA DIRECT Micro Kit were added prior to lysis. This buffer contains 5 mM dithiothreitol, an RNase inhibitor,

which should increase the stability of the target *hsp70* mRNA. Samples were then shipped on dry ice and upon arrival all samples were thawed. RNA was isolated, and amplified as previously described. As shown in *Figure 2.2*, all 8 of the samples containing 1 oocyst of *C. parvum* scored positive. Additionally, all 8 replicates containing 2, 3, 4, 5 and 10 oocysts scored positive; indicating that our assay is capable of detecting a single oocyst.



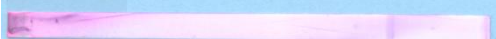
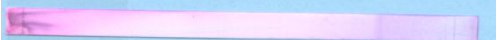


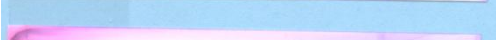
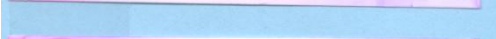

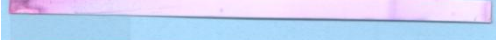
Sample	Test Strip	Visual	Signal
Negative Control		-	10
1 oocyst		+	29
1 oocyst		+	30
1 oocyst		+	17
1 oocyst		+	34
1 oocyst		+	23
1 oocyst		+	26
1 oocyst		+	19
1 oocyst		+	19
Positive Control		+	22

Figure 2.2: Lateral flow test strips from 1 oocyst *C. parvum* samples
Samples containing 1 oocyst of *C. parvum* were prepared by flow cytometry and processed through heat shock, lysis, mRNA isolation and NASBA amplification yielding obvious signals.

Discrimination between Viable and Non-viable Oocysts

Upon examining the boiled sample, 315 oocysts were counted all of which score DAPI-/PI+ with no oocysts scoring in any other category, yielding a 0% viable score. Examination of the control sample yielded 50 oocysts scoring DAPI+/PI-, with the

DAPI staining localized to the nuclei indicating that there are in fact viable oocysts in the control. As staining was only to confirm the presence of viable oocysts, counting was limited to this category even though DAPI-/PI- oocysts could be viable. It should be noted that during counting no PI+ oocysts were noted, though there were several DAPI- oocysts observed. Examples of the stained oocysts from both samples are shown in *Figure 2.3*.

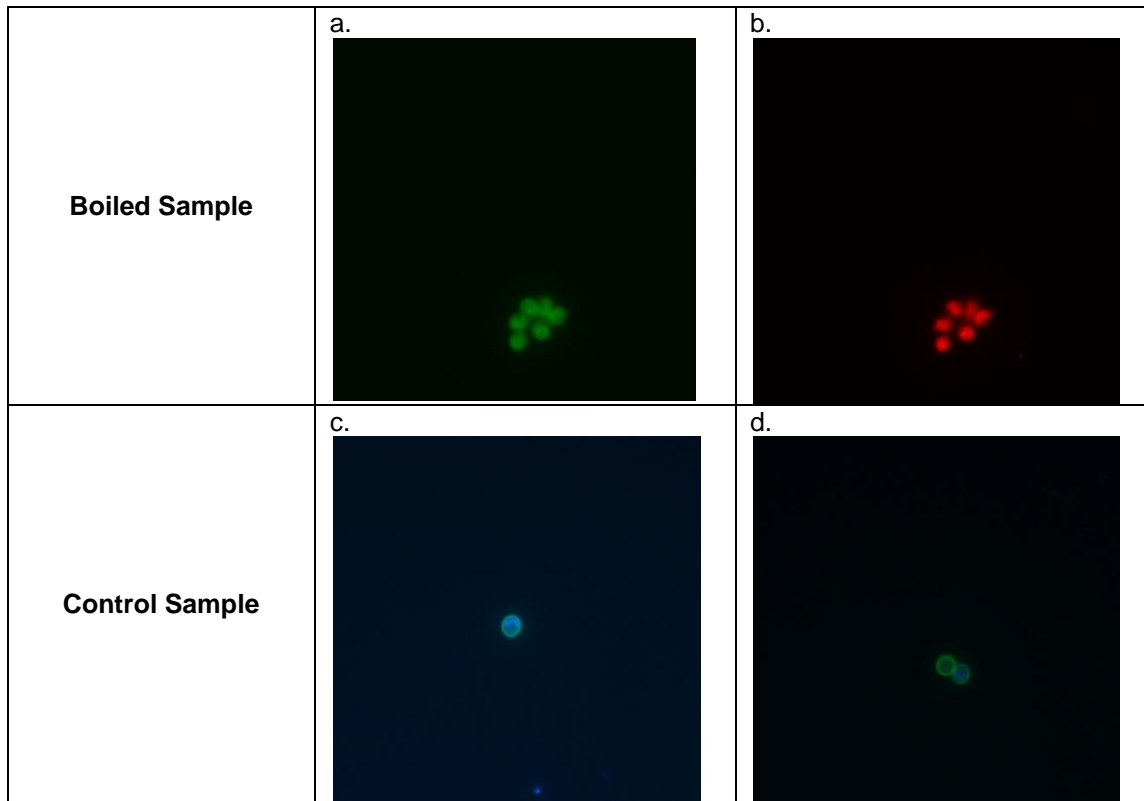


Figure 2.3: DAPI/PI Viability Staining Results

The images from the boiled sample show a cluster of 6 oocysts stained with the (a) FITC-labeled antibody on the oocyst wall and (b) PI inclusion in the cytoplasm. It is evident from the FITC-labeled antibody (a) that there is deformation of the oocysts common in dead oocysts, note the brighter locations indicating crumpling of the oocyst walls. The control sample yielded viable oocysts; shown (c, d) are two different oocysts that showed DAPI staining localized to the nuclei. A DAPI- oocysts can be seen (d) next to a DAPI+ oocyst.

From both the boiled and the control non-boiled samples, 24 aliquots of 10 oocysts per 100 μ L were processed through mRNA isolation and NASBA along with 3 positive and 3 negative controls. All 24 aliquots from the boiled sample provided no signal, correlating to the 0% viability assessed via DAPI/PI staining. Also, all 24 aliquots of the control non-boiled sample yielded positive signals, which also correlates to the observed viable oocysts via DAPI/PI staining.

Comparison to EPA Method 1622

Samples containing nominally 10 oocysts or 25 oocysts of *C. parvum* were prepared and half were processed through the IMS, staining and enumeration procedures of EPA Method 1622 by Clancy Environmental Consultants, Inc. (6). The remaining samples were heat shocked, had 100 μ L Lysis/Binding Buffer added, and were lysed via the previously described freeze/thaw procedure. These samples were then shipped frozen, thawed and mRNA isolated and amplified via NASBA prior to being quantified using the lateral flow assay. The actual concentration of the samples was determined by staining and counting additional samples from the same IMS procedure, as would normally be done at the end of Method 1622 (6); the actual concentration was 4 to 11 oocysts for those labeled to contain 10, and 17 to 32 oocysts for those labeled to contain 25.

The results shown in *Table 2.6* indicates that the detection system described here is highly comparable to EPA Method 1622. While it cannot provide quantitative results, i.e. only a yes/no answer, it is very rapid, easy to perform and does not require

expensive equipment, aside from a freezer and a heating bath. The signal values obtained with the biosensor were lower than expected when compared to all previous analyses. We assume that either the oocysts were not all viable that were contained in the sample (thus reducing the number of detectable oocysts for the biosensor close to or below the detection limit), or that the two-step detection process in which samples were shipped frozen prior to RNA extraction and amplification resulted in partial loss of RNA in the samples.

Table 2.6: Comparison of results obtained from experimental method and EPA Method 1622 for samples containing 10 or 25 oocysts of *C. parvum*

<i>Testing Method</i>	<i>Sample ID</i>	<i>Signal or Oocyst Count</i>	<i>Interpretation</i>
Experimental Method	10 A	8	Positive
	10 B	30	Positive
	10 C	37	Positive
	25 A	12	Positive
	25 B	12	Positive
	25 C	0	Negative
Method 1622	10 D	11 oocysts	Positive
	10 E	9 oocysts	Positive
	10 F	10 oocysts	Positive
	25 D	17 oocysts	Positive
	25 E	10 oocysts	Positive
	25 F	24 oocysts	Positive

Spiked Environmental Water Samples

All four replicates of the control sample, consisting of 100 counted oocysts in 5 mL of nuclease-free water, yielded positive signals as did all four replicates of samples 201-1, 243-2, 270-3, 256-6, and 094-3. This result, shown in *Figure 2.4*, all samples tested yielding positive results – indicates that the system described can be used to detect viable *C. parvum* oocysts in concentrated pellet material from environmental water samples following IMS.

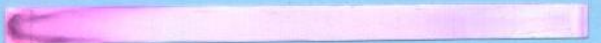



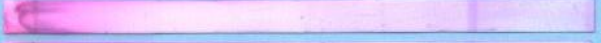
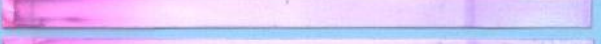


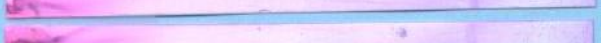







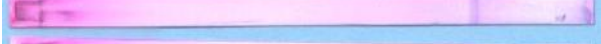










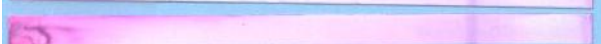
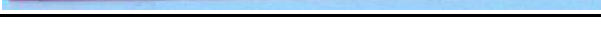
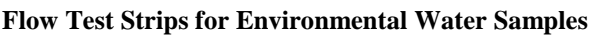
<i>Sample</i>	<i>Test Strip</i>	<i>Signal</i>
Negative		-
Control		+
Control		+
Control		+
Control		+
201-1		+
201-1		+
201-1		+
201-1		+
Positive		+
Negative		-
243-2		+
243-2		+
243-2		+
243-2		+
270-3		+
270-3		+
270-3		+
270-3		+
Positive		+
Negative		-
256-6		+
256-6		+
256-6		+
256-6		+
094-3		+
094-3		+
094-3		+
094-3		+
Positive		+

Figure 2.4: Lateral Flow Test Strips for Environmental Water Samples

Samples containing 100 oocysts counted by flow cytometry were spiked with packed pellet material in a total volume of 5 mL and processed through IMS. All samples yielded positive signals

Conclusions

Employing IMS, heat shock, freeze–thaw lysis, mRNA isolation, NASBA amplification and a nucleic acid hybridization lateral flow sandwich assay, the described method specifically detects as few as one oocyst of a viable human pathogenic *Cryptosporidium* species. Assuming a single oocyst present in a 5 mL sample is captured by IMS, the described method would hence be capable of detecting one oocyst per 5 mL as proven here. In addition, because large environmental water samples were filtered and used as sample matrix, we can safely assume that one oocyst captured through filtration and IMS from large samples (hundreds to thousands of liters of water) can indeed be detected with this method. Detection of these oocysts is possible in the presence of large numbers of microorganisms commonly found in contaminated water samples and in packed pellet material collected from environmental water samples. The entire method, from IMS to readable signals on the test strips, takes only 4.5 h with IMS running 90 min, a 20-min heat shock, 10 min for freeze–thaw lysis, 5 min for mRNA isolation, 115 min for NASBA (including steps prior to incubation), a 20-min liposome-target hybridization incubation, and 10 min for the lateral flow assays to produce signals. Most importantly, results obtained with the method compared very well with those from EPA Method 1622.

Acknowledgement

This study was funded in part by EPA Contract Number EP-D-06–034, NYSTAR. This research was also supported in part by the Cornell University Agricultural Experiment Station federal formula funds, Project No. 123–314 received from

Cooperative State Research, Education and Extension Service, US Department of Agriculture. Any opinions, findings, conclusions, or recommendations expressed in this publication are those of the author(s) and do not necessarily reflect the view of the US Department of Agriculture. The authors would like to thank Jennifer Clancy and Randi McQuin of Clancy Environmental Consultants, Inc., Becky Hoffman and Martin Collins of the Wisconsin State Laboratory of Hygiene, and Giovanni Widmer and Sal Tzipori of Tufts University School of Veterinary Medicine for providing samples used in this study.

REFERENCES

1. Yagita K, Izumiyama S, Tachibana H, Masuda G, Iseki M, Furuya K, et al. Molecular characterization of *Cryptosporidium* isolates obtained from human and bovine infections in Japan. *Parasitology Research* 2001;87:950-5.
2. Leoni F, Amar C, Nichols G, Pedraza-Diaz S, McLauchlin J. Genetic analysis of *Cryptosporidium* from 2414 humans with diarrhoea in England between 1985 and 2000. *Journal of Medical Microbiology* 2006;55:703-7.
3. Wilkinson SL. Eating Healthy in a Dirty World. *Chemical & Engineering News* 1997;75:24-33.
4. Mead P, Slutsker L, Dietz V, McCaig LF, Bresee JS, Shapiro C, et al. Food-Related Illness and Death in the United States. *Emerging Infectious Diseases* 1999;5:607-25.
5. Chappell CL, Okhuysen PC, Sterling CR, DuPont HL. *Cryptosporidium parvum*: Intensity of infection and oocyst excretion patterns in healthy volunteers. *Journal of Infectious Diseases* 1996;173:232-6.
6. Environmental Protection Agency. Method 1622: *Cryptosporidium* in Water by Filtration/IMS/FA. Vol., 2005:45-60.
7. Robertson LJ, Campbell AT, Smith HV. *In vitro* excystation of *Cryptosporidium parvum*. *Parasitology* 1993;106:13-9.
8. Hou L, Li X, Dunbar L, Moeller R, Palermo B, Atwill ER. Neonatal-Mouse Infectivity of Intact *Cryptosporidium parvum* Oocysts Isolated after Optimized In Vitro Excystation. *Applied and Environmental Microbiology* 2004;70:642-6.
9. Baeumner AJ, Humiston M, Montagna RA, Durst RA. Detection of Viable Oocysts of *Cryptosporidium parvum* Following Nucleic Acid Sequence Based Amplification. *Analytical Chemistry* 2001;73:1176-80.
10. Hartley HA, Baeumner AJ. Biosensor for the Specific Detection of a Single Viable *B. anthracis* Spore. *Analytical and Bioanalytical Chemistry* 2003;376:319-27.

11. Baeumner AJ, Schlesinger NA, Slutzki NS, Romano J, Lee EM, Montagna RA. A Biosensor for Dengue Virus Detection: Sensitive, Rapid and Serotype specific. *Analytical Chemistry* 2002;74:1442 – 8.
12. Baeumner AJ, Cohen RN, Miksic V, Min JH. RNA Biosensor for the Rapid Detection of Viable *Escherichia coli* in Drinking Water. *Biosensors & Bioelectronics* 2003;18:405 – 13.
13. Esch MB, Baeumner AJ, Durst RA. Detection of *Cryptosporidium parvum* Using Oligonucleotide-Tagged Liposomes in a Competitive Assay Format. *Analytical Chemistry* 2001;73:3162-7.
14. Aguilar ZP, Fritsch I. Immobilized Enzyme-Linked DNA-Hybridization Assay with Electrochemical Detection for *Cryptosporidium parvum* hsp70 mRNA. *Analytical Chemistry* 2003;75:3890-7.
15. Stinear T, Matusan A, Hines K, Sandery M. Detection of a Single Viable *Cryptosporidium parvum* Oocyst in Environmental Water Concentrates by Reverse Transcription-PCR. *Applied and Environmental Microbiology* 1996;62:3385-90.
16. Edwards KA, Baeumner AJ. Optimization of DNA-tagged dye-encapsulating liposomes for lateral-flow assays based on sandwich hybridization. *Analytical and Bioanalytical Chemistry* 2006;386 1335-43.
17. Baeumner AJ, Pretz J, Fang S. A Universal Nucleic Acid Sequence Biosensor with Nanomolar Detection Limits. *Analytical Chemistry* 2004;76:888-94.

CHAPTER 3

INTEGRATED MICROFLUIDIC PRE-CONCENTRATOR AND IMMUNOBIOSENSOR

Abstract

We present a microfluidic biosensor that integrates membrane-based preconcentration with fluorescence detection. The concentration membrane was fabricated in polyacrylamide by an *in-situ* photopolymerization technique at the junction of glass microchannels. Liposomes entrapping sulforhodamine B (SRB) dye molecules were used for signal amplification. The biotin-streptavidin binding system was a model system for evaluating device performance. Biotinylated liposomes were preconcentrated at the membrane by applying an electric field across the membrane. The electric field causes the liposomes to migrate towards the membrane where they are concentrated by a sieving effect. Two orders of magnitude concentration was achieved after applying the electric field for only 2 min. The concentrated bolus was then eluted towards the detection unit, where the biotinylated liposomes were captured by immobilized streptavidin. The integrated system with the preconcentration module shows a fourteen-fold improvement in signal as opposed to a system that does not include preconcentration.

Introduction

Microfluidic systems have become increasingly popular in biological and chemical analyses owing to the advantages of minimal reagent use, cost-effectiveness and automation (1, 2). An important application of microfluidic systems has been in the

field of biosensors for pathogen detection and clinical diagnostics (3-5). However, the use of microfluidic devices for the total analysis of a whole sample has been limited due to the challenges associated with integration of the different processing steps like sample preparation, preconcentration, analysis and detection on the same device (6-10). In this paper, we present an integrated microfluidic immunobiosensor that combines preconcentration and fluorescence detection steps to enable sensitive detection in dilute samples.

Pre-concentration of sample prior to analysis is an important step in microfluidic systems as it enables detection of very small concentrations of analytes and also improves detection sensitivity and signal-to-noise ratios. A number of pre-concentration techniques have been developed that can achieve high concentration factors in small time durations. Some examples include surface-binding techniques like solid-phase extraction (11-13) and electrokinetic manipulation techniques like isoelectric focusing (14-16), field-amplified sample stacking (17, 18), isotachopheresis (19-21) and dielectrophoresis (22, 23). However, the limitations of these techniques are that they either involve buffer handling challenges or fabrication complexities making them difficult to integrate with lab-on-chip systems. Porous membrane-based pre-concentration systems, on the other hand, do not require complex buffer systems to concentrate samples. Khandurina *et al.* (24, 25) demonstrated the use of a porous silicate membrane while Wang *et al.* (26) used a nanofluidic filter for pre-concentration. However, in the former case, the authors reported that the silicate membranes were hard to fabricate in a reproducible manner and the latter approach

involves the fabrication of micro- and nanochannels in the same device. More recently, Kim *et al.* (27) have developed self-sealed nanoporous junctions inside PDMS microchannels for pre-concentration. However, PDMS-based devices are less robust than glass-based microfluidic devices and are prone to surface adhesion and reusability issues.

We use an *in-situ* photopolymerized nanoporous membrane (28-30) in our integrated glass microfluidic device for the pre-concentration step. Song *et al.* (28) have shown high concentration factors (four orders of magnitude local concentration) using these nanoporous membranes. The *in-situ* fabrication technique allows for easy integration with total analysis systems. Our membranes are fabricated in polyacrylamide as it is hydrophilic, biocompatible and shows minimal non-specific adhesion (30). The pore-size of acrylamide gels can be easily adjusted by changing the percentage of monomer components (31, 32). Moreover, unlike other membrane-based concentration methods, the response of this system is linear with the voltage-time product (28).

Figure 3.1 shows the integrated microfluidic biosensor with the inset showing the concentration membrane. The membrane is nanoporous and is made using polyacrylamide at the intersection of the glass channels by an *in-situ* photopolymerization technique (28-30). We use liposomes, which can encapsulate a very large number of fluorescent dye molecules in their core for signal amplification in the biosensor. Fluorescence from the dye molecules is quenched when they are encapsulated at a high concentration within the liposome core. The analytes to be

detected are tagged with liposomes (33) and these complexes are injected into the inlet well of the device. An electric field is applied across the membrane, causing the liposome-analyte complexes to migrate towards the membrane. However, since the size of the pores in the membranes is much smaller than the size of these complexes, they are concentrated at the membrane by a sieving effect. The concentrated bolus is then eluted towards the detection region, where these complexes are captured using immobilized antibodies. The captured liposomes are then lysed by flowing a detergent and the released fluorophores result in a significant signal enhancement due to the elimination of self-quenching of the dye molecules.

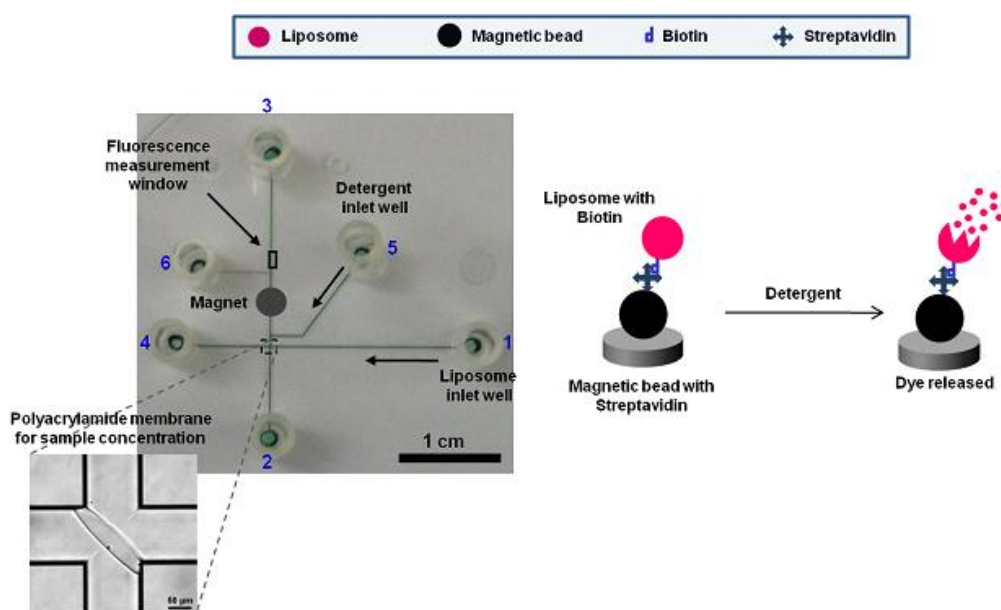


Figure 3.1: Image of the integrated glass microfluidic device used for the biotin-streptavidin experiments, with the channels filled with food dye to appear dark and show contrast. The inset shows a picture of the polyacrylamide membrane-based concentrator at the junction of microchannels. Biotinylated liposomes are captured by streptavidin-conjugated magnetic beads localized at the magnet. The fluorescence from the lysed liposomes is imaged downstream from the magnet in the region marked as the fluorescence measurement window.

In this paper, we present results showing improved detection sensitivity with the inclusion of the pre-concentration system using proof-of-concept experiments performed with biotin-streptavidin binding.

Experimental Methods

Fabrication of microfluidic channels

Schott D263 glass wafers (100 mm diameter, 0.55 mm thick; S I Howard Co., Worcester, MA) were used for etching microfluidic channels. Device geometry was defined using L-Edit CAD software (Tanner Research) and a photomask was created using GCA/Mann 3600F Optical Pattern Generator. A 225 nm thick layer of amorphous silicon deposited on the glass wafers by PECVD was used as the hard mask for etching. The wafers were then coated with a 3 μm thick layer of Shipley 1818 positive photoresist and soft-baked at 115°C for 1 min. The mask pattern was transferred to the photoresist using an EV 620 contact aligner and the wafers were developed using a 300MIF resist developer. The exposed silicon was etched using an Oxford 80 (#1) reactive ion etching (RIE) system and the photoresist was stripped using a mixture of acetone and isopropanol. The exposed glass was etched using a 16% HF solution (Shape Products Company, Oakland, CA). The glass wafers were exposed to HF for 14 min, resulting in channel depths of 20 μm (etch rate of D263 glass in 16% HF is about 1.4 $\mu\text{m}/\text{min}$ when left unagitated). Finally, the remaining silicon on the wafers was removed by reactive ion etching using the Oxford 80 (#1) system. In the final device, the wide channel width was 120 μm and the narrow

channel width was 50 μm . The depths of the channels in both cases were 20 μm . Connection holes were made in the wafers by sandblasting.

Wafer bonding

The glass microchannels were sealed by a plain borofloat glass wafer (100 mm diameter, 500 μm thick; Mark Optics, Santa Ana, CA) using a low temperature glass bonding technique ([24](#), [25](#), [34](#), [35](#)). The etched and the plain glass wafers were cleaned by sonicating in acetone for about 5 min. The wafers were then hydrolyzed in RCA cleaning solution (prepared by mixing 5N ammonium hydroxide, 30% w/w hydrogen peroxide and deionized water in 3:2:9 ratio by volume) for 20 min at 70-80°C, rinsed in deionized water and dried under nitrogen. This was followed by plasma cleaning to activate the surfaces of both the wafers prior to bonding. A thin layer of potassium silicate (KASIL 2130, The PQ Corp., Valley Forge, PA) was coated on the plain glass wafer by spinning a diluted solution (1:10 by weight in deionized water) at 2000 rpm for 8 sec. As the spin-coated wafer was then brought into contact with the etched glass wafer, the bonding region spread instantaneously across the entire area of the wafers. The bonded wafers were then placed in a hot press at 90°C for an hour to reinforce the bonding.

Membrane fabrication and surface treatment

The channels of the bonded devices were treated with 1 M NaOH for 20 min to remove the potassium silicate layer in the microchannels. The wafers were then rinsed with DI water and dried in nitrogen. Prior to membrane fabrication, the glass channels

were coated with an acrylate-terminated self-assembling monolayer to enable covalent attachment of the polyacrylamide membrane to the channel walls (36-38). For this, the channels were prepared by exposing to 1 M HCl for 30 min, rinsing in DI water and then exposing to 1 M NaOH for 30 min. The channels were thoroughly rinsed with DI water and then exposed to a freshly mixed coating solution containing 2:3:5 mixture (by volume) of 3-(trimethoxysilyl)propyl acrylate, glacial acetic acid and deionized water for exactly 30 min. The channels were finally rinsed in 1-propanol and DI water and dried with vacuum.

The polyacrylamide membrane was fabricated at the intersection of the glass microchannels by a photopolymerization technique (28-30). For this, a 355 nm laser beam was shaped using a train of lenses and mirrors into a long narrow beam to match the dimensions of the channel junction. The optical train also helps to direct the beam through a microscope to enable visualization of the polymerization process. The channels were filled with a freshly prepared and degassed solution of 22% (15.7:1) acrylamide/bisacrylamide containing 0.2% (w/v) VA-086 photoinitiator (30). All the reservoirs were capped with tape to prevent evaporation, and the solution was allowed to equilibrate for 20 min to eliminate pressure-driven flow. The membrane was then fabricated by directing the shaped laser beam towards the junction and exposing for approximately 15 sec. The unpolymerized acrylamide solution was purged from the channels and the channels were rinsed thoroughly with DI water.

Finally, the channels were coated with linear polyacrylamide to suppress the electroosmotic flow (36-38). The channels were filled with a degassed solution of 50 mg/ml acrylamide in deionized water containing 250 ppm hydroquinone and 2 mg/ml V-50 photoinitiator and exposed to UV light in a UV oven for 30 min. The unpolymerized solution was rinsed out of the channels and the channels were cleaned with DI water.

Liposome and magnetic bead preparation

Liposomes were prepared by a modified version (33) of the reversed-phase evaporation technique described by Siebert *et al.* (39). All lipids used were obtained from Avanti Polar Lipids (Alabaster, AL). Fluorescent liposomes encapsulate 150 mM sulforhodamine B (SRB) dye in 0.02 M HEPES, pH 7.5 in the core and also contain 0.33 mol% dipalmitoyl phosphoethanolamine(DPPE)-rhodamine in the bilayer. Biotinylated lipids were used in the preparation of the liposomes in order to add functionality to the outer surface of the bilayer. The remainder of the bilayer consists of 35 mol% dipalmitoyl phosphatidylcholine (DPPC), 15 mol% dipalmitoyl phosphatidylglycerol (DPPG), 42 mol% cholesterol, and 6 mol% N-(glutaryl)-1,2-dipalmitoyl-*sn*-glycero-3-phosphoethanolamine. After formation of the vesicles, extrusions through 1 μm and 0.4 μm filters was performed to assure unilamellar liposomes with a uniform size distribution. Removal of unencapsulated SRB was facilitated by application of the liposome preparation to a Sephadex G-50 column equilibrated with 0.01 M HEPES, 0.2 M NaCl, 0.2 M sucrose, 0.01% sodium azide

(NaN₃), pH 7.5 (1X HSS), also used for elution. Fractions containing liposomes were collected and dialyzed 1X HSS in the dark overnight.

To capture these biotinylated liposomes in the microfluidic device, commercially available streptavidin-conjugated superparamagnetic beads (Dynabeads MyOne Streptavidin, 1 µm in diameter; Invitrogen, Carlsbad, CA) were used. Prior to use, the stock was vortexed to homogenize the suspension and the necessary volume was removed. In order to remove preservatives and introduce the working buffer, the beads were then washed twice with an equal volume of 1X HSS by applying the tube to a magnet rack, removing the supernatant, and resuspending.

Sample loading, concentration and detection

Prior to performing concentration and detection experiments, the channels of the device were primed with 1X HSS buffer. A permanent magnet was positioned on the top surface of the device upstream of the detection region using adhesive putty. One microliter of Dynabeads MyOne streptavidin-conjugated superparamagnetic beads prepared in 1X HSS buffer was injected towards the magnet through the port 5 (*Figure 3.1*) using a syringe pump at a flow rate of 1 µl/min. For the electrokinetic concentration experiments, a solution of 10,000x diluted fluorescent liposomes (biotinylated with SRB dye in the core) in 1X HSS buffer was used. For the direct injection experiments, the liposome solution was further diluted by a factor of 10 in 1X HSS buffer (due to lowest achievable flow rate limitations with our existing

equipment) so that the same number of liposomes is flowed through the device for performance comparison.

For the direct injection experiments, the biotinylated liposome solution in 1X HSS buffer was injected towards the magnet with a syringe pump at a flow rate of 10 $\mu\text{l/hr}$ for 90 sec through inlet port 1 (*Figure 3.1*). On the other hand, for the electrokinetic concentration experiment, all the wells were filled with 60 μl of plain 1X HSS buffer except the inlet well which was filled with the liposome-1X HSS solution. The pressure driven flow in the system was eliminated by adjusting the heights of the solutions in the wells. The liposomes were then electrophoretically concentrated at the membrane by applying a voltage difference of 150 V across the membrane. After concentrating for a duration of 90 sec, the concentrated bolus of liposomes was eluted towards the bead bed by applying a voltage of 150 V to the outlet port 3 downstream of the magnet. In both cases, after liposome injection, wash buffer was injected at a flow rate of 20 $\mu\text{l/hr}$ to wash off any unbound liposomes in the device through port 5. A detergent solution of 60 mM octyl- β -D-glucopyranoside (OG) was then flowed through the same port 5 towards the bead bed at a flow rate of 40 $\mu\text{l/hr}$ and the emitted fluorescence from the lysis of the liposomes was recorded downstream of the bead bed.

For each experiment, the background was calculated as the average of the total fluorescence intensity values estimated in the region of interest during the first 60 frames of the detergent injection videos.

After each run, the device was thoroughly rinsed with deionized water multiple times followed by a final rinse which involves flowing deionized water at a rate of 2 $\mu\text{l}/\text{min}$ with a syringe pump for 15 min.

Concentration factors during the experiments were estimated analytically as the ratio of the swept volume of liposomes at a given electrophoretic velocity to the volume of the measurement window around the membrane. The electrophoretic velocity of liposomes was estimated from Zetasizer measurements.

Results

Electrophoretic concentration of fluorescent liposomes

Concentration and elution experiments were performed using fluorescent liposomes to estimate the concentration factors for the membrane-based pre-concentration system.

Figure 3.2 shows snapshots of the channel junction during the concentration and elution steps achieved by switching electric fields between the vertical and horizontal channels. *Figure 3.3* shows the concentration factor plotted as a function of time for which the high voltage is applied across ports 1 and 4 (*Figure 3.2(a)*). It can be seen from *Figure 3.3* that after a concentration time of 160 sec, the estimated concentration factor was around 230. Analytical calculations (as described in the materials and methods section) resulted in concentration factors of around 350 for 160 sec of applying high voltage which is on the same order of magnitude as the experimental value. For these calculations, the zeta potential of the liposomes estimated from

Zetasizer measurements was -28.8 ± 2.9 mV (resulting in a mean electrophoretic velocity of $103.1 \mu\text{m}/\text{sec}$), while the inferred zeta potential from the experiments was -19 mV. The trend in *Figure 3.3* is linear as expected since the liposomes migrate with a constant electrophoretic velocity.

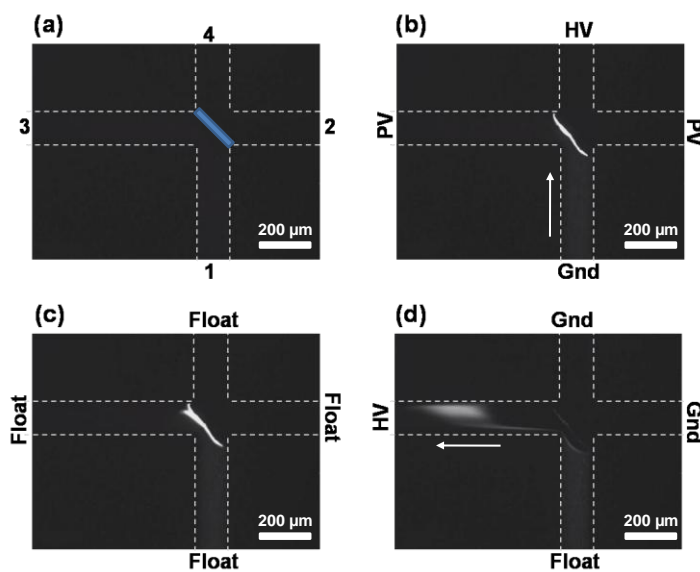


Figure 3.2: Image sequence showing liposome concentration and elution. Microchannel edges have been drawn for clarity. The membrane has also been highlighted in (a). HV denotes high voltage (100 V), PV pinch voltage (40 V), Gnd ground. (a) Before loading (b) Sample concentration (c) After concentration (d) Sample elution. Pinch voltage is applied to minimize the diffusion of the sample away from the membrane.

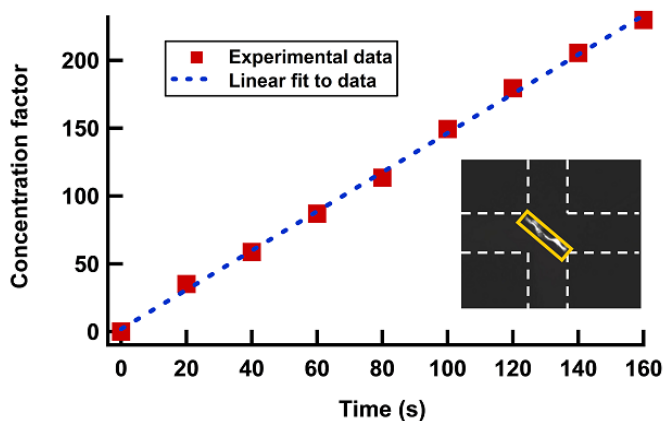


Figure 3.3: Concentration factors during liposome concentration as a function of time. The intensities were averaged over a measurement window (23 x 180 pixels) shown as a box in the inset. The concentration factors are consistent with analytical values estimated using a liposome zeta potential of -19 mV.

Integrated concentration and detection experiments

Concentration and detection experiments were performed with the biotin-streptavidin binding system in the integrated microfluidic device. For these experiments, biotinylated fluorescent liposomes (with SRB dye in the core and bilayer) were used as the analytes to be detected. Streptavidin coated magnetic beads immobilized in the channels using a permanent magnet served as the capture region. The liposomes were electrophoretically concentrated at the membrane by applying a high voltage across the membrane. The concentrated bolus of liposomes was eluted by switching the electric field towards the bead bed where the liposomes are captured. *Figure 3.4* shows an image of the bead bed with the captured fluorescent liposomes. The unbound liposomes were washed away by flowing 1X HSS as wash buffer over the bead bed. The OG solution was then injected into the channels, resulting in the lysis of the bound liposomes. The released fluorescence from the liposomes was captured downstream in the region indicated as the fluorescence measurement window in *Figure 3.1*. Snapshots from the fluorescence burst during OG injection in the region of interest are shown in *Figure 3.5*.

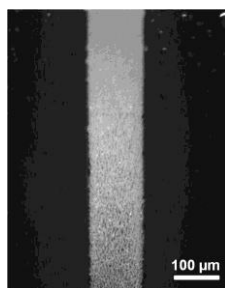


Figure 3.4: Fluorescent liposomes captured at the bead bed immobilized using a permanent magnet.

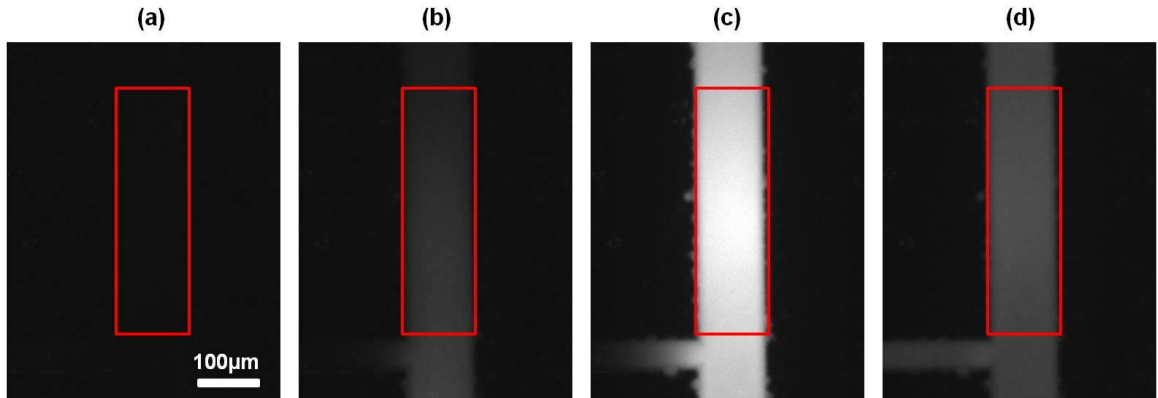


Figure 3.5: Snapshots of the fluorescence measurement window (shown as a box) during OG injection. (a): Background image before the start of injection. (b), (c), (d): Snapshots during fluorescence burst from the lysed liposomes during OG injection.

Comparison of device performance with and without concentration

In order to evaluate the effect of the pre-concentration step on the performance of the system, direct injection experiments were performed where the liposomes were injected towards the bead bed using a syringe pump bypassing the concentration step. The number of liposomes in the device was maintained the same for both sets of experiments – with and without the pre-concentration step.

The total fluorescence intensity in the measurement window during OG injection was estimated from the captured videos of fluorescence burst and plotted as a function of time. These intensity profiles are shown in *Figure 3.6(a)*. This figure shows data from both the electrokinetic concentration (shown in red) and direct injection (shown in blue) experiments. The area under these curves gives the integrated fluorescence intensities for each of these experiments. These integrated intensities for the electrokinetic concentration and direct injection cases are compared in *Figure 3.6(b)*. This figure shows that the inclusion of the pre-concentration step increases the signal by a factor of 14. The increased signal is a result of a concentrated bolus of liposomes

flowing over the bead bed resulting in better capture efficiencies than in the case where a dilute solution of the same number of liposomes is flowed.

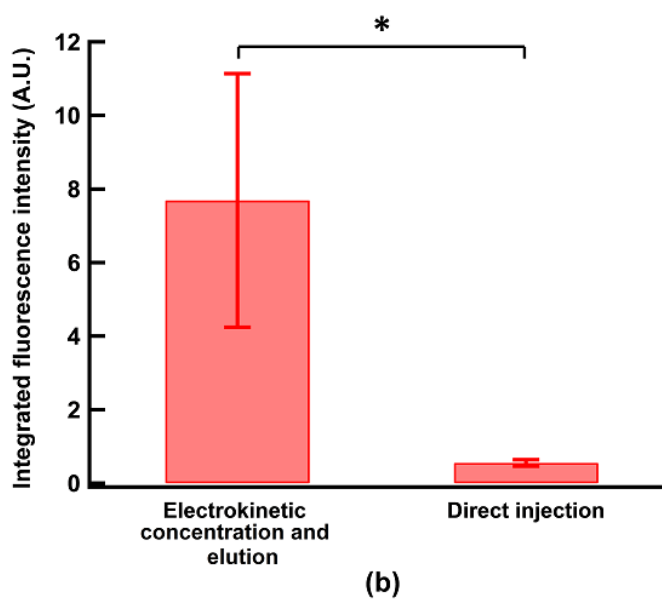
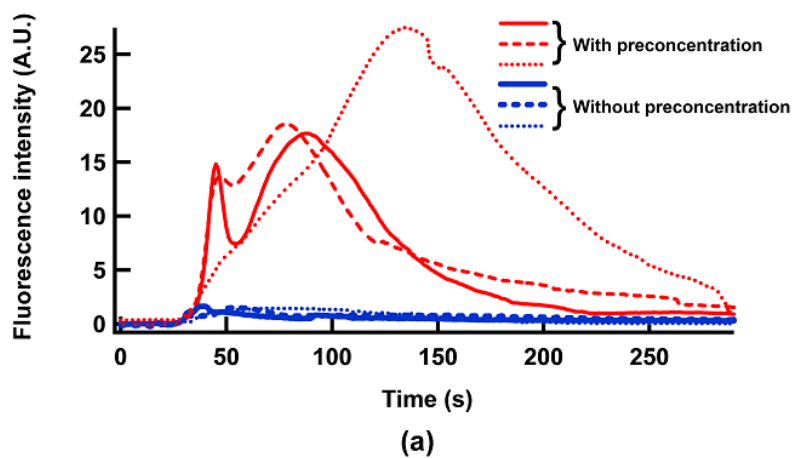


Figure 3.6(a): Fluorescence intensity profiles from the bead bed during OG injection for the two experiments including the pre-concentration step (shown in red lines) and excluding it (shown in blue lines). (b): Comparison of the effect of pre-concentration on the integrated fluorescence intensities from the bead bed during OG injection. The data is reported as mean \pm SD with $n=3$. * indicates $p<0.05$.

Discussion

The detection sensitivity of the biosensor depends on the binding kinetics between the low concentration of an analyte and the surface immobilized biorecognition element. This process is usually diffusion-limited (40-42), and an increase in the local analyte concentration in the capture region greatly improves the binding kinetics. Singh and coworkers (8, 30) have used similar membrane-based preconcentrators in conjunction with microchip SDS-PAGE and electrophoretic immunoassays to show improved separation resolution and detection limits. Wang *et al.* (43) have shown 500-fold improvement in sensitivity (from 50 pM to sub 100 fM) and improved dynamic range of immunoassay detection using nanofluidic filter based electrokinetic preconcentrator. However, the improvement in sensitivity has been reported for molecular analytes like proteins and does not include any post-binding amplification steps.

Our design and fabrication techniques are compatible for integrating electrochemical detection into the device. The device can be operated in electrochemical detection mode by patterning gold interdigitated electrodes downstream from the membrane and using electrochemical liposomes instead of fluorescent ones (44). The low temperature bonding technique is suitable for bonding etched glass wafers with gold-patterned wafers as it does not lead to delamination of the gold electrodes as seen in the conventional high temperature bonding techniques. Also, the core of the liposomes can be filled with electrochemical species such as potassium ferri/ferro hexacyanide molecules instead of fluorophores for detection. This straightforward extension to an

electrochemical system is advantageous as electrochemical detection methods offer several benefits over popularly used optical detection techniques. These include low capital cost for equipment, portability, low power requirement and absence of photobleaching issues (45, 46).

Conclusion

We have presented an integrated microfluidic biosensor that integrates on-chip concentration with liposome-based signal amplification on the same device. We have achieved two orders of magnitude concentration with the membrane-based system within 160 sec of applying high voltage across the membrane. The electric field can be switched to elute the concentrated sample bolus towards the detection region where it is captured efficiently at the immobilized bead bed. The inclusion of the pre-concentration step results in a fourteen-fold improvement in the signal as opposed to a system without the pre-concentration step, when the same number of liposomes is introduced in both cases. The functionality of the membrane can be extended to a filtering device for removing small interfering particles that competitively bind to the target probes, further increasing the signal-to-noise ratio. The inclusion of the pre-concentration system in the integrated device along with the post-binding amplification achieved using liposomes help to improve the limit of detection of the biosensor. By extending the biosensor operation to electrochemical detection format, we can build an inexpensive and portable system that can be used for pathogen detection.

Acknowledgments

This chapter is included in this dissertation as background for the following chapters.

The first author of this chapter is Sowmya Kondapalli. This work was supported by the United States Environmental Protection Agency and was performed in part at the Cornell Nanofabrication Facility. The authors would like to thank Dr. Katie A. Edwards for providing fluorescent liposomes used in the early concentration experiments.

REFERENCES

1. Arora A, Simone G, Salieb-Beugelaar GB, Kim JT, Manz A. Latest Developments in Micro Total Analysis Systems. *Anal Chem* (Washington, DC, U S) 2010;82:4830-47.
2. Ohno K-i, Tachikawa K, Manz A. Microfluidics: applications for analytical purposes in chemistry and biochemistry. *Electrophoresis* 2008;29:4443-53.
3. Mairhofer J, Roppert K, Ertl P. Microfluidic systems for pathogen sensing: a review. *Sensors* 2009;9:4804-23.
4. Liu P, Mathies RA. Integrated microfluidic systems for high-performance genetic analysis. *Trends Biotechnol* 2009;27:572-81.
5. Chen L, Manz A, Day PJR. Total nucleic acid analysis integrated on microfluidic devices. *Lab Chip* 2007;7:1413-23.
6. Beyor N, Yi L, Seo TS, Mathies RA. Integrated Capture, Concentration, Polymerase Chain Reaction, and Capillary Electrophoretic Analysis of Pathogens on a Chip. *Anal Chem* (Washington, DC, U S) 2009;81:3523-8.
7. Sista R, Hua Z, Thwar P, Sudarsan A, Srinivasan V, Eckhardt A, et al. Development of a digital microfluidic platform for point of care testing. *Lab Chip* 2008;8:2091-104.
8. Herr AE, Hatch AV, Throckmorton DJ, Tran HM, Brennan JS, Giannobile WV, Singh AK. Microfluidic immunoassays as rapid saliva-based clinical diagnostics. *Proc Natl Acad Sci U S A* 2007;104:5268-73.
9. Easley CJ, Karlinsey JM, Bienvenue JM, Legendre LA, Roper MG, Feldman SH, et al. A fully integrated microfluidic genetic analysis system with sample-in-answer-out capability. *Proc Natl Acad Sci U S A* 2006;103:19272-7.

10. Lagally ET, Scherer JR, Blazej RG, Toriello NM, Diep BA, Ramchandani M, et al. Integrated Portable Genetic Analysis Microsystem for Pathogen/Infectious Disease Detection. *Anal Chem* 2004;76:3162-70.
11. Jemere AB, Oleschuk RD, Ouchen F, Fajuyigbe F, Harrison DJ. An integrated solid-phase extraction system for sub-picomolar detection. *Electrophoresis* 2002;23:3537-44.
12. Ramsey JD, Collins GE. Integrated microfluidic device for solid-phase extraction coupled to micellar electrokinetic chromatography separation. *Anal Chem* 2005;77:6664-70.
13. Yu C, Davey MH, Svec F, Frechet JMJ. Monolithic porous polymer for on-chip solid-phase extraction and preconcentration prepared by photoinitiated in situ polymerization within a microfluidic device. *Anal Chem* 2001;73:5088-96.
14. Li Y, DeVoe DL, Lee CS. Dynamic analyte introduction and focusing in plastic microfluidic devices for proteomic analysis. *Electrophoresis* 2003;24:193-9.
15. Tan W, Fan ZH, Qiu CX, Ricco AJ, Gibbons I. Miniaturized capillary isoelectric focusing in plastic microfluidic devices. *Electrophoresis* 2002;23:3638-45.
16. Cabrera CR, Yager P. Continuous concentration of bacteria in a microfluidic flow cell using electrokinetic techniques. *Electrophoresis* 2001;22:355-62.
17. Jung B, Bharadwaj R, Santiago JG. Thousandfold signal increase using field-amplified sample stacking for on-chip electrophoresis. *Electrophoresis* 2003;24:3476-83.
18. Lichtenberg J, Verpoorte E, de Rooij NF. Sample preconcentration by field amplification stacking for microchip-based capillary electrophoresis. *Electrophoresis* 2001;22:258-71.

19. Jung B, Bharadwaj R, Santiago JG. On-Chip Millionfold Sample Stacking Using Transient Isotachopheresis. *Anal Chem* 2006;78:2319-27.
20. Wainright A, Williams SJ, Ciambone G, Xue Q, Wei J, Harris D. Sample pre-concentration by isotachopheresis in microfluidic devices. *J Chromatogr, A* 2002;979:69-80.
21. Wang J, Zhang Y, Mohamadi MR, Kaji N, Tokeshi M, Baba Y. Exceeding 20 000-fold concentration of protein by the on-line isotachopheresis concentration in poly(methyl methacrylate) microchip. *Electrophoresis* 2009;30:3250-6.
22. Lapizco-Encinas BH, Davalos RV, Simmons BA, Cummings EB, Fintschenko Y. An insulator-based (electrodeless) dielectrophoretic concentrator for microbes in water. *J Microbiol Methods* 2005;62:317-26.
23. Moncada-Hernandez H, Lapizco-Encinas BH. Simultaneous concentration and separation of microorganisms: insulator-based dielectrophoretic approach. *Anal Bioanal Chem* 2010;396:1805-16.
24. Khandurina J, Jacobson SC, Waters LC, Foote RS, Ramsey JM. Microfabricated Porous Membrane Structure for Sample Concentration and Electrophoretic Analysis. *Anal Chem* 1999;71:1815-9.
25. Foote RS, Khandurina J, Jacobson SC, Ramsey JM. Preconcentration of proteins on microfluidic devices using porous silica membranes. *Anal Chem* 2005;77:57-63.
26. Wang Y-C, Stevens AL, Han J. Million-fold Preconcentration of Proteins and Peptides by Nanofluidic Filter. *Anal Chem* 2005;77:4293-9.
27. Kim SJ, Han J. Self-sealed vertical polymeric nanoporous-junctions for high-throughput nanofluidic applications. [Erratum to document cited in CA148:373127]. *Anal Chem (Washington, DC, U S)* 2008;80:7179.

28. Song S, Singh AK, Kirby BJ. Electrophoretic Concentration of Proteins at Laser-Patterned Nanoporous Membranes in Microchips. *Anal Chem* 2004;76:4589-92.
29. Song S, Singh AK, Shepodd TJ, Kirby BJ. Microchip dialysis of proteins using in situ photopatterned nanoporous polymer membranes. *Anal Chem* 2004;76:2367-73.
30. Hatch AV, Herr AE, Throckmorton DJ, Brennan JS, Singh AK. Integrated Preconcentration SDS-PAGE of Proteins in Microchips Using Photopatterned Cross-Linked Polyacrylamide Gels. *Anal Chem* 2006;78:4976-84.
31. Holmes DL, Stellwagen NC. Estimation of polyacrylamide gel pore size from Ferguson plots of normal and anomalously migrating DNA fragments. I. Gels containing 3% N,N'-methylenebisacrylamide. *Electrophoresis (Weinheim, Fed Repub Ger)* 1991;12:253-63.
32. Holmes DL, Stellwagen NC. Estimation of polyacrylamide gel pore size from Ferguson plots of linear DNA fragments. II. Comparison of gels with different crosslinker concentrations, added agarose and added linear polyacrylamide. *Electrophoresis (Weinheim, Fed Repub Ger)* 1991;12:612-19.
33. Edwards K, Curtis K, Sailor J, Baeumner A. Universal liposomes: preparation and usage for the detection of mRNA. *Analytical and Bioanalytical Chemistry* 2008;391:1689-702.
34. Wang HY, Foote RS, Jacobson SC, Schneibel JH, Ramsey JM. Low temperature bonding for microfabrication of chemical analysis devices. *Sens Actuators, B* 1997;B45:199-207.
35. Khandurina J, McKnight TE, Jacobson SC, Waters LC, Foote RS, Ramsey JM. Integrated system for rapid PCR-based DNA analysis in microfluidic devices. *Anal Chem* 2000;72:2995-3000.

36. Kirby BJ, Wheeler AR, Zare RN, Fruetel JA, Shepodd TJ. Programmable modification of cell adhesion and zeta potential in silica microchips. *Lab on a Chip* 2003;3:5-10.
37. Hjerten S. Free zone electrophoresis. *Chromatogr Rev* 1967;9:122-219.
38. Hjerten S. High-performance electrophoresis. Elimination of electroendosmosis and solute adsorption. *J Chromatogr* 1985;347:191-8.
39. Siebert STA, Reeves SG, Durst RA. Liposome immunomigration field assay device for Alachlor determination. *Anal Chim Acta* 1993;282:297-305.
40. Munir A, Wang J, Li Z, Zhou HS. Numerical analysis of a magnetic nanoparticle-enhanced microfluidic surface-based bioassay. *Microfluid Nanofluid* 2010;8:641-52.
41. Sadana A, Sii D. Binding kinetics of antigen by immobilized antibody: influence of reaction order and external diffusional limitations. *Biosens Bioelectron* 1992;7:559-68.
42. Kusnezow W, Syagailo YV, Rueffer S, Klenin K, Sebald W, Hoheisel JD, et al. Kinetics of antigen binding to antibody microspots: strong limitation by mass transport to the surface. *Proteomics* 2006;6:794-803.
43. Wang Y-C, Han J. Pre-binding dynamic range and sensitivity enhancement for immuno-sensors using nanofluidic preconcentrator. *Lab Chip* 2008;8:392-4.
44. Goral VN, Zaytseva NV, Baeumner AJ. Electrochemical microfluidic biosensor for the detection of nucleic acid sequences. *Lab Chip* 2006;6:414-21.
45. Kwakye S, Goral VN, Baeumner AJ. Electrochemical microfluidic biosensor for nucleic acid detection with integrated minipotentostat. *Biosens Bioelectron* 2006;21:2217-23.

46. Kwakye S, Baeumner A. An embedded system for portable electrochemical detection. *Sens Actuators, B* 2007;B123:336-43.

CHAPTER 4

MICRO-TOTAL ANALYSIS SYSTEM FOR VIRUS DETECTION: MICROFLUIDIC PRE-CONCENTRATION COUPLED TO LIPOSOME-BASED DETECTION

Abstract

An integrated microfluidic biosensor is presented that combines sample pre-concentration and liposome-based signal amplification for the detection of enteric viruses present in environmental water samples. This microfluidic approach overcomes the challenges of long assay times of cell culture-based methods and the need to extensively process water samples to eliminate inhibitors for PCR-based methods. Here, viruses are detected using an immunoassay sandwich approach with the reporting antibodies tagged to liposomes. Described is the development of the integrated device for the detection of environmentally relevant viruses using feline calicivirus (FCV) as a model organism for human norovirus. *In-situ* fabricated nanoporous membranes in glass microchannels were used in conjunction with electric fields to achieve pre-concentration of virus-liposome complexes and therefore enhance the antibody-virus binding efficiency. The concentrated complexes were eluted to a detection region downstream where captured liposomes were lysed to release fluorescent dye molecules that were then quantified using image processing. This system was compared to an optimized electrochemical liposome-based microfluidic biosensor without pre-concentration. The limit of detection of FCV of the integrated device was at 1.6×10^5 PFU/mL an order of magnitude lower than that obtained using the microfluidic biosensor without pre-concentration. This significant improvement demonstrates that the integrated device has the potential to serve as an early screening

system for viruses in environmental water samples as it can serve as pre-concentrator and pre-purification step for a highly sensitive rapid immunoassay.

Introduction

Enteric viruses are any one of over 100 species that infect humans or animals via the fecal-oral route and primarily infect and replicate in the gastrointestinal tract.

Although these viruses are commonly associated with gastroenteritis, they can cause a range of diseases, including respiratory infections, hepatitis, conjunctivitis, and meningitis (1). They have even been linked to chronic diseases like insulin-dependent diabetes (2).

Once infected, humans or host animals shed virus particles in feces. Enteric viruses are then introduced into water systems mostly through leaking sewage and septic systems, urban and agricultural runoff, and directly from untreated or under-treated wastewater. Outbreaks have been linked not only to contaminated drinking water, but also contaminated recreational and irrigation water as well as shellfish harvested from contaminated waters (3). These pathogenic viruses are highly resistant to changes in pH and temperature, as well as to common methods of wastewater treatment. It has been shown that these viruses can remain infective for up to 130 days in seawater, 120 days in freshwater and sewage, and 100 days in soil (1). Depending on the source of contamination and water supply in question, virus particles can be present in low concentrations, complicating both detection and sterilization methods.

Current detection methods for enteric viruses can be divided into two main categories: cell culture assays and molecular methods. The cell culture technique was the most popular method for detection of enteric viruses prior to the development of the Polymerase Chain Reaction (PCR) and remains the method of choice to isolate and determine infectivity of viruses. The cell culture technique requires the inoculation of a cell line, chosen based on the virus of interest, and incubating for days to weeks as it is evaluated for the cytopathogenic effects of a viral infection (4). This long incubation time is an obvious drawback of the cell culture assay, though it is not the only one; some viruses do not grow on established cell lines, grow too slowly, or just do not show any visible cytopathogenic effects.

The molecular methods most commonly used for the detection of enteric viruses are variations of conventional PCR (5) or reverse transcriptase-PCR (RT-PCR) (6), including real-time PCR (7) and multiplex PCR (8), as well as Nucleic Acid Sequence-Based Amplification (NASBA) (9). These methods allow for the rapid, sensitive, and specific detection of enteric viruses of interest. The primary drawback to these molecular methods is the inability to limit detection to only infective viruses. However, this can be remedied by the use of integrated cell culture RT-PCR. This method involves inoculating a cell line with the sample and incubating for a short time, usually far before cytopathogenic effects are evident. Nucleic acids can then be extracted from the culture and processed through RT-PCR, testing for viral mRNA that would be produced only if the sample contained infective viruses. This process can, however, decrease the efficiency of detection (10).

As some enteric viruses are not cultivable and molecular techniques sacrifice efficiency of detection for an ability to identify infective viruses, many countries, including the United States, rely on indicators of fecal contamination - enterococci, coliform bacteria - rather than direct testing. Reliance on these indicators is flawed, as viruses are more resistant to disinfection processes and natural environmental conditions (11, 12).

Feline calicivirus (FCV) is a member of the *caliciviridae* family that causes respiratory and potentially severe systemic disease in cats. FCV is used as a model for human pathogenic noroviruses, as it is a member of the same family as these viruses but is non-pathogenic to humans (13). Enzyme-Linked Immunosorbent Assays (ELISAs) for the detection of FCV have been previously described, which use either two antibodies (14) or one antibody and one transmembrane glycoprotein (15). Detection limits were not reported, as the developed ELISAs were used to screen antibodies (14) or determine the binding domain of the glycoprotein (15). However, methods have been reported employing Atomic Force Microscopy (AFM) and Surface-Enhanced Raman Spectroscopy (SERS) for detection of FCV with limits of detection of 3 million and 1million virions/mL, respectively (16).

Biosensors are an attractive detection method for molecules and small particles, such as virions, as they can produce rapid, sensitive and specific signals (17-22). Both microfluidic and lateral flow assays using liposome nanovesicles as a visual or electrochemical signal generation and amplification system have been well-established

using nucleic acids ([17-22](#)) and antibodies ([23-25](#)) as capture molecules, depending on the target being detected. Additionally, novel biological recognition elements have been employed in similar assays, such as using ganglioside-incorporating liposomes for the detection of cholera toxin subunit B ([26](#)).

The often-low concentration of virions in water samples can be a challenge ([11](#)). Addressing this, herein described is the use of a microfluidic device combining pre-concentration and fluorescent detection, previously described ([27](#)), to detect FCV. As shown in Figure 4.1.a, pre-concentration of the virus particles can be achieved by first allowing liposomes tagged with specific anti-FCV antibodies to bind, and then actuating the complexes toward a nanoporous membrane via electrokinesis ([27, 28](#)). These complexes can then be eluted from the membrane as a bolus and applied to a downstream capture and detection zone, where the non-specifically bound liposomes may be washed away prior to lysis and signal quantification. This was compared to an optimized microfluidic electrochemical detection assay, outlined in Figure 4.1.b, in which all incubation steps are conducted off-chip, in suspension.

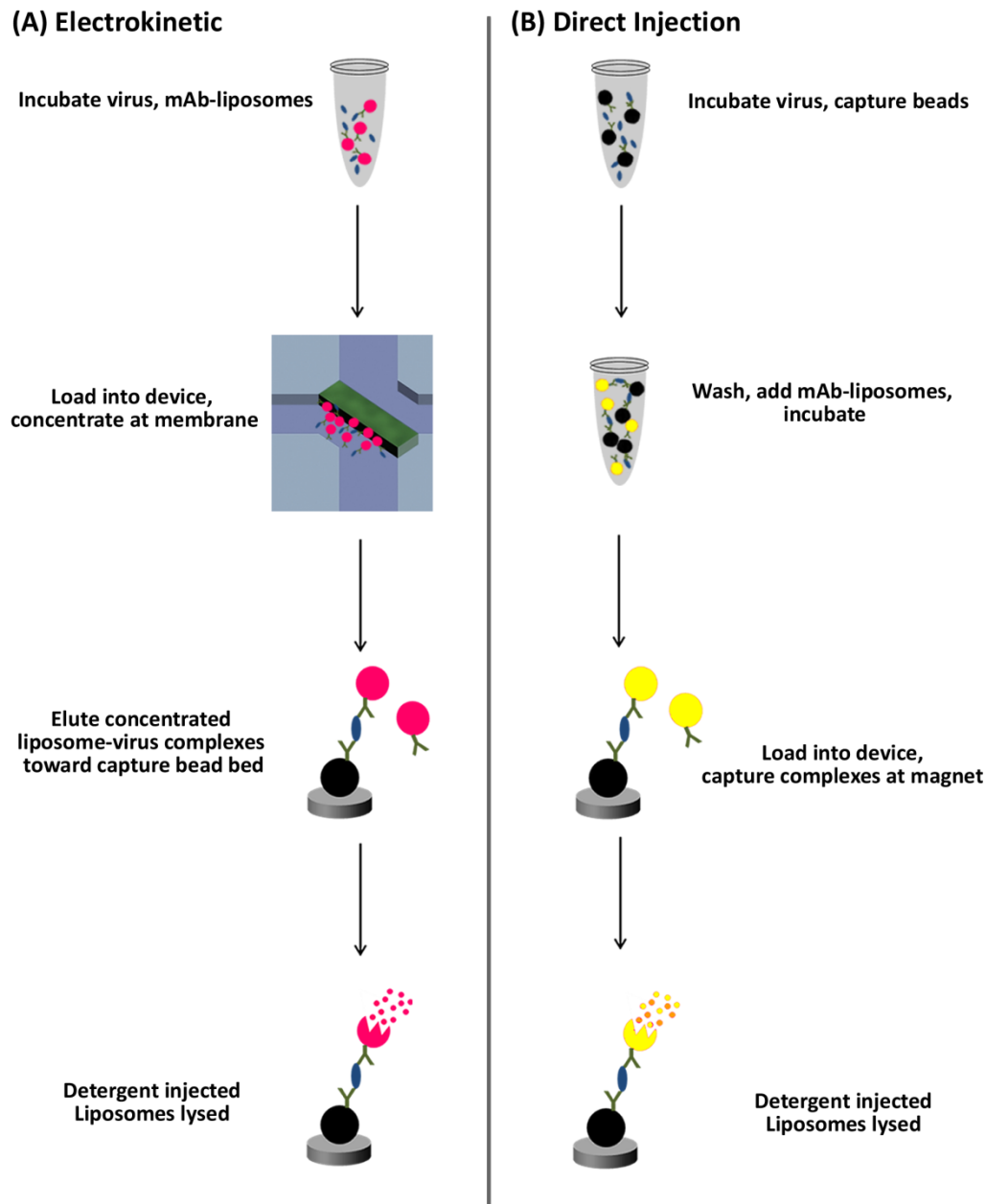


Figure 4.1: Schematic of Assays with and without Pre-concentration.

The assay employing electrokinetic pre-concentration (A) begins with loading the device with anti-FCV pAb-labeled Protein A superparamagnetic beads to create a capture bed and incubating the anti-FCV mAb-labeled fluorescent liposomes with FCV. The sample is then loaded into the inlet well, concentrated at the nanoporous membrane and eluted toward the capture bead bed. Following washing, detergent is injected to lyse the liposomes, releasing the fluorescent dye for quantification. The assay without pre-concentration (B) begins with incubating an FCV sample with the same capture beads as before. The virus-bead complexes are washed and incubated with electrochemical liposomes. This sample is pulled into the microfluidic channel, where the detection complexes are captured at a magnet and washed and the bound liposomes are lysed with detergent. This releases the electroactive species, which undergoes redox cycling at a downstream IDUA.

Materials & Methods

FCV purification and titration

The F9 vaccine strain of FCV (ATCC; VR-782) was propagated on Crandell-Reese feline kidney (CRFK) cells (ATCC; CCL-94). Viral stocks were prepared from twice plaque-purified viruses. Purified FCV-F9 was prepared and titrated as previously described (29, 30), by extraction from cell lysates using trichlorotrifluoroethane followed by banding of virus on CsCl gradients (1.30 - 1.45 g/ml). Purified virus was dialysed into 150 mM NaCl, 10 mM Tris base, 15 mM MgCl₂, pH 7.2 then stored at 4°C prior to use.

Biotinylation of antibodies

Biotin was conjugated to antibodies using the EZ-Link® NHS-PEG₄-Biotin kit and purified using the Slide-A-Lyzer® mini-dialysis kit (Pierce Rockford, IL). Briefly, 100µL of 1mg/mL antibodies were added to the Slide-A-Lyzer tubes and dialyzed against 1X PBS, pH 7.0, to exchange the buffer and assure appropriate pH. Biotin was then added at more than a 20-molar excess to assure good conjugation at the relatively low antibody concentration, and the samples were incubated for 30 min at room temperature. The samples were again dialyzed against 1X PBS, pH 7.0, in order to remove the excess biotin. Samples were collected out of the dialysis tubes and stored in the refrigerator.

Preparation of capture beads

Polyclonal anti-FCV antibodies (Baker Institute, Ithaca, NY) were purified from rabbit serum with a HiTrap Protein A HP column (GE Healthcare Uppsala, SE) as per manufacturer suggestions. Once purified, polyclonal antibodies were then conjugated to Protein-A magnetic beads from Dynabeads Immunoprecipitation kit (Invitrogen, Carlsbad, CA) as per manufacturer provided instructions.

Preparation of streptavidin-conjugated liposomes

Fluorescent streptavidin-conjugated liposomes were prepared via the reverse-phase evaporation method with 150 mM sulforhodamine B (SRB), 20 mM HEPES, pH 7.5, as the encapsulant as previously described (31) with modification. To allow for visualization of the liposomes during the concentration procedure, a fluorophore-labeled lipid (Avanti Polar Lipids Alabaster, AL), 0.33 mol% 1,2-dipalmitoyl-*sn*-glycero-3-phosphoethanolamine-N-(lissamine rhodamine B sulfonyl), was added to the initial lipid mixture. Liposomes coupled to streptavidin were incubated for 15 minutes at room temperature with 1 µg anti-FCV monoclonal antibody (Abcam Cambridge, MA), biotinylated as above. The liposome-antibody conjugate was then diluted to a working phospholipid concentration of 0.7 mM.

Liposomes with the same bilayer composition and streptavidin-modification were also prepared with an encapsulant of potassium ferri/ferrohexacyanide with a combined concentration of 200 mM for experiments using amperometric detection. These liposomes were prepared in 1X HEPES-Saline-Sucrose (1X HSS), containing 10 mM

HEPES, 200 mM NaCl, and 200mM sucrose, pH 7.5, but the liposomes were then dialyzed against 1X PBS, 20 mM sucrose, pH 7.5, as HEPES has been shown to interfere with electrochemistry (32, 33).

Microtiter plate liposome immunoassay (LIA) for antibody selection

Previously reported protocols for the use of liposomes in microtiter (34) were adapted and modified for virus detection. High-binding Nunc Maxisorb® polystyrene plates were prepared for a Liposome Immunoassay (LIA) by washing each well with 200 μ L of 1X PBS. Anti-FCV antibodies were diluted with 1X PBS to 5 μ g/mL and 200 μ L were added to each well. The plates were then incubated overnight in the refrigerator. After incubation, wells were emptied, tapped dry, and washed with 200 μ L of 1X PBS. Wells were blocked for 1 hour at room temperature with 200 μ L of blocking reagents containing either 0.05% Tween-20 or 0.1% Tween-20 in 1X PBS. Plates were then emptied, dried and washed twice with 200 μ L per well of 1X PBS.

Prepared plates were then loaded with 100 μ L per well of varying concentrations of FCV in 1X PBS in triplicate and incubated for 2 hours in the refrigerator with gentle shaking. Wells were tapped dry and washed twice with 200 μ L of 1X PBS.

Biotinylated anti-FCV antibodies were diluted in 1X PBS to a concentration of 1 μ g/mL, and 100 μ L of solution was added to each well. Plates were incubated for 1 hour at room temperature with gentle shaking.

The plates were washed twice in 200 μL per well of 1X HSS. Streptavidin-conjugated liposomes diluted to 50 μM phospholipids concentration and 100 μL were added to each well. Plates were again incubated for 1 hour at room temperature with gentle shaking.

Plates were emptied, dried, and washed three times with 200 μL per well 1X HSS, respectively. For measuring the fluorescence emission at 590 nm, 50 μL of 30 mM octyl- β -D-glucopyranoside (OG) was added to each well.

Concentration and Detection of FCV

Prior to performing concentration and detection experiments, the channels of the device, shown in Figure 4.2, were primed with 1X HSS. A permanent magnet was positioned on the top surface of the device upstream of the detection region by use of adhesive putty. One microliter of polyclonal-antibody-conjugated superparamagnetic beads was injected towards the magnet through port 5 using a syringe pump at a flow rate of 1 $\mu\text{L}/\text{min}$. The packed bead bed at the magnet constitutes the capture region of the device. The liposome-antibody conjugate was then mixed with FCV of the required concentration and incubated for two hours. This virus-liposome solution was loaded into the inlet well of the device whereas all the other wells were filled with 1X HSS. The pressure-driven flow in the system was eliminated by adjusting the heights of the solutions in the wells. The virus-liposome complexes were then electrokinetically concentrated at the membrane by applying a voltage difference of 150 V across the membrane. After concentrating for a 90 seconds, the concentrated

bolus was eluted towards the bead bed by applying a voltage of 150 V to the outlet port 3 downstream of the magnet. This results in the capture of the virus-liposome complexes at the bead bed, as illustrated in Figure 4.1. Wash buffer was injected at a flow rate of 20 $\mu\text{L/h}$ to wash off any unbound liposomes in the device through port 5. A detergent solution of 60 mM OG was then introduced through the same port towards the bead bed at a flow rate of 40 $\mu\text{L/h}$ and the emitted fluorescence from the lysis of the bound liposomes was recorded downstream of the bead bed. Video was captured during lysis, and the fluorescent intensity was integrated over time to yield the final signal.

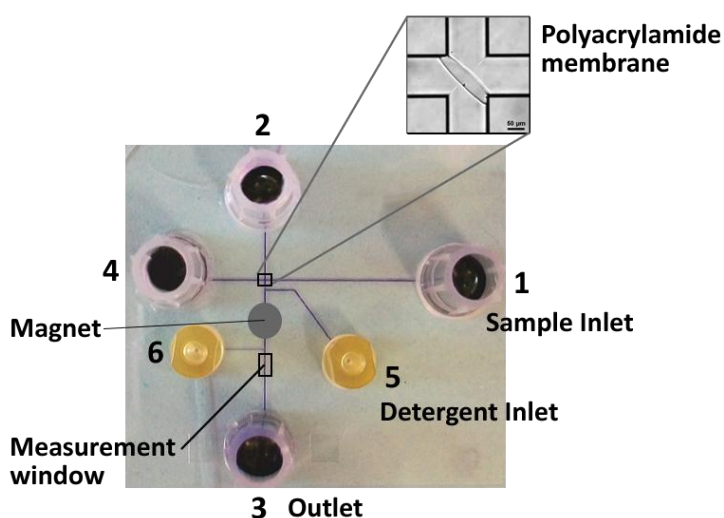


Figure 4.2: Combined Concentration and Detection Device.

After the channels are filled with 1XHSS and the capture bead bed is packed at the magnet, a virus-liposome solution is introduced to port 1 and a potential is applied across the membrane (inset). Once concentrated, the virus-liposome bolus is eluted from the membrane by switching the potential to port 3, downstream of the magnet. Once the sample is captured, non-specifically bound liposomes are washed away by wash buffer, applied via port 5 using pressure-driven flow. Liposomes are then lysed using a detergent introduced through the same port. (Note: device filled with visible dye for illustrative purposes)

Detection of FCV without Electrokinetic Concentration

To show the effect of pre-concentration on detection of FCV, the assay was also carried out in a microfluidic device outfitted with an interdigitated ultramicroelectrode array (IDUA) fabricated on polymethylmethacrylate (PMMA), shown in Figure 4.3, as previously described (35). The assay without electrokinetic concentration is similar to the procedure outlined above with several modifications required for the electrochemical transducer and pressure-driven flow. Streptavidin-conjugated liposomes encapsulating the ferri/ferrohexacyanide redox couple were substituted for those encapsulating SRB. To provide the most pertinent comparison, the procedure used was that which proved optimal for the device. Polyclonal antibody-conjugated Protein A superparamagnetic beads were prepared as described and 5 μL were mixed with 70 μL of FCV in Dulbecco's Modified Eagle's Media (DMEM) with 10% fetal bovine serum (FBS) and incubated, gently shaking at room temperature for 10min. The sample was then applied to a magnet, separating the beads such that they could be washed twice with 75 μL 1X PBS, once with 75 μL 1X PBS with 0.2 M Sucrose (1X PBSS), and finally resuspended in 5 μL 1X PBSS. To this sample, 5 μL monoclonal antibody-coupled electrochemical liposomes were added and incubated, gently shaking at room temperature for 10 min. This sample was then pulled into the device, captured at the magnet and washed with 20 μL 1X PBSS at 5 $\mu\text{L}/\text{min}$ to remove any unbound liposomes. Liposomes were then lysed, releasing the electroactive species to produce a signal, by the injection of 30 μM OG at 1 $\mu\text{L}/\text{min}$ until the signal returned to baseline. Potential was applied and signals recorded using an Epsilon Electrochemical Analyzer (BASi, West Lafayette, IN) as previously described (26).

Though using a different signal transduction method, previous work has shown detection limits on the same order of magnitude for fluorescent and electrochemical transduction (36).

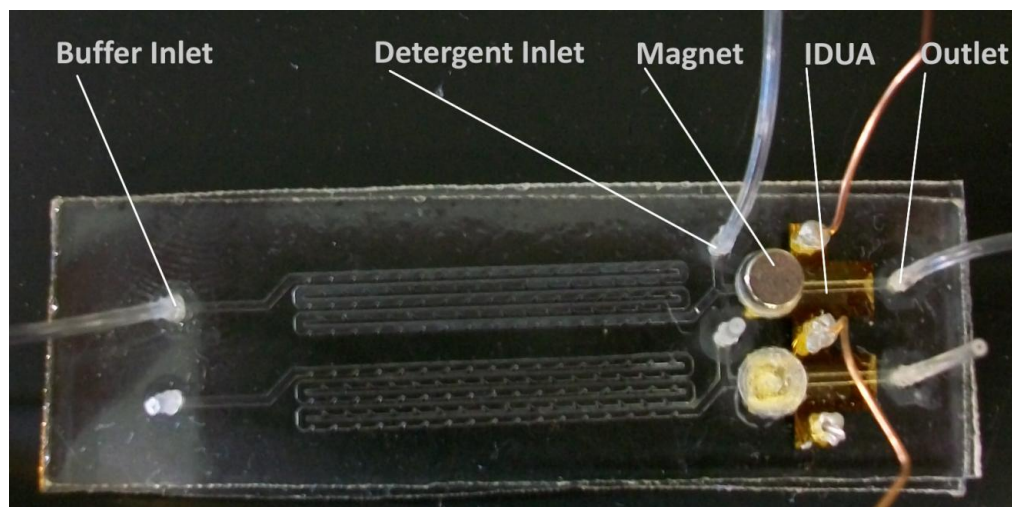


Figure 4.3: Device without pre-concentration module.

The device, fabricated in PMMA has two microfluidic channels and IDUAs side-by-side for two separate samples. The sample is pulled into the device through the Outlet via negative pressure on the Buffer Inlet, allowing for the capture of the detection complexes at the magnet. The sample is then washed by buffer flow actuated via the Buffer Inlet and bound liposomes are lysed with the introduction of OG through the detergent inlet. Signals are obtained by applying a potential across the IDUA and recording the current resulting from the oxidation-reduction cycling of the electroactive encapsulant.

Results & Discussion

For the development of the integrated device for pre-concentration and detection of viruses, a standard immunoassay using liposome amplification was initially developed using a microtiter plate format. This was subsequently transformed to capture antibodies immobilized on superparamagnetic beads and implemented with fluorescent liposomes in the integrated device. Secondly, the assay was adapted to a microfluidic electrochemical biosensor using electrochemical liposomes as these have

been found to be as sensitive as fluorescent liposomes (36) and enable the development of portable and rapid microfluidic biosensors requiring little hardware (37).

Selection of Antibodies and Assay Optimization

A series of commercially available and custom antibodies were screened via the microtiter plate LIA described and a sample of highly-purified FCV in PBS. It was found that many antibody pairs would not result in effective capture and detection of FCV. Some pairs generated highly reproducible results and representative data of two combinations are shown in Figure 4.4; here, antibody pairs employing the polyclonal antibody as capture antibody generated high signals and signal-to-noise ratios (SNR). Based on all combinations tried, it was determined that using a custom polyclonal rabbit-derived anti-FCV for capture was best in conjunction with the monoclonal labeled mAb1 (Abcam clone number FCV1-43) as it yielded an SNR just under 9 for a concentration of 5000 ng/mL.

Further optimization of the assay employed FCV in lysed cell culture medium, containing DMEM with 10% FBS, and focused on blocking to reduce non-specific binding. A dose-response curve was developed for the microtiter LIA for future comparison to microfluidic devices, as shown in Figure 4.5. Here, the limit of detection is approximately 4×10^4 PFU/mL.

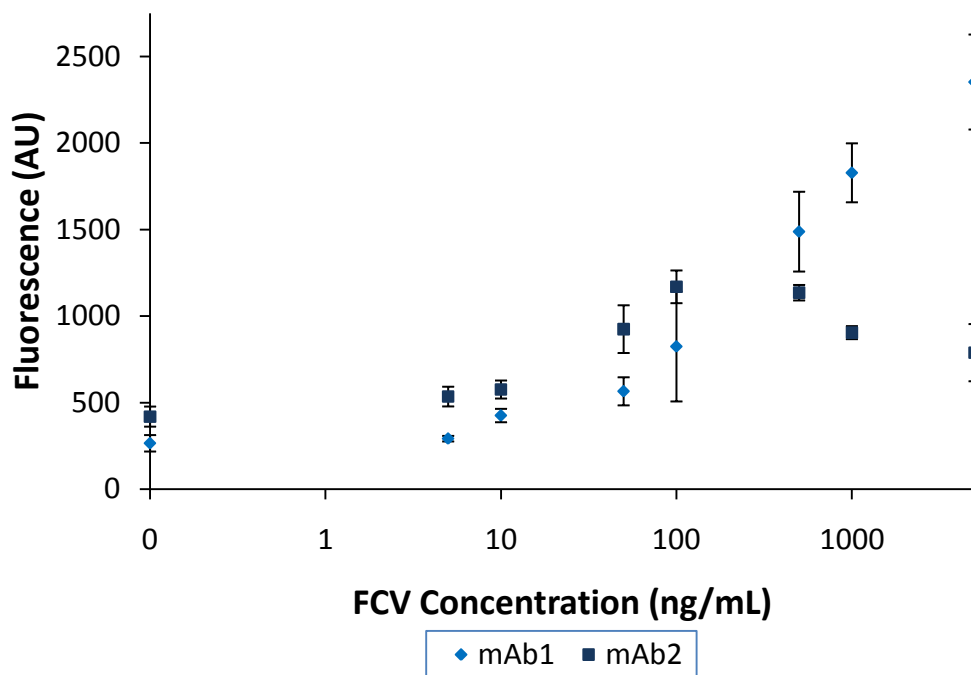


Figure 4.4: Dose-response curves for polyclonal capture antibody with monoclonal reporter antibodies. The best antibody pair for the detection of FCV was determined by screening all variations in a microtiter plate liposome immunoassay (LIA). Here a custom polyclonal anti-FCV was immobilized to the plate and biotinylated anti-FCV monoclonal antibodies and streptavidin-conjugated fluorescent liposomes were used for signal generation.

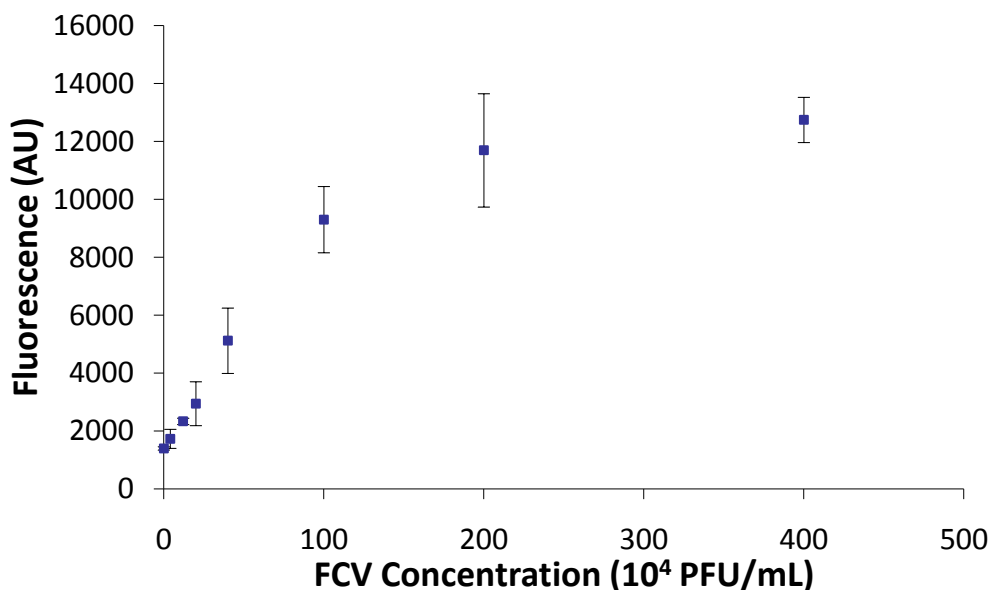


Figure 4.5: Optimized assay for FCV detection in cell culture lysate.

Using the previously optimized antibody pairs, FCV was detected in cell culture lysate consisting of DMEM and 10% FBS in a microtiter plate LIA.

Comparison of FCV detection with and without electrokinetic concentration:

FCV detection experiments were performed to show the improvement in detection sensitivity with the inclusion of the electrokinetic pre-concentration step. In the first set of experiments, FCV was detected by use of the integrated microfluidic device that includes the pre-concentration step. Fluorescent liposomes were used in these experiments and the fluorescence intensity signal from the lysis of the captured liposomes was estimated using image processing. These experiments were done for different concentrations of FCV ranging from 0 – 6.0×10^5 PFU/ml. The limit of detection for these experiments performed with the integrated device was estimated, from the data shown in Figure 4.6, to be 1.6×10^5 PFU/ml.

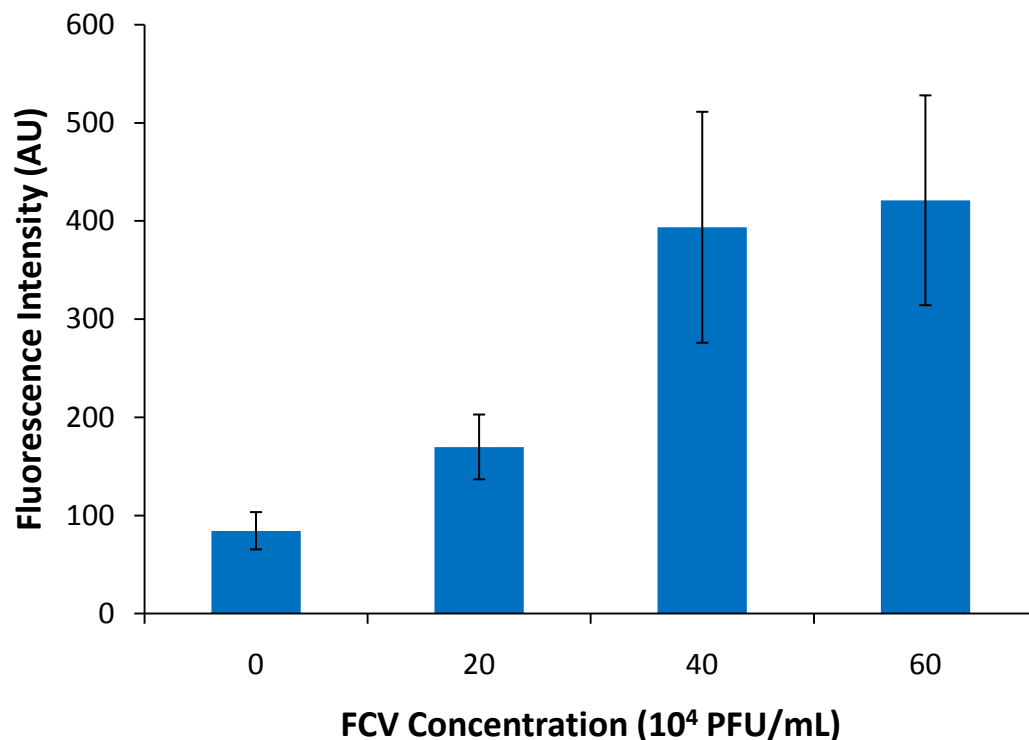


Figure 4.6: FCV detection after electrokinetic concentration.

FCV samples were incubated with anti-FCV-coupled liposomes for two-hours at the indicated concentrations. Samples were then concentrated for 90 sec by application of a potential across a nanoporous membrane and then eluted to the capture bead bed. After washing, liposomes were lysed with detergent and the fluorescence intensity downstream was integrated over time.

A second set of experiments were performed excluding the pre-concentration step by directly injecting the virus-liposome-bead detection complexes towards the magnet. Electrochemical liposomes were used in these experiments and the integrated current signal from the lysis of the captured liposomes is plotted as a function of the concentration of FCV as shown in Figure 4.7. The limit of detection in this case was estimated as 3.2×10^6 PFU/mL, as it is more than 3 standard deviations above the negative control.

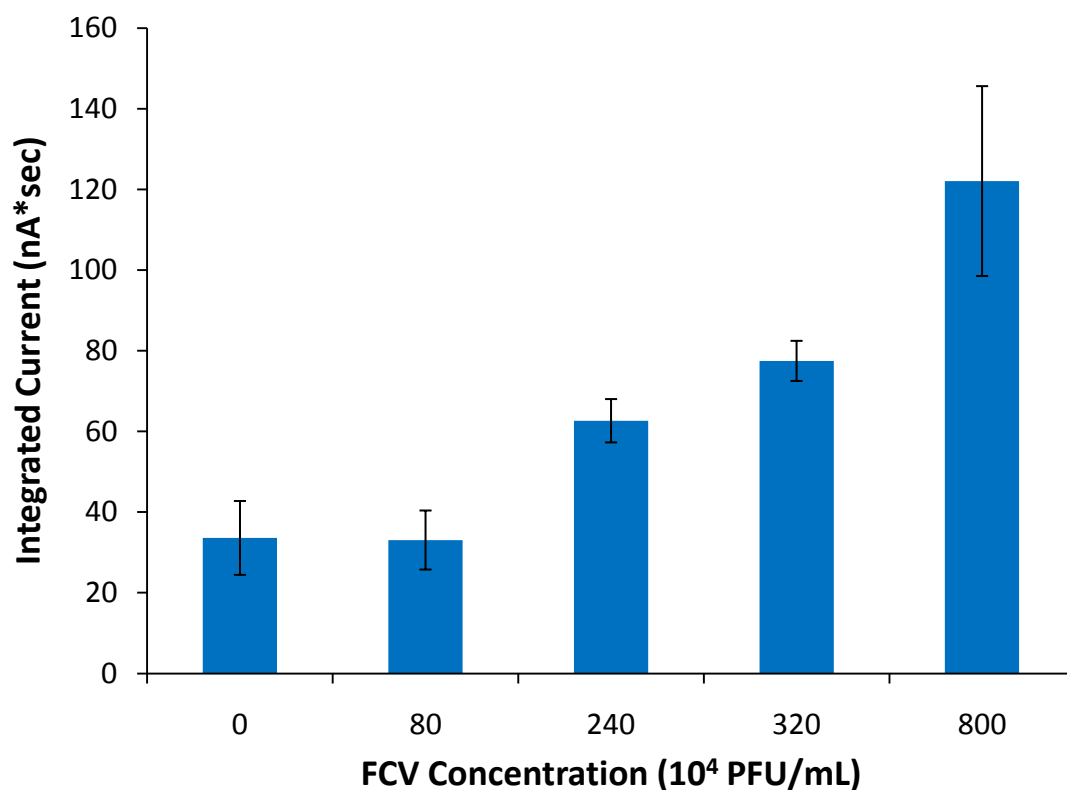


Figure 4.7: FCV detection without pre-concentration.

FCV samples were incubated with anti-FCV-coupled magnetic beads and anti-FCV-coupled liposomes for a total of 20 min, with wash steps, at the indicated concentrations. Samples were then injected into a microfluidic channel toward a magnet, where the detection complexes were captured and washed. Bound liposomes were lysed with detergent and the current measured across the IDUA resulting from the released electroactive species was integrated over time.

There is an order of magnitude improvement in the limit of detection with the integrated microfluidic device over the direct injection system as the increased concentration of the analytes improves the antibody-antigen binding kinetics in the detection region. This improvement is more remarkable as the direct injection device employed an optimized procedure allowing the magnetic beads, virus and liposomes to incubate, sequentially, off-chip in solution. This takes advantage of the bead surface area and should provide ample antibody-antigen interaction. Future planned experiments will include the addition of electrochemical detection into the integrated device in order to render it more field-portable. The equipment needed for electrochemical detection is relatively inexpensive, portable and can provide quantitative signal read-out making it better suited for on-site detection than the currently employed fluorescence-based detection described here (38).

Current literature reports limits of detection of FCV on the order of 10^6 particles/mL using Surface Enhanced Raman Spectroscopy (SERS) (39). Concentration is not easily converted from virus particles/mL to PFU/mL as they require the estimation of the infectivity, which is dependent not just on the particular strain but also the cell culture media and cell line. Based on an approximate ratio of infectious to non-infectious particles for enteric viruses in general (40), this corresponds to a limit of detection on the order of 10^4 PFU/mL, which is comparable, though lower, than that reported herein. Although there have been strides in the miniaturization of SERS instruments, the equipment costs approximately \$15,000 (41) and is best suited to laboratory analysis, particularly due to the approximately 20 hours of incubation time required for the

assay. Instead, the reported device, adapted for electrochemical detection, will be well suited to field portable assays due to its significantly shorter assay time of only xxx hours, small size, and comparable sensitivity.

Most of the portable microfluidic biosensors for enteric virus detection reported in the literature are based on RT-PCR techniques (42-44). PCR is highly susceptible to inhibitors, primarily humic acid, that are present in environmental water samples, which can reduce sensitivity or completely inhibit the signal (45). Further, microfluidic PCR systems also face the challenges of adsorption of enzymes to channel walls (46), difficulty in precisely controlling temperature, sample evaporation and formation of bubbles in the channels (47). The advantage of our integrated microfluidic device is that it has on-chip detection times on the order of a few minutes and does not involve any temperature cycling issues.

Conclusion

Using a device integrating a liposome immunoassay with an upstream pre-concentration of the virus-liposome complexes, we have shown a limit of detection of 1.6×10^5 PFU/mL for FCV. This detection limit is an order of magnitude lower than that obtained with an equivalent detection device that does not include pre-concentration. The here described system can be extended to electrochemical detection by patterning gold electrodes in the device and using electrochemical liposomes similar to those used in the described PMMA device. Electrochemical detection is inexpensive and portable with quantitative signal readout.

In addition, the current protocol described uses a concentration time of 90 seconds. This does by no means deplete the 60 μ L sample of virus-liposome complexes. However, it was chosen as the high voltage employed coupled with the high conductivity of liposome diluent lead to resistive heating of the sample when longer times were used. In the future, we intend to avoid this problem by using several short pulses, sending several boluses of highly concentrated virus-liposome complexes to the capture bead bed. As significantly more liposome-virus complexes would end up concentrated on the membrane, we predict that this would result in a limit of detection decreased at least by an order of magnitude.

Acknowledgments

This publication was made possible by USEPA cooperative agreement #CR-83360101. Its contents are solely the responsibility of the recipient and do not necessarily represent the official views of the USEPA. Further, USEPA does not endorse the purchase of any commercial products or services mentioned in the publication.

REFERENCES

1. Fong T-T, Lipp EK. Enteric Viruses of Humans and Animals in Aquatic Environments: Health Risks, Detection, and Potential Water Quality Assessment Tools. *Microbiol Mol Biol Rev* 2005;69:357-71.
2. Wagenknecht LE, Roseman JM, Herman WH. Increased incidence of insulin-dependent diabetes mellitus following an epidemic of coxsackievirus B5. *American Journal of Epidemiology* 1991;133:1024–31.
3. Le Guyader FS, Atmar RL. Viruses in Shellfish. In: Bosch A, ed. *Human Viruses in Water*, Vol. 17. Amsterdam, The Netherland: Elsevier, 2007:205-26.
4. Block JC, Schwartzbrod L. *Viruses in water systems : detection and identification*. New York, N.Y.; Weinheim, Federal Republic of Germany: VCH Publishers ; VCH Verlagsgesellschaft, 1989.
5. Saiki RK, Gelfand DH, Stoffel S, Scharf SJ, Higuchi R, Horn GT, et al. Primer-directed enzymatic amplification of DNA with a thermostable DNA polymerase. *Science* 1988;239:487-91.
6. Parshionikar SU, Willian-True S, Fout GS, Robbins DE, Seys SA, Cassady JD, Harris R. Waterborne Outbreak of Gastroenteritis Associated with a Norovirus. *Appl Environ Microbiol* 2003;69:5263-8.
7. Pusch D, Oh DY, Wolf S, Dumke R, Schröter-Bobsin U, Höhne M, et al. Detection of enteric viruses and bacterial indicators in German environmental waters. *Archives of Virology* 2005;150:929-47.
8. Fout GS, Martinson BC, Moyer MWN, Dahling DR. A Multiplex Reverse Transcription-PCR Method for Detection of Human Enteric Viruses in Groundwater. *Appl Environ Microbiol* 2003;69:3158-64.
9. Rutjes SA, van den Berg HHJL, Lodder WJ, de Roda Husman AM. Real-Time Detection of Noroviruses in Surface Water by Use of a Broadly Reactive Nucleic Acid Sequence-Based Amplification Assay. *Appl Environ Microbiol* 2006;72:5349-58.

10. Wyn-Jones P. The Detection of Waterborne Viruses. In: Bosch A, ed. Human Viruses in Water, Vol. 17. Amsterdam, The Netherlands: Elsevier, 2007:177-204.
11. Jofre J. Indicators of Waterborne Enteric Viruses. In: Bosch A, ed. Human Viruses in Water, Vol. 17. Amsterdam, The Netherlands: Elsevier, 2007:227-49.
12. Bosch A. Human enteric viruses in the water environment: a minireview. *International Microbiology* 1998;1:191-6.
13. Tree JA, Adams MR, Lees DN. Disinfection of feline calicivirus (a surrogate for Norovirus) in wastewaters. *Journal of Applied Microbiology* 2005;98:155-62.
14. Tajima T, Takeda Y, Tohya Y, Sugii S. Reactivities of Feline Calicivirus Field Isolates with Monoclonal Antibodies Detected by Enzyme-Linked Immunosorbent Assay. *The Journal of Veterinary Medical Science* 1998;60:753-5.
15. Ossiboff RJ, Parker JSL. Identification of Regions and Residues in Feline Junctional Adhesion Molecule Required for Feline Calicivirus Binding and Infection. *Journal of Virology* 2007;81:13608-21.
16. Porter MD, Driskell JD, Kwartka KM, Lipert RJ, Neill JD, Ridpath JF. Detection of Viruses: Atomic Force Microscopy and Surface Enhanced Raman Spectroscopy. *Developments in Biologicals* 2006;126:31-9.
17. Esch MB, Baeumner AJ, Durst RA. Detection of *Cryptosporidium parvum* Using Oligonucleotide-Tagged Liposomes in a Competitive Assay Format. *Analytical Chemistry* 2001;73:3162-7.
18. Hartley HA, Baeumner AJ. Biosensor for the Specific Detection of a Single Viable *B. anthracis* Spore. *Analytical and Bioanalytical Chemistry* 2003;376:319-27.
19. Connelly J, Nugen S, Borejsza-Wysocki W, Durst R, Montagna R, Baeumner A. Human pathogenic *Cryptosporidium* species bioanalytical detection method

with single oocyst detection capability. *Analytical and Bioanalytical Chemistry* 2008;391:487-95.

20. Baeumner AJ, Schlesinger NA, Slutzki NS, Romano J, Lee EM, Montagna RA. A Biosensor for Dengue Virus Detection: Sensitive, Rapid and Serotype specific. *Analytical Chemistry* 2002;74:1442 – 8.
21. Zaytseva NV, Montagna RA, Lee EM, Baeumner AJ. Multi-analyte single-membrane biosensor for the serotype-specific detection of Dengue virus. *Analytical and Bioanalytical Chemistry* 2004:46-53.
22. Baeumner AJ, Cohen RN, Miksic V, Min JH. RNA Biosensor for the Rapid Detection of Viable *Escherichia coli* in Drinking Water. *Biosensors & Bioelectronics* 2003;18:405 – 13.
23. DeCory T, Durst RA, Zimmerman S, Garringer L, Paluca G, DeCory H, Montagna RA. Development of an Immunomagnetic Bead-Immunoliposome Fluorescence Assay for Rapid Detection of *Escherichia coli* O157:H7 in Aqueous Samples and Comparison of the Assay with Standard Microbiology Method. *Applied and Environmental Microbiology* 2005;71:1856-64.
24. Kim M, Oh S, Durst RA. Detection of *Escherichia coli* O157:H7 Using Combined Procedure of Immunomagnetic Separation and Test Strip Liposome Immunoassay. *Journal of Microbiology and Biotechnology* 2003;13:509-16.
25. Park S, Durst RA. Modified Immunoliposome Sandwich Assay for the Detection of *Escherichia coli* O157:H7 in Apple Cider. *Journal of Food Protection* 2004;67:1568-73.
26. Bunyakul N, Edwards K, Promptmas C, Baeumner A. Cholera toxin subunit B detection in microfluidic devices. *Analytical and Bioanalytical Chemistry* 2008.
27. Kondapalli S, Connelly JT, Baeumner AJ, Kirby BJ. Integrated microfluidic preconcentrator and immunobiosensor for pathogen detection. *Microfluidics and Nanofluidics* 2011;Accepted.

28. Song S, Singh AK, Kirby BJ. Electrophoretic Concentration of Proteins at Laser-Patterned Nanoporous Membranes in Microchips. *Anal Chem* 2004;76:4589-92.
29. Ossiboff RJ, Sheh A, Shotton J, Pesavento PA, Parker JSL. Feline caliciviruses (FCVs) isolated from cats with virulent systemic disease possess *in vitro* phenotypes distinct from those of other FCV isolates. *Journal of General Virology* 2007;88:506-17.
30. Ossiboff RJ, Zhou Y, Lightfoot PJ, Prasad BVV, Parker JSL. Conformational Changes in the Capsid of a Calicivirus upon Interaction with Its Functional Receptor. *J Virol* 2010;84:5550-64.
31. Edwards K, Curtis K, Sailor J, Baeumner A. Universal liposomes: preparation and usage for the detection of mRNA. *Analytical and Bioanalytical Chemistry* 2008;391:1689-702.
32. Masson J-F, Gauda E, Mizaikoff B, Kranz C. The interference of HEPES buffer during amperometric detection of ATP in clinical applications. *Analytical & Bioanalytical Chemistry* 2008;390:2067-71.
33. Welch KD, Davis TZ, Aust SD. Iron Autoxidation and Free Radical Generation: Effects of Buffers, Ligands, and Chelators. *Archives of Biochemistry and Biophysics* 2002;397:360-9.
34. Edwards KA, Baeumner AJ. Optimization of DNA-tagged liposomes for use in microtiter plate analyses. *Analytical & Bioanalytical Chemistry* 2006;386:1613-23.
35. Nugen SR, Asiello PJ, Connelly JT, Baeumner AJ. PMMA biosensor for nucleic acids with integrated mixer and electrochemical detection. *Biosensors and Bioelectronics* 2009;24:2428-33.
36. Goral VN, Zaytseva NV, Baeumner AJ. Electrochemical microfluidic biosensor for the detection of nucleic acid sequences. *Lab on a Chip* 2006;6:414-21.
37. Kwakye S, Baeumner A. An embedded system for portable electrochemical detection. *Sensors and Actuators B: Chemical* 2007;123:336-43.

38. Kwakye S, Baeumner A. An embedded system for portable electrochemical detection. *Sensors and Actuators, B: Chemical* 2007;B123:336-43.
39. Driskell JD, Kwarta KM, Lipert RJ, Porter MD, Neill JD, Ridpath JF. Low-Level Detection of Viral Pathogens by a Surface-Enhanced Raman Scattering Based Immunoassay. *Analytical Chemistry* 2005;77:6147-54.
40. Kopecka H, Dubrou S, Prevot J, Marechal J, Lopez-Pila JM. Detection of naturally occurring enteroviruses in waters by reverse transcription, polymerase chain reaction, and hybridization. *Appl Environ Microbiol* 1993;59:1213-19.
41. Porter MD, Lipert RJ, Siperko LM, Wang G, Narayanan R. SERS as a bioassay platform: fundamentals, design, and applications. *Chem Soc Rev* 2008;37:1001-11.
42. Lee W-C, Lien K-Y, Lee G-B, Lei H-Y. An integrated microfluidic system using magnetic beads for virus detection. *Diagnostic Microbiology and Infectious Disease* 2008;60:51-8.
43. Li Y, Zhang C, Xing D. Fast identification of foodborne pathogenic viruses using continuous-flow reverse transcription-PCR with fluorescence detection. *Microfluidics and Nanofluidics* 2011;10:367-80.
44. Lien K-Y, Lee W-C, Lei H-Y, Lee G-B. Integrated reverse transcription polymerase chain reaction systems for virus detection. *Biosens Bioelectron* 2007;22:1739-48.
45. Kopecka H, Dubrou S, Prevot J, Marechal J, Lopez-Pila JM. Detection of naturally occurring enteroviruses in waters by reverse transcription, polymerase chain reaction, and hybridization. *Appl Environ Microbiol* 1993;59:1213-9.
46. Zhang C, Xu J, Ma W, Zheng W. PCR microfluidic devices for DNA amplification. *Biotechnology Advances* 2006;24:243-84.
47. Zhang C, Xing D. Miniaturized PCR chips for nucleic acid amplification and analysis: latest advances and future trends. *Nucleic Acids Research* 2007;35:4223-37.

CHAPTER 5

OPTIMIZATION OF MICROFLUIDIC ELECTROCHEMICAL DETECTION CHANNELS FOR LIPOSOME NANOVESICLE-BASED SIGNAL AMPLIFICATION

Abstract

Microfluidic electrochemical biosensors for pathogen detection have been developed previously relying on liposome signal amplification. Here, liposomes entrap an electrochemically active redox couple and are tagged at their outer surface with DNA probes. In the assay, the liposome-coupled probe hybridizes to a nucleic acid target sequence, which in turn hybridizes to a second probe immobilized on a superparamagnetic bead via a sandwich approach. Bound target sequences are isolated in the capture zone via a magnet and subsequently quantified by lysing the liposomes using a detergent. Thus, the entrapped redox couple is released and measured on an electrode downstream of the magnet. Optimization of these systems was investigated leading to a dramatic decrease in the limit of detection achievable. First, the current measured by the interdigitated ultramicroelectrode array (IDUA) was enhanced via changes to the metal layers and assay buffer conditions. Second, the effects of the detection channel dimensions were investigated. It was found that a reduction in the channel height from 50 μm to 20 μm produced an order of magnitude reduction in the limit of detection of a DNA target sequence, a decrease from 0.1fmol to 0.01fmol per assay. This was due to the smaller volume into which liposomes were lysed and hence an overall increased concentration in the microfluidic channels. Additionally, it was determined that too small dimensions resulted in too low volumetric flow rates and

prevented assay conduction as the superparamagnetic beads settled in the inlet hole. Thus, it is concluded that an optimal dimensional range can be identified striking the balance between increased limits of detection and successful execution of assay protocols under realistic time constraints.

Introduction

Microfluidic devices offer a number of advantages as a result of miniaturization, particularly the ability to analyze small sample volumes, integrate multi-step processes into one device, increased portability and potential for high throughput analysis. The pairing of microfluidics and amperometric detection is particularly advantageous as electrodes are readily miniaturized and the reduction in electrode size and spacing allows for the measurements of very low currents (1).

For sensors employing electrochemical transduction that rely on liposome lysis for signal generation, the limit of detection for any analyte can theoretically be decreased by reducing the overall channel volume into which the liposomes are lysed. Since the liposomes contain a set concentration of the oxidation-reduction couple, lysing the same number in a smaller volume will produce a higher overall concentration of the electroactive species. Previous work determined that the lowest detectable concentration of potassium ferri/ferrohexacyanide in 0.1M phosphate buffer, pH 7.0, for a gold IDUA on Pyrex® glass consisting of two sets of 420 interdigitated fingers each being 2.5µm wide and high, separated by a 4.5µm gaps, is 0.5µM (2). Also as previously reported, liposomes extruded through 0.4µm pore polycarbonate filters

have been shown to be unilamellar and have a diameter of approximately 275nm (3). Assuming spherical geometry and that the combined concentration of the encapsulated redox couple is the same as the initial concentration added, 200mM, one can predict the concentration of liposomes needed to reach the limit of detection of 0.5 μ M. Here, that would be approximately 230 liposomes/nL. With the previously reported channel dimensions of 500 μ m wide and 50 μ m deep and assuming that the bead-target complexes are captured within the first 100 μ m of the magnet edge, 574 liposomes would need to be captured in order to produce a detectable concentration. It has also been established that increases in the height of the electrodes yield improved signals and signal-to-noise ratios, as the active surface of the IDUA is the gap face of the individual fingers, and 0.2M potassium phosphate is the optimal concentration of supporting electrolyte for detection of this redox couple using these electrodes (4). Based on these calculations, channels 500 and 50 μ m in width and 50 and 20 μ m deep were tested using a nucleic acid hybridization assay with a synthetic target that has been previously established (2, 5), in order to assess improvements in the analytical sensitivity.

Materials & Methods

All microfabrication was conducted at the Cornell NanoScale Science and Technology Facility (CNF), which also provided chemicals, silicon wafers, and consumables required for processing. Pyrex® borosilicate glass wafers were purchased from Mark Optics (Santa Ana, CA), Ultem™ macro-to-microfluidic connectors and PEEK™ tubing were purchased from LabSmith (Livermore, CA), polyimide-sheathed glass

capillary tubing was obtained from Polymicro Technologies (Phoenix, AZ), Tygon® tubing and thumb screws were purchased from Small Parts, Inc (Miami Lakes, FL), Sylgard® 184 silicone elastomer kit containing polydimethylsiloxane (PDMS) pre-polymer and catalyst was procured from Dow Corning (Midland, MI), and Epo-Tek H20E conductive epoxy was purchased from Epoxy Technology Inc. (Billerica, MA). All experiments were carried out using a BASi Epsilon EC (West Lafayette, IN) and KD Scientific syringe pumps (Holliston, MA).

Lipids used for liposomes were purchased from Avanti Polar Lipids (Alabaster, AL), all nucleotides were provided by Eurofins MWG Operon (Huntsville, AL), and Dynabeads® MyOne™ streptavidin superparamagnetic beads were purchased from Invitrogen (Carlsbad CA). All other chemicals were procured from VWR International (Radnor, PA).

Fabrication of microfluidic channels

Soft lithography was employed for the rapid prototyping of microfluidic channels (6) employing a channel design previously described (7). Briefly, a 100mm silicon wafer was patterned via standard photolithographic techniques and plasma etched using a Bosch process Unaxis 770. Prior to use, the remaining photoresist was stripped in a hot solvent bath (propylene glycol, N-methylpyrrolidone, tetramethylammonium hydroxide) and the master was treated with Rain-X® to create an anti-stiction coating. PDMS elastomer and catalyst were mixed 7:1, degassed, and 15mL was applied to the center of the silicon master, confined in a housing machined to exactly fit the wafer,

and cured for 1 hour at 80°C. Individual channels were peeled from the master, trimmed and ports were punched through to make the necessary connections. PDMS channel layers were sealed, reversibly, to a borosilicate glass slip patterned with an IDUA by sandwiching the device in a polymethylmethacrylate (PMMA) housing with pressure applied using thumbscrews as shown in *Figure 5.1*. Macro-to-microfluidic connections were made using ULTEM™ bonded port connectors for inlets and a PEEK™ tubing post at the outlet attached to the housing. The bottom portion of the housing includes a hole to accommodate a neodymium-iron-boron rare earth magnet.

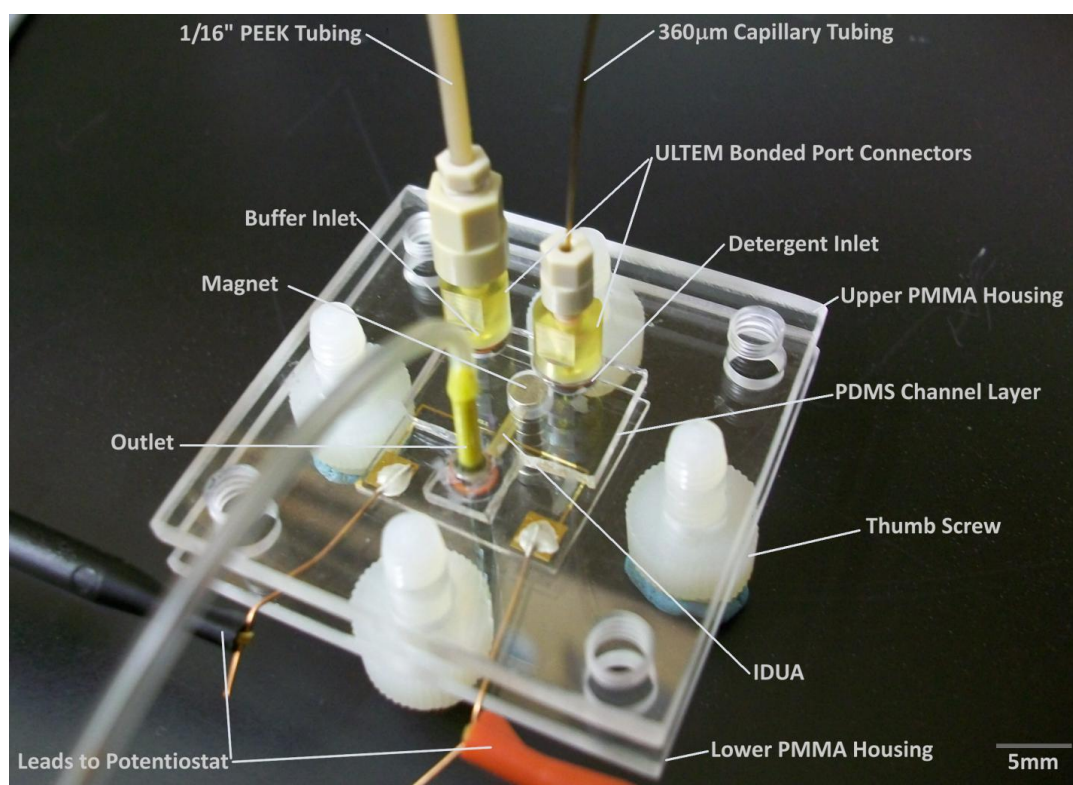


Figure 5.1: Fully assembled microfluidic device. The PDMS is reversibly sealed to a Pyrex® glass slip patterned with an IDUA such that the main channel passes over the electrode finger array. These layers are then sandwiched between two layers of PMMA, bearing the necessary ports for the introduction of sample, buffer, and detergent and removal of waste as well as the positioning of the magnet for bead capture.

Fabrication of IDUAs

IDUAs were fabricated using standard projection photolithographic and lift-off techniques, as previously described (2), with modifications. Here, the metal stack consisted of a 10nm thermally evaporated chromium adhesion layer, 10nm e-gun evaporated platinum diffusion barrier and a 90nm thermally evaporated gold active electrode surface. A batch with the previously used stack, 7nm titanium adhesion layer and 50nm gold active layer, was also prepared. After lift-off, each electrode pair was diced to produce the necessary slips and copper leads were attached to the contact pads using electrically conductive silver epoxy.

IDUA characterization

To rapidly test the response of the electrodes to the redox couple, 10 μ L drops of 0.2M phosphate buffer, pH 7.0, and 10 μ M ferri/ferrohexacyanide in 0.2M phosphate buffer, pH 7.0, were applied to the IDUA fingers for 5min with an applied potential of 400mV, washing with deionized water and drying under nitrogen flow between droplets. Recorded current was then averaged as the signal for each IDUA.

IDUA flow response

To determine the response of the IDUA to varying concentrations of the electroactive species, pulses of ferri/ferrohexacyanide in 0.2M phosphate buffer, pH 7.0, were flowed through the channels of varying dimensions for 10 minutes, long enough to reach a steady-state current response. The IDUA was connected to the potentiostat and a 400mV potential was applied across the two electrodes.

Liposome and magnetic bead preparation

In this study, a synthetic DNA target based on the sequence of the *hsp70* mRNA of *Cryptosporidium parvum* and the corresponding probes, developed previously, were used (8). Liposomes were made using the reverse phase evaporation method and cholesterol-tagged DNA oligonucleotide reporter probes as previously described with modifications (3). Here, the encapsulant was an equimolar 200mM potassium ferri/ferrohexacyanide in 20mM HEPES, pH7.5. These liposomes were prepared in 1X HEPES-Saline-Sucrose (1XHSS), containing 10mM HEPES, 200mM NaCl, and 200mM sucrose, pH 7.5, and quantified based on phospholipid concentration via the Bartlett Assay (9, 10). As HEPES has been shown to interfere with electrochemistry (11, 12), an additional batch was made with an encapsulant of the same concentration of the redox couple but in 10mM sodium borate, 200mM NaCl, pH.7.5, and both batches were examined dialyzed against 1XHSS, 1XPBS, 200mM sucrose, pH7.5 (1XPSS), and 1X Borate-Saline-Sucrose (1XBSS), containing 100mM sodium borate, 200mM NaCl, 200mM sucrose, pH7.0, and lysed by mixing with 60mM n-octyl- β -D-glucopyranoside (OG).

Superparamagnetic beads coated in a monolayer of streptavidin were tagged with biotinylated oligonucleotide probes according to the manufacturer's specifications. Briefly, 20 μ L of beads were washed twice in 2X Binding and Washing (B&W) Buffer, containing 10mM Tris-HCl, 1mM EDTA, 2M NaCl, pH7.5, and then resuspended in 18 μ L 1X B&W buffer and 2 μ L of 300 μ M biotinylated capture probe

and incubated for 15min, shaking at room temperature. The beads were then washed three times in 1X B&W buffer.

DNA hybridization assay

To assess the effect of channel dimensions on the analytical sensitivity of microfluidic biosensor assays with liposome-based signal amplification, a DNA sandwich hybridization assay was conducted. Per assay, 1 μ L of liposomes, 1 μ L of hybridization solution (20% formamide, 4X SSC, 0.2% Ficoll type 400, 0.8% dextran sulfate, 0.2M sucrose), 1 μ L capture beads, and 1 μ L target were mixed and incubated for 15min, shaking at room temperature. Each 4 μ L sample was drawn into PEEK™ tubing attached to a 1mL syringe filled with running buffer (20% formamide, 4X SSC, 0.2% Ficoll type 400, 0.2M sucrose) and then injected into the channels, maintaining a constant linear velocity of 20cm/min to avoid bead loss. The flow of running buffer was continued for 20 μ L to wash away any unbound liposomes, during which time a potential of 400mV was applied to equilibrate the system prior to the lysis of the liposomes via the injection of 30mM OG, 0.2M phosphate buffer, pH7.0 at a constant linear velocity of 6cm/min. Signals were recorded and the area under the curve was evaluated using OriginPro 8.5 (Northampton, MA).

Results & Discussion

Electrochemical microfluidic biosensors for pathogen detection have successfully used liposome amplification previously ([2](#), [13-15](#)). Though the IDUAs have been optimized for detection using ferri/ferrohexacyanide ([4](#)), until this point, no optimization of the

electrochemical detection had been performed as experiments were focused on the development of the microfluidic systems and the biological aspects of the assays. Here, we focused on the optimization of the electrochemical microfluidic assay by further investigating the fabrication of robust IDUAs and optimizing channel dimensions to best suit the bioanalytical assay involving liposome amplification.

IDUA fabrication

Previous work was conducted using IDUAs with a 7nm Ti adhesion layer and a 50nm Au layer (2). While many of the IDUAs worked well, they tended to become non-functioning due to short circuiting, adhesion loss or large variability between electrodes even from the same wafer (34 - 43% CV) and between wafers (55% CV). We therefore investigated improving their performance by changing the metal stack and by further investigating supporting electrolyte solutions. The new metal stack consists of a 10nm Cr layer for adhesion and a 90nm Au layer for detection with a 10nm Pt barrier layer in between to prevent the diffusion of Cr through the Au layer causing electrode failure (16). This resulted in highly stable IDUAs that could be re-used for many analyses and also re-used in several microfluidic system set ups, i.e. PMDS-based devices could be disassembled and reassembled with the same IDUA. Also, the variability within one wafer and between wafers was significantly improved to 9 - 15% CV and 19% CV, respectively. Combining these new IDUAs with the increase from 0.1M phosphate buffer previously used (2) to the optimized supporting electrolyte concentration of 0.2M phosphate buffer (4), the signals increased from 47 nA to 164 nA above the background signals.

Buffer optimization

Liposomes are synthesized entrapping a highly concentrated solution of the ferro/ferrihexacyanide redox couple at 200 mM in buffer. In order to stabilize the entrapped solutions, liposomes are kept in a surrounding buffer solution with an equi- or slightly hyperosmolarity. However, phosphate buffer cannot be used for liposome synthesis as it prevents the ability to quantify liposome yields based on the Bartlett assay (10). Stable liposomes encapsulating fluorescent dyes have been successfully produced using HEPES buffers with sucrose to balance the osmolarity (3, 10). To assure that this change from phosphate buffer would not hamper the signals obtained from the release of ferro/ferrihexacyanide from liposomes, signals obtained in various supporting electrolytes were investigated. Here, we studied 5 μ M ferri/ferrohexacyanide in phosphate, HEPES, and borate buffers and all were tested at supporting electrolyte concentrations of 0.01 and 0.1M and all but borate were evaluated at 0.2M. Borate buffer is saturated around 0.14M and it was tested at this concentration. It was found that 0.01M HEPES reduced the signal 60% with increasing concentrations eliminating the signal above background. The interference of HEPES and other Good's buffers with electrochemical reactions has been documented (11), and in reactions with iron ions has been shown to stabilize the reduced form (12), which, here, would disrupt redox cycling generating a lower current. Further, saturated borate buffer provided the greatest improvement over 0.2M phosphate buffer, with over a 400% increase in signal.

With this knowledge, the synthesis of liposomes using HEPES or borate buffer, and subsequent dialysis against various buffers (1X HSS, BSS and PSS) was investigated in order to optimize subsequent electrochemical quantification.

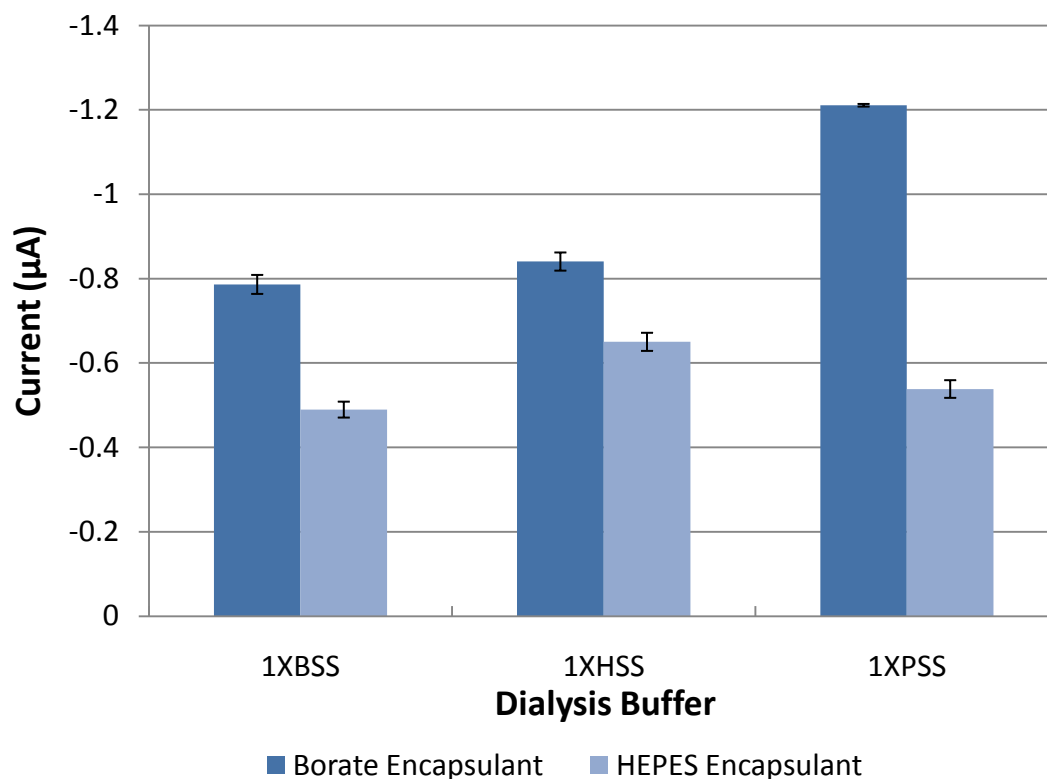


Figure 5.2: Effect of Encapsulant and Diluent Buffers on Liposome Performance. Liposomes made in either HEPES or borate buffers were dialysed against 1XBSS, 1XHSS, or 1XPSS, mixed with 30mM OG and 8µL were applied to the fingers of an IDUA. Liposomes made in borate buffer generally performed better, and liposomes with HEPES encapsulant buffer performed best with HSS diluent buffer.

Liposomes were lysed by mixing with 30mM OG and 8µL was applied to the fingers of an IDUA held at 400mV. As shown in *Figure 5.2*, the liposomes made in borate buffer generated signals higher than those of liposomes prepared in HEPES buffer. However, borate buffer liposomes were highly unstable and could not be synthesized reliably. Further studies were therefore continued with our traditional HEPES buffer

supported liposomes. Instead, we will include phosphate buffer in the OG detergent solution in order to further increase signal to noise ratios.

IDUA electrochemical response with varying channel dimensions

To determine the response of these IDUAs to the redox couple, dose-response curves were developed using these and microchannels of varying dimensions prior to experiments with the full hybridization assay.

Maintaining a channel depth of 50 μ m, channels 500 and 50 μ m in width were assembled over the IDUAs. As shown in *Figure 5.3*, the wider channel produced consistently higher signals. However, the calculated detection limit for the concentration of the redox couple, based on a signal three times the standard deviation of the background, is approximately 0.2 μ M and 0.02 μ M ferri/ferrohexacyanide for 500 and 50 μ m wide channels, respectively, as the narrower channel produced higher signal-to-noise ratios. For channels of the same width, here 500 μ m, but varying depth, either 50 or 20 μ m, produced similar signals as shown in *Figure 5.4*. This correlates to the fact that wider channels provide access to a greater surface area of the IDUA, allowing for more of the electroactive species to engage in redox cycling between the fingers of the array.

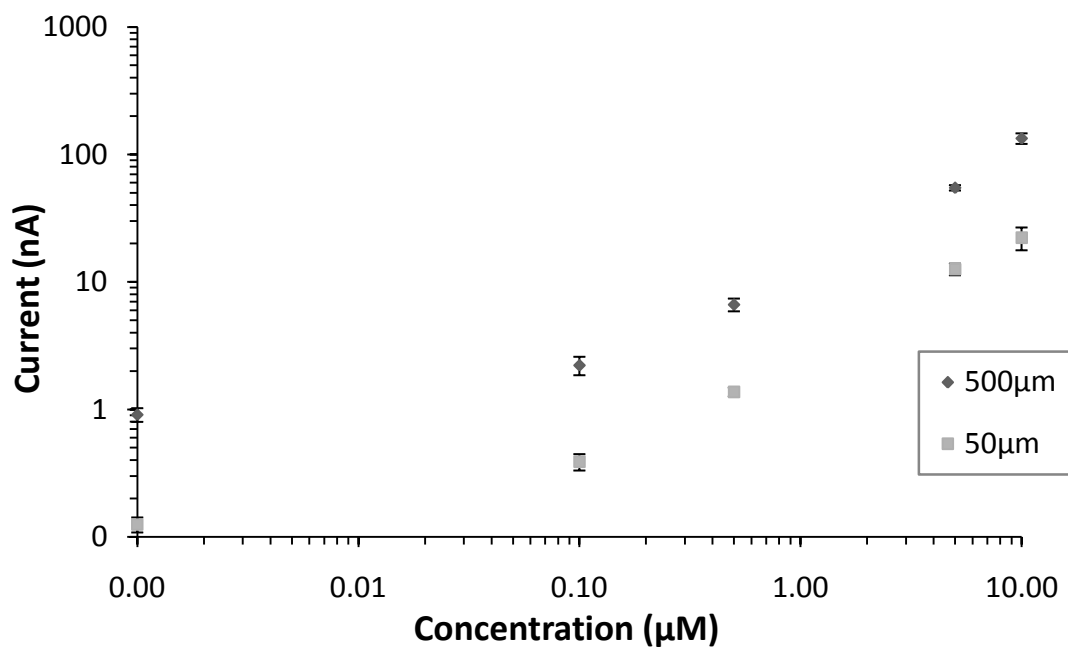


Figure 5.3: Calibration curve for 50µm deep channels of specified widths. Wider channels produce consistently higher signals; however, the narrower channels provide greater sensitivity due to the reduction in background noise (n = 3).

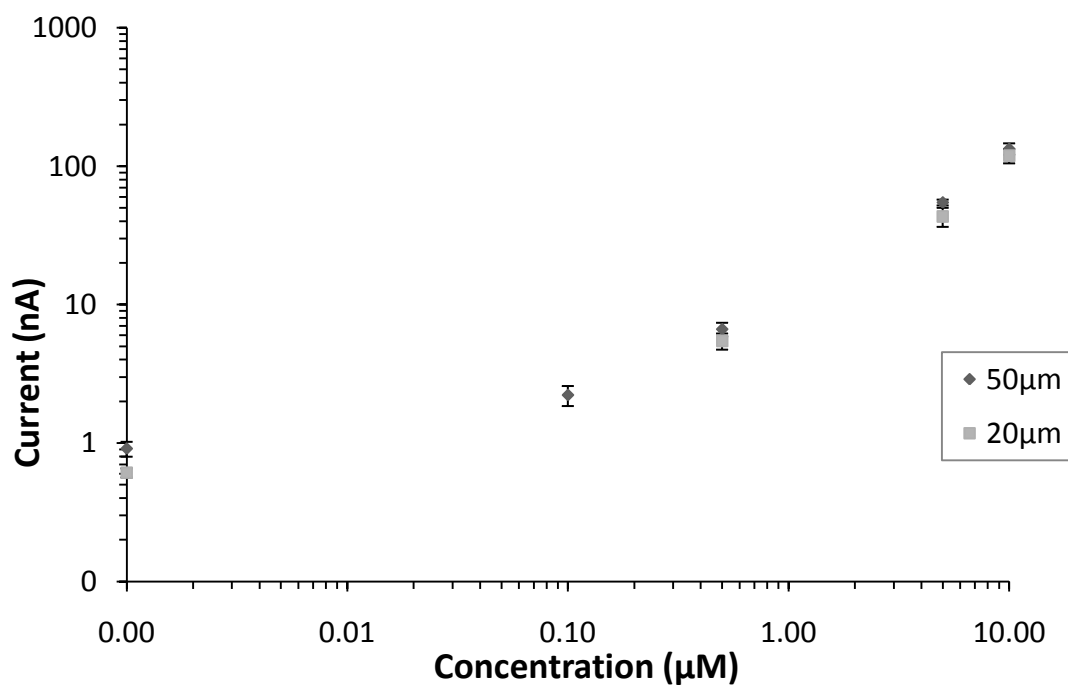


Figure 5.4: Calibration curves for 500µm wide channels with specified depths. Channels of the same width with a varying depth produce the same signals as the active surface area of the IDUA is the same (n = 3).

Effect of dimension changes on DNA hybridization assay

The true impact of the reduced channel volume over the IDUA is most clear when employing liposome signal amplification in the DNA hybridization assay. Flow rates for loading/washing and lysing of liposomes were previously optimized using a channel 500 μm wide and 50 μm deep (2). As the cross-sectional area of the detection channel decreases, the flow rate must also be reduced in order to control for linear velocity from channel to channel. The two flow rates required for the assay in the varying channels used are shown in *Table 5.1*.

Table 5.1: Flow Rates Required for Equal Linear Velocities in Channels of Varying Cross-Sections

<i>Width (μm)</i>	<i>Depth (μm)</i>	<i>Flow Rate at 20cm/min ($\mu\text{L}/\text{min}$)</i>	<i>Flow Rate at 6cm/min ($\mu\text{L}/\text{min}$)</i>
500	50	5.00	1.50
500	20	2.00	0.60
50	50	0.50	0.15

Simply decreasing the depth of the channel from 50 to 20 μm provides a significant enhancement in the limit of detection of the target DNA, as shown in *Figure 5.5*. The analytical sensitivity, calculated to be 3 standard deviations above the background noise, was approximately 0.1fmol of target DNA per assay for the 50 μm deep channels. This was reduced to approximately 10 amol per assay for the 20 μm deep channels. This is an improvement of an order of magnitude from simply decreasing the depth of the channel by 60%. Further decreasing the depth of the channel could lead to further improvements, however, the lower flow rates required to retain the beads, and not lose sample, could lead to clogging as the superparamagnetic beads have time to settle in the inlet. This was observed for the 50x50 μm channels; bead

settling blocked the inlet, allowing for increase pressure and, ultimately, bonding failure and leakage.

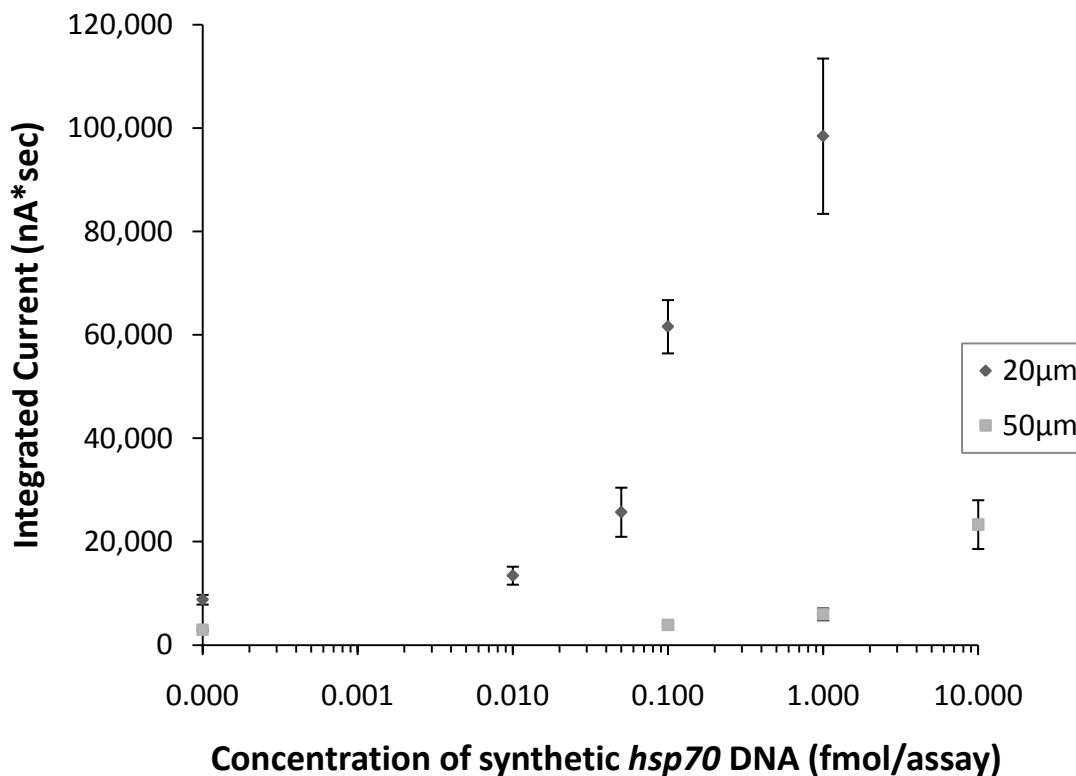


Figure 5.5: Dose-response curves for channels of two different depths using a DNA sandwich-hybridization assay. The linear velocity of the detergent flow for liposome lysis was controlled for the varying depth ($n = 3$).

Conclusions

Improvements in the signal generation and transduction of the microfluidic electrochemical biosensor using liposomes were achieved by implementing optimal supporting electrolyte concentration, liposome diluents and fabricating a thicker metal stack. Furthermore, reductions in the cross-sectional dimensions of a microfluidic channel positioned over an IDUA for electrochemical detection yielded a significant

decrease in the limit of detection of a model DNA hybridization assay employing liposome lysis for signal amplification. Channels 500 μm wide were tested with two different depths, 50 and 20 μm , yielding detection limits of 0.1fmol and 10 amol of target DNA per assay. Additionally, it was shown that, though current response to the redox couple was lower, signal-to-noise improvements were noted for narrower channels. The use of these channels in detection assays was, unfortunately, prohibited by the clogging of the sample inlet due to bead settling during loading at the low flow rate required to avoid bead loss at the magnet. This ultimately caused leakage as the backpressure disrupted the reversible seal of the device. To investigate the benefits of even smaller channels, permanent sealing of the device and improvements in bead capture will need to be investigated to permit higher flow rates.

Acknowledgements

This work was performed in part at the Cornell NanoScale Science and Technology Facility, a member of the National Nanotechnology Infrastructure Network, which is supported by the National Science Foundation (Grant ECS-0335765). This work was developed in part under the auspices of the Cornell University Center for Life Science Enterprise, a New York State Center for Advanced Technology supported by New York State and industrial partners.

REFERENCES

1. Fritsch I, Aguilar ZP. Advantages of downsizing electrochemical detection for DNA assays. *Analytical and Bioanalytical Chemistry* 2007;387:159-63.
2. Goral VN, Zaytseva NV, Baeumner AJ. Electrochemical microfluidic biosensor for the detection of nucleic acid sequences. *Lab on a Chip* 2006;6:414-21.
3. Edwards KA, Baeumner AJ. Optimization of DNA-tagged dye-encapsulating liposomes for lateral-flow assays based on sandwich hybridization. *Analytical and Bioanalytical Chemistry* 2006;386:1335-43.
4. Min J, Baeumner AJ. Characterization and optimization of interdigitated ultramicroelectrode arrays as electrochemical biosensor transducers. *Electroanalysis* 2004;16:724-9.
5. Connelly J, Nugen S, Borejsza-Wysocki W, Durst R, Montagna R, Baeumner A. Human pathogenic *Cryptosporidium* species bioanalytical detection method with single oocyst detection capability. *Analytical and Bioanalytical Chemistry* 2008;391:487-95.
6. Duffy DC, McDonald JC, Schueller OJA, Whitesides GM. Rapid Prototyping of Microfluidic Systems in Poly(dimethylsiloxane). *Analytical Chemistry* 1998;70:4974-84.
7. Zaytseva NV, Goral VN, Montagna RA, Baeumner AJ. Development of a microfluidic biosensor module for pathogen detection. *Lab on a Chip* 2005;5:805-11.
8. Baeumner AJ, Humiston M, Montagna RA, Durst RA. Detection of Viable Oocysts of *Cryptosporidium parvum* Following Nucleic Acid Sequence Based Amplification. *Analytical Chemistry* 2001;73:1176-80.
9. Itoh YH, Itoh T, Kaneko H. Modified Bartlett assay for microscale lipid phosphorus analysis. *Analytical biochemistry* 1986;154:200-4.

10. Edwards K, Curtis K, Sailor J, Baeumner A. Universal liposomes: preparation and usage for the detection of mRNA. *Analytical and Bioanalytical Chemistry* 2008;391:1689-702.
11. Masson J-F, Gauda E, Mizaikoff B, Kranz C. The interference of HEPES buffer during amperometric detection of ATP in clinical applications. *Analytical & Bioanalytical Chemistry* 2008;390:2067-71.
12. Welch KD, Davis TZ, Aust SD. Iron Autoxidation and Free Radical Generation: Effects of Buffers, Ligands, and Chelators. *Archives of Biochemistry and Biophysics* 2002;397:360-9.
13. Kwakye S, Goral VN, Baeumner AJ. Electrochemical microfluidic biosensor for nucleic acid detection with integrated minipotentiostat. *Biosensors & Bioelectronics* 2006;21:2217-23.
14. Bunyakul N, Edwards K, Promptmas C, Baeumner A. Cholera toxin subunit B detection in microfluidic devices. *Analytical and Bioanalytical Chemistry* 2008.
15. Nugen SR, Asiello PJ, Connelly JT, Baeumner AJ. PMMA biosensor for nucleic acids with integrated mixer and electrochemical detection. *Biosensors and Bioelectronics* 2009;24:2428-33.
16. Rairden JR, Neugebauer CA, Sigsbee RA. Interdiffusion in thin conductor films—chromium/gold, nickel/gold and chromium silicide/gold. *Metallurgical and Materials Transactions B* 1971;2:719-22.

CHAPTER 6

CONCLUSION

The work described in this dissertation focused on improvements to biosensor technologies to tackle two obstacles commonly faced in the detection of waterborne pathogens. These obstacles, namely low concentration of the analyte of interest and presence of contaminants in environmental matrices, must be overcome in order to produce a robust biosensor that is capable of detection at levels consistent with water quality regulations and with the clinically significant infectious doses that typically inform those regulations.

The strategy presented for the detection of *Cryptosporidium parvum* successfully overcomes the presence of contaminants and low oocyst concentrations by the implementation, first, of immunomagnetic separation (IMS) and, second, a series of steps increasing specificity and sensitivity while further purifying, concentrating, and amplifying the target mRNA. This assay achieved the ultimate goal of extreme sensitivity – capable of detecting mRNA from a single oocyst – while still being able to process real environmental samples. Future work with this assay is the development of a micro-total analysis system (μ TAS).

Microfluidic devices have great promise not just for the reduction of user error but also increased sensitivity, reduced sample volumes and reagent costs, and novel and efficient pre-processing methods. Herein, work focused on integration of microfluidic nanoporous membrane pre-concentration with liposome-based detection and its application to enteric virus detection. The integration into one device of these two

modules provided improvements in the limit of detection. Nonetheless, the sensitivity needs further enhancement to reach levels competitive with other technologies. This may be achieved, in part, by implementing electrochemical detection and replacing magnetic bead-based capture with immobilized antibodies, which will reduce error associated with bead packing variability.

Optimization of channel design and dimensions is crucial in microfluidic biosensor, as is demonstrated by the order of magnitude improvement in analytical sensitivity achieved simply by reducing channel height by 60%. This data can, and should, be used to seek further improvements in all microfluidic detection schemes reliant on lysis of liposomes for signal generation and amplification, including the described combined concentration-detection device. This, as well as reducing the distance between the nanoporous membrane and capture region to reduce diffusion of the bolus, will be crucial to future developments.

Ultimately, the goal of biosensors for any analyte, including those for waterborne pathogens, is to provide a rapid, sensitive and specific result in as little time as possible with as little effort as possible. As discussed and demonstrated in the preceding chapters, there are trade-offs to be made when selecting how to detect a target – antibodies versus nucleic acid sequences, for example – that favor one criterion over another. The described system for detecting *C. parvum* targets a specific mRNA, permitting the detection of a single, viable oocyst. This does, however, sacrifice time as it requires a lengthy enzymatic amplification step. Research efforts should continue to pursue vigorously amplification-free nucleic acid sensors by

pursuing novel signal generation schemes, for example upconverting phosphors (UCP) and electrochemiluminescence (ECL), while harnessing the promise that miniaturization provides.

With much focus on miniaturization, microfluidics and μ TAS, one must not lose sight of real world needs. As we continually reduce the sample volumes that our devices can handle we must remember that regulations often require the testing of large samples. For instance, the US Environmental Protection Agency (US EPA) requires that at least 100mL of drinking water be tested for the presence of fecal coliform as an indicator organism, a volume far greater than any microfluidic device can accommodate. It may seem attractive to simply divide large samples amongst several assays until the entire volume is processed. Doing so would require a method with high analytical sensitivity and a high-throughput, parallelized process, which may be attainable with microfluidic molecular biological techniques. However, this alone would not address the commonly present contaminants in these samples. Pre-concentration and purification methods are a must for any device that seeks to analyze real samples.

Robust processing modules capable of handling larger samples via a combination of higher flow rates and larger volume channels and chambers should be pursued in order to realize the potential of microfluidic biosensors. These should exploit the filtration and concentration methods currently employed on the macro-scale. For example, non-specific concentration techniques, like charged filters are commonly used to retain pathogens of interest, particularly viruses, until elution for analysis and, as discussed in the preceding chapters, some have explored this on the micro-scale. Charged

nanofibers, beads/particles, or micro-patterned structures can increase surface area, provide increased capture efficiency, and should be further explored. However, water samples may easily foul a device, as sources may contain small rocks, occasionally consisting of iron ore complicating magnetic separations, clay colloids, and plant detritus. Thus, filter-based methods should always address fouling and best practices should call for designs that allow for possible backwashing or other means of assuring proper function during processing.